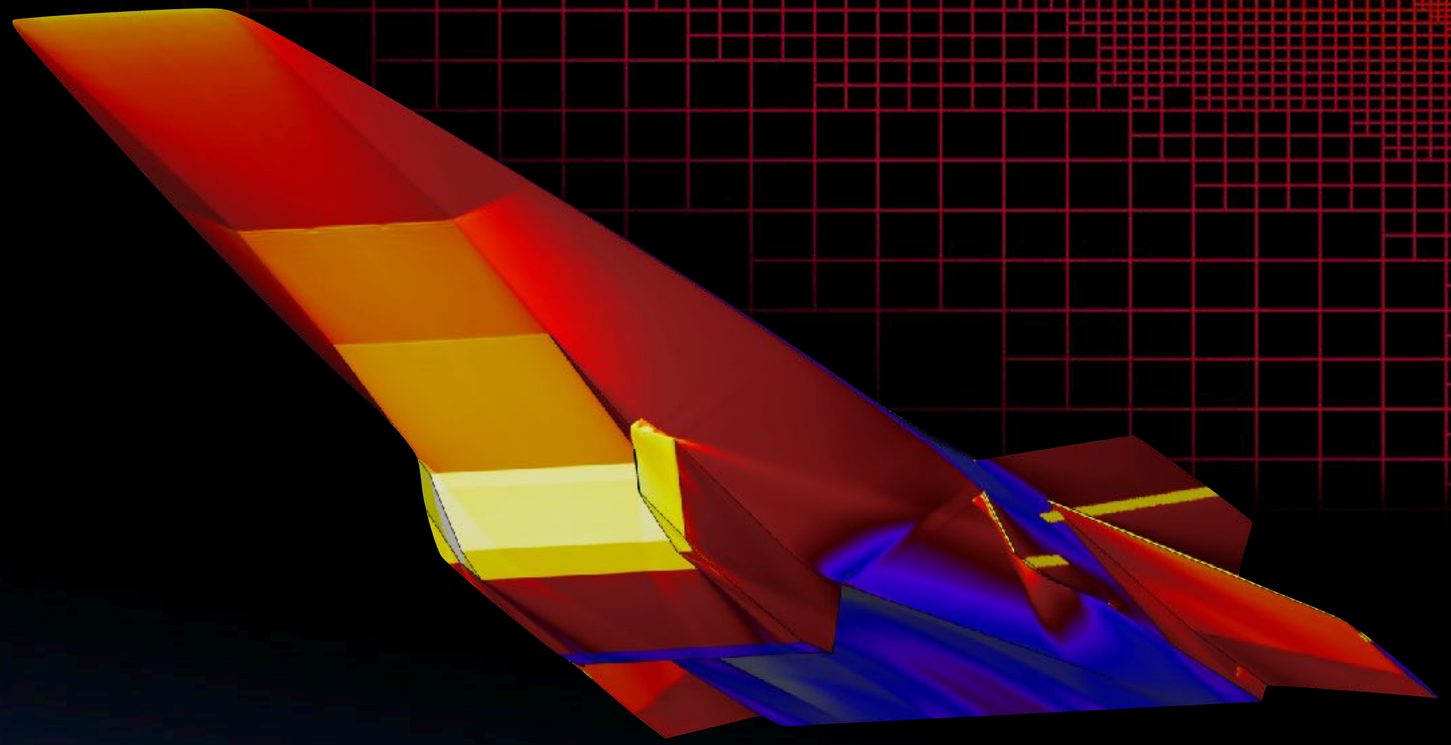
NASA Ames Research Center
Advanced Modeling & Simulation Seminar Series

Smarter Grids, Faster Solvers: Advances and Applications with NASA's Cart3D

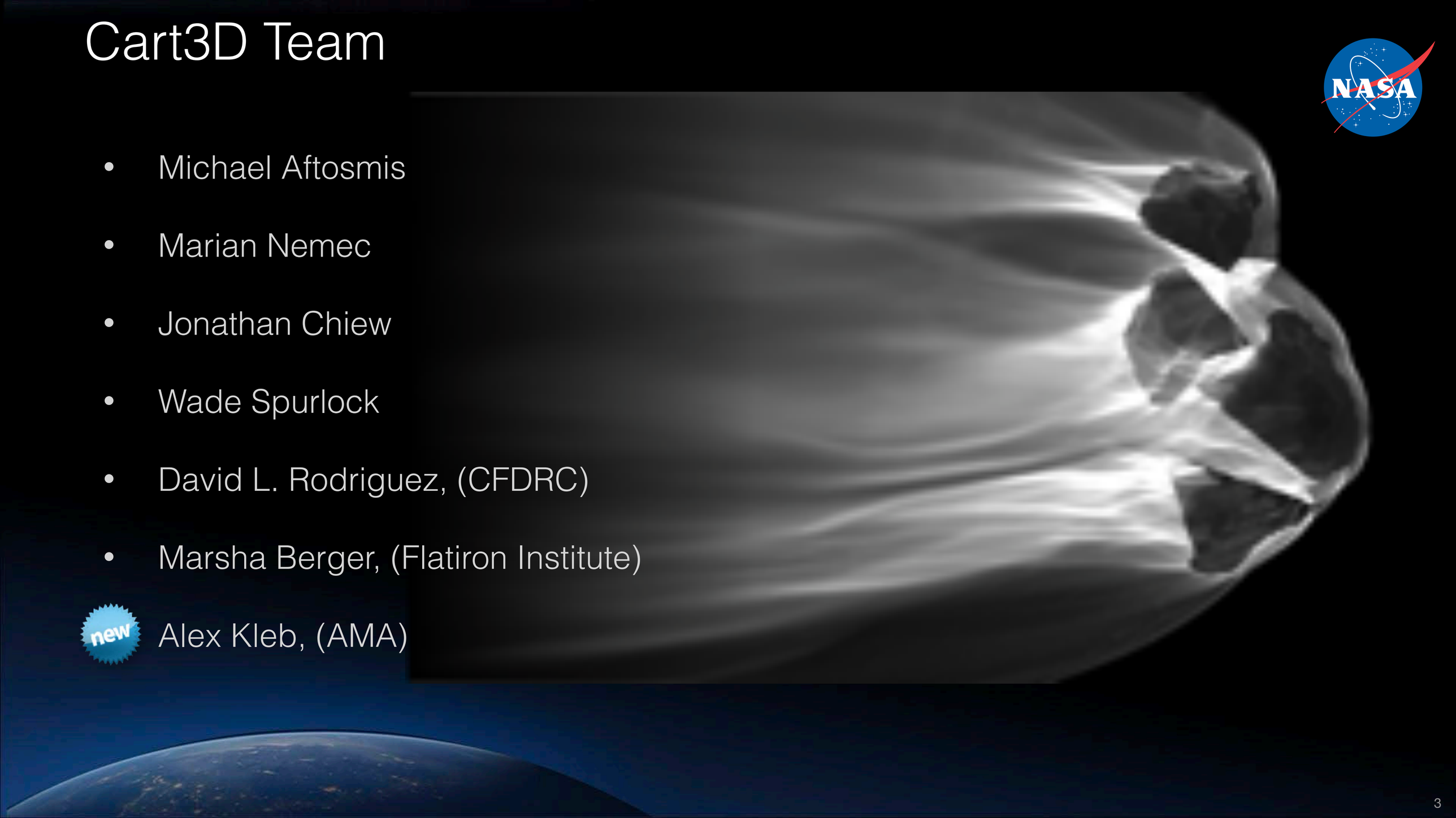


Michael J. Aftosmis
Computational Aerosciences Branch
NASA Advanced Supercomputing Division
NASA Ames Research Center
michael.aftosmis@nasa.gov

11 December, 2025

NASA SILICON VALLEY
AMES RESEARCH CENTER

Cart3D Team



- Michael Aftosmis
- Marian Nemec
- Jonathan Chiew
- Wade Spurlock
- David L. Rodriguez, (CFDRC)
- Marsha Berger, (Flatiron Institute)
- new Alex Kleb, (AMA)

Funding, mission support & key collaborators

FY24-25

Aeronautics Research Mission Directorate

- Commercial Supersonic Transport (CST)
- Low Boom Flight Demonstrator (LBFD)
- Transformative Aeronautics Concepts Program (TACP/TTT)
- Convergent Aeronautics Solutions Project (CAS)

Science Mission Directorate

- Planetary Defense Coordination Office - Asteroid Threat Assessment Project (ATAP)

Exploration Systems Development Mission Directorate & Space Technology Mission Directorate

External Collaborations

- Flatiron Institute & UW
- Lawrence Livermore Nat. Lab. (LLNL)
- MIT & U.Mich
- Nat. Air and Space Intel. Center (NASIC)
- National Geospatial Intel. Agency (NGA)
- Defense Intel. Center (DIA)
- NAVAIR & ARL

Outline

Cart3D Overview

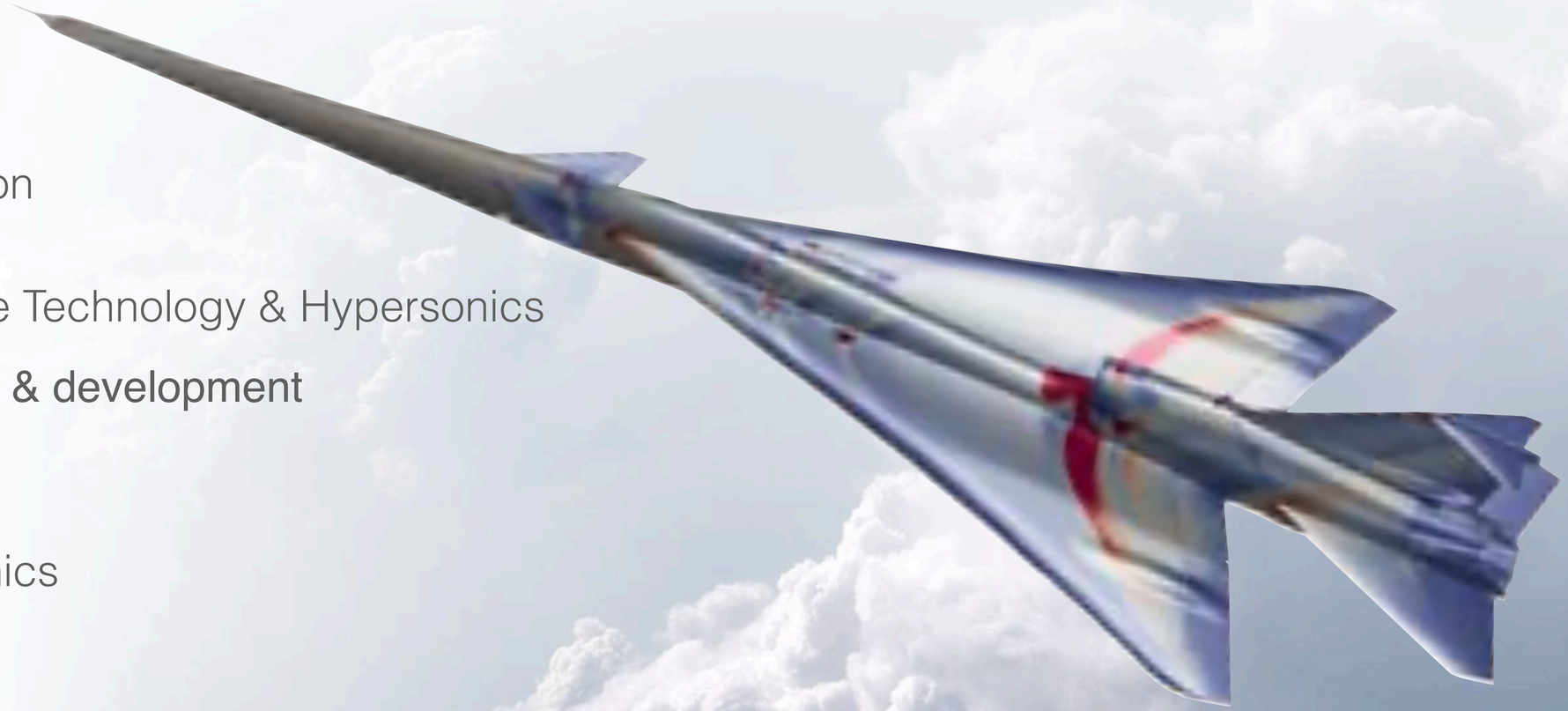
- Usage & application areas
- Current release
- Automation

Recent highlights

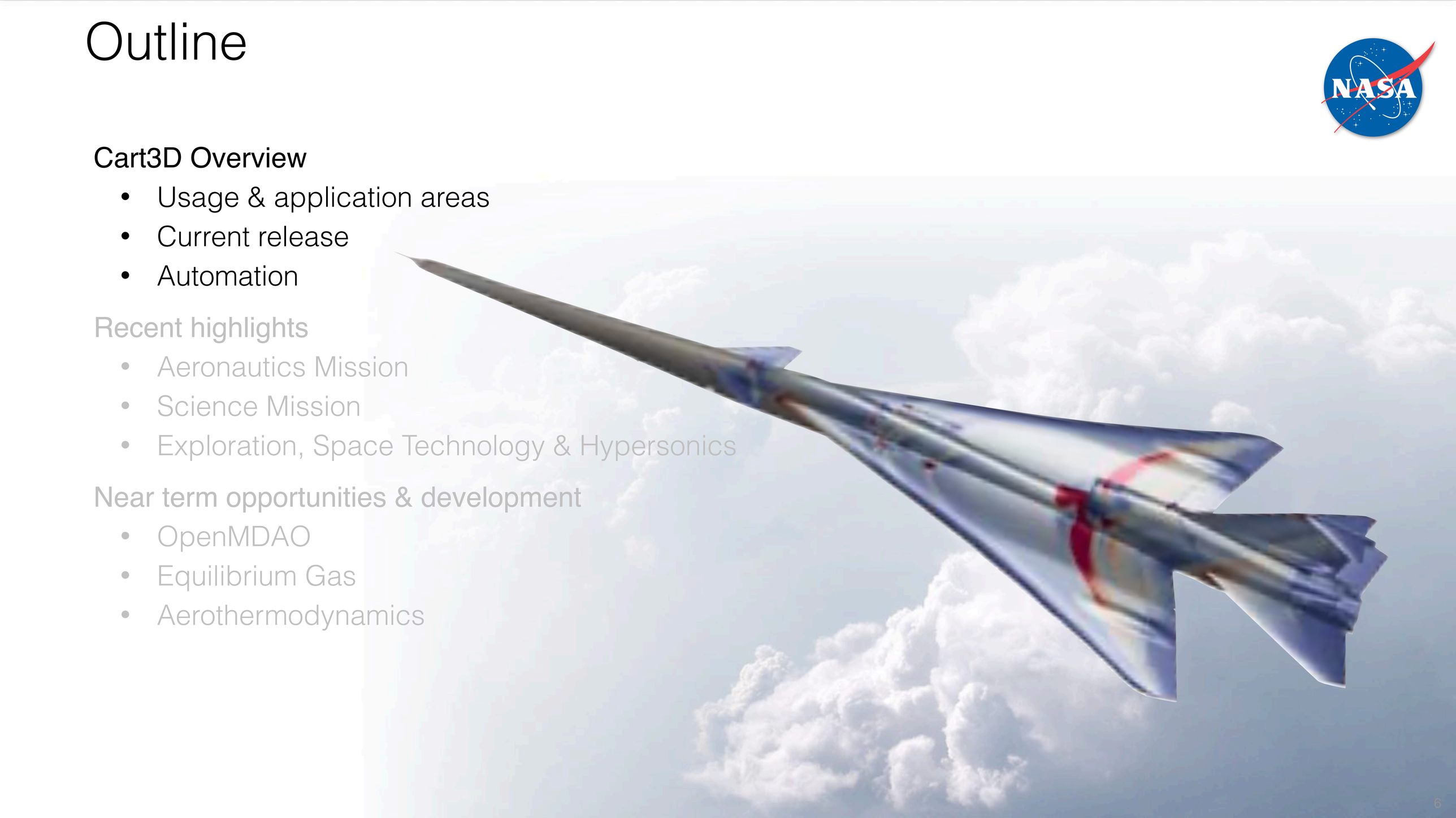
- Aeronautics Mission
- Science Mission
- Exploration, Space Technology & Hypersonics

Near term opportunities & development

- OpenMDAO
- Equilibrium Gas
- Aerothermodynamics



Outline



Cart3D Overview

- Usage & application areas
- Current release
- Automation

Recent highlights

- Aeronautics Mission
- Science Mission
- Exploration, Space Technology & Hypersonics

Near term opportunities & development

- OpenMDAO
- Equilibrium Gas
- Aerothermodynamics

Cart3D Basics

High-fidelity inviscid analysis

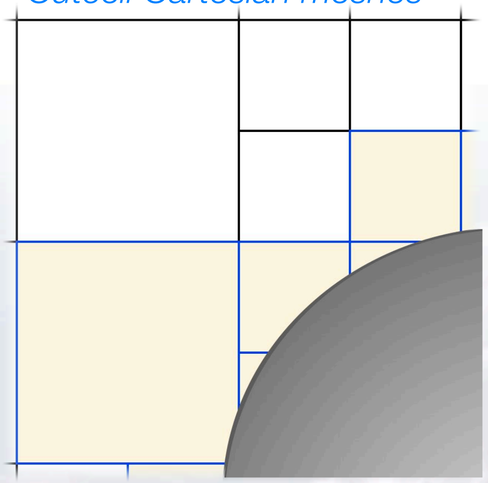
Meshing

- Fully-automated mesh generation for complex geometry
- Unstructured Cartesian cells
- Cutcell boundaries
- Fully integrated adjoint-based mesh adaptation

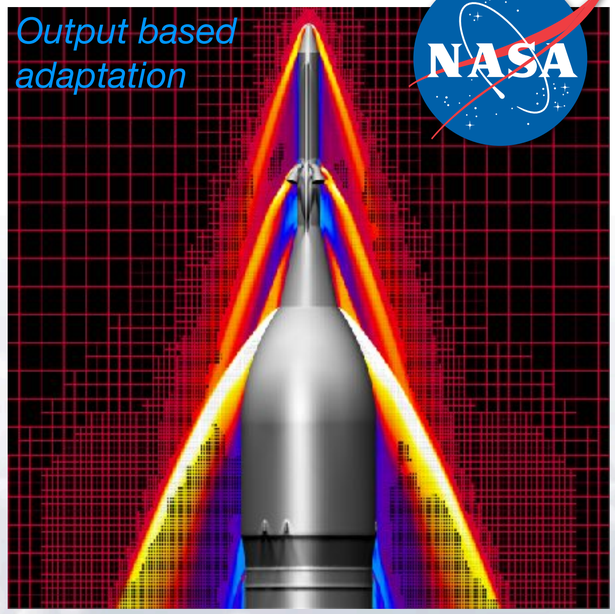
Solver

- Fully-conservative finite-volume method
- Multigrid accelerated 2nd-order upwind scheme
- Dual-time approach for unsteady simulation
- SFC-based domain decomposition, scalable to thousands of cores
- One of NASAs most heavily used production solvers, large validation database

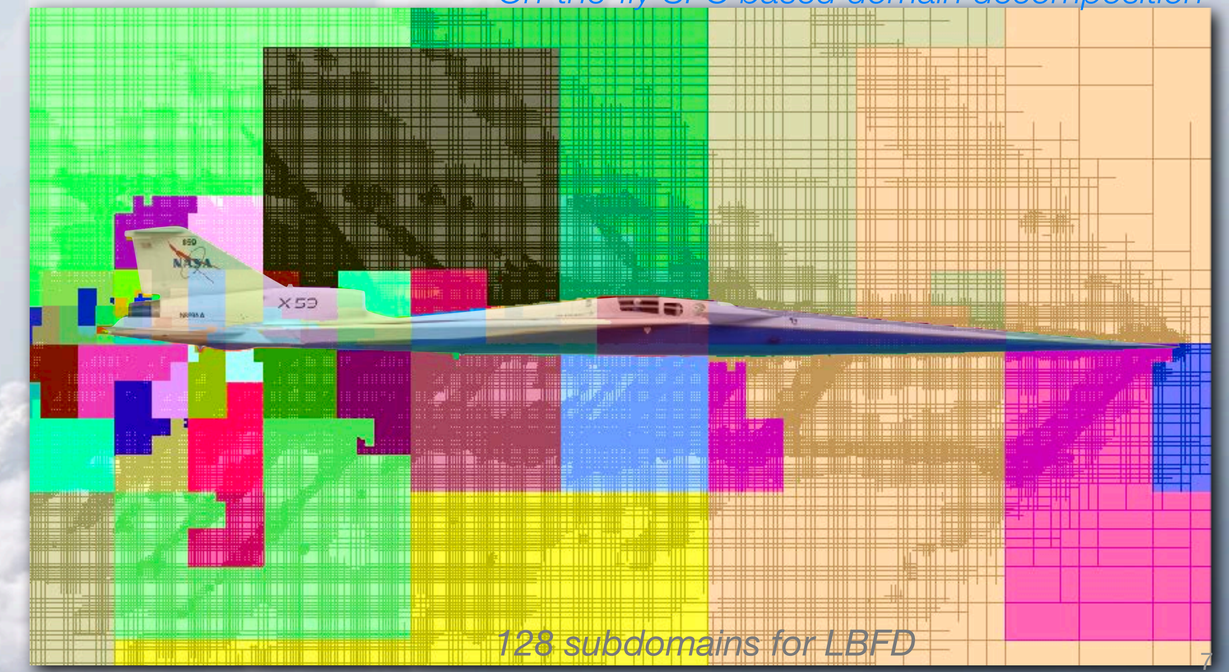
Cutcell Cartesian meshes



Output based adaptation



On-the-fly SFC based domain decomposition

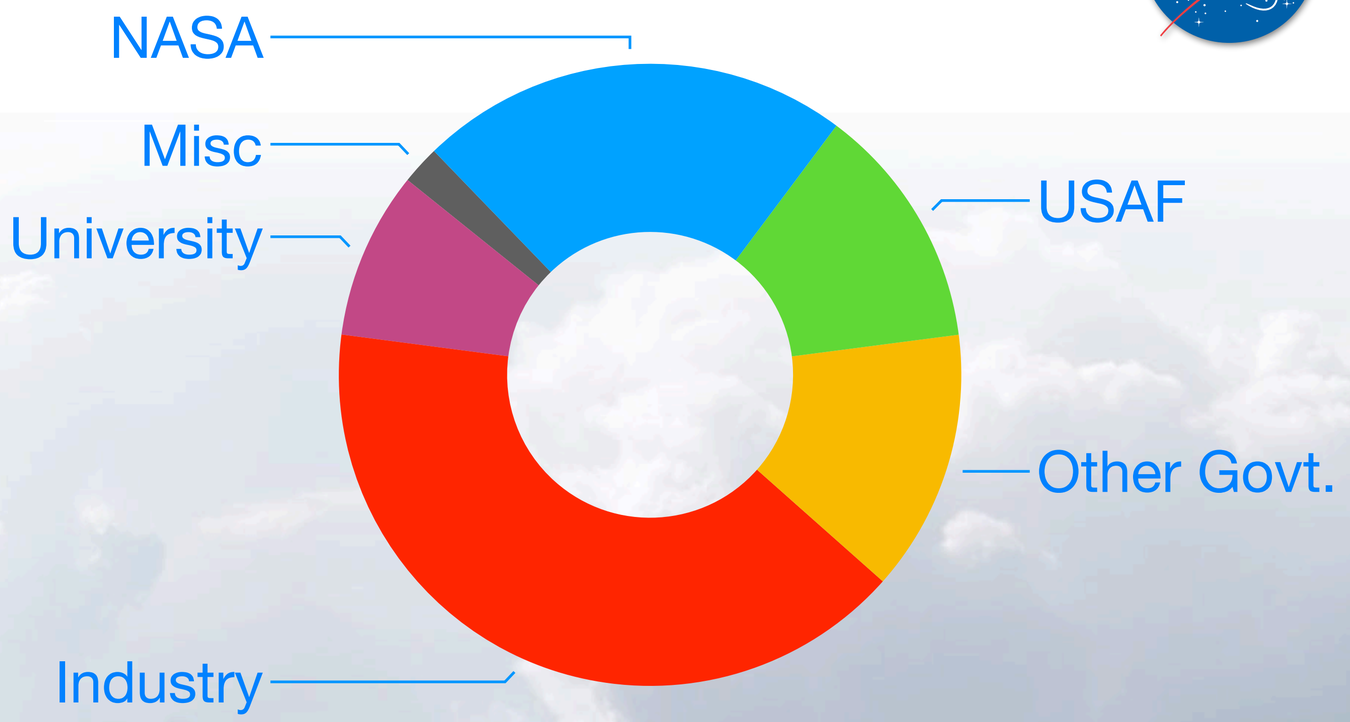


128 subdomains for LBFD

Overview & usage

Current usage

- NASA
  - ARMD, ESDMD, STMD & SMD
- DoD & DOE
  - USAF, NAVAIR, ARL
  - NASIC, DIA, NGA
  - LLNL, Sandia, JHUAPL
- Industry
  - Launch & entry vehicles
  - Aircraft industry (~50% supersonic)
  - Defense
- External to NASA, hypersonics has been the fastest growing applications area over the past decade



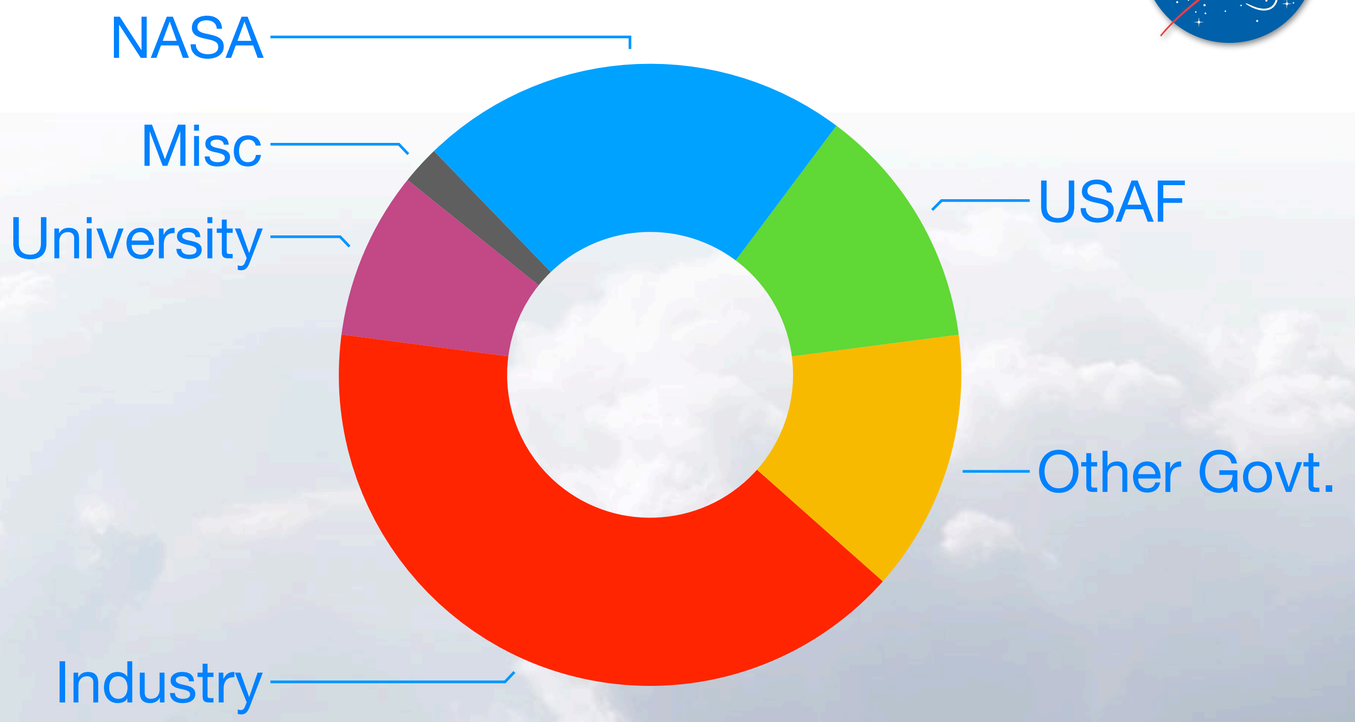
~950 Registered users

Aug 2025

Overview & usage

Industry growth areas

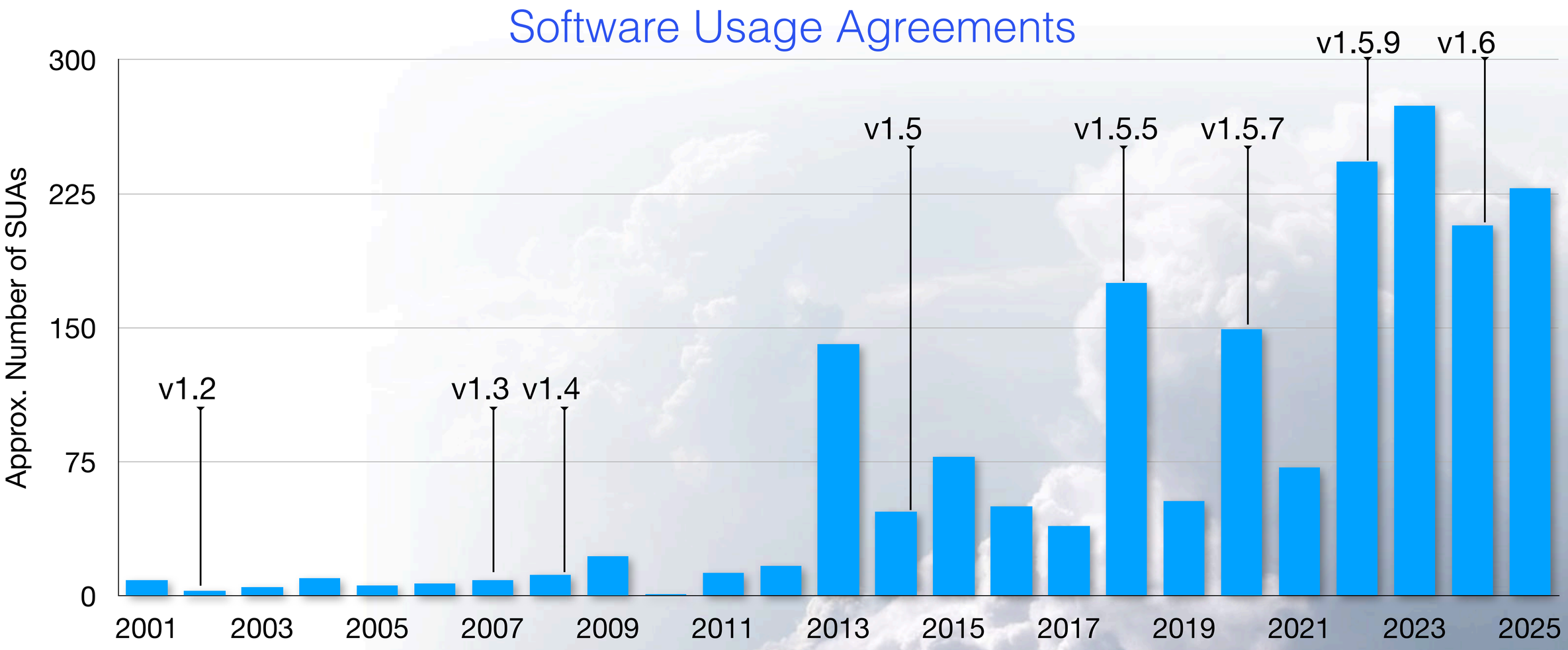
- Commercial space
  - Launch & booster flyback
  - Re/entry
- Commercial supersonics
- Drone & UAV aerodynamics
- Hypersonics
  - Some commercial re/entry
  - Largely driven by DoD emphasis
  - Big boost in fy25



Supersonics & hypersonics have been the fastest growing application areas over the past decade

Overview & usage

Software Usage Agreements (SUAs)



Current Release

Cart3D v1.6.0 & Cart3D Design v1.0

Cart3D v1.6.0

- Released Dec. 2024 (NASA Software Catalog & NASA.box)
- Tighter integration with sBOOM for sonic boom analysis
- Output-based adaptation and error control for ground noise functionals (A/B/C-SEL)
- Integration with NASA's QUEST UQ package
- Symbolic geometry deformation and component labeling
- Support for aeroheating analysis with CBAERO v6.5+
- Improved solver speed and performance

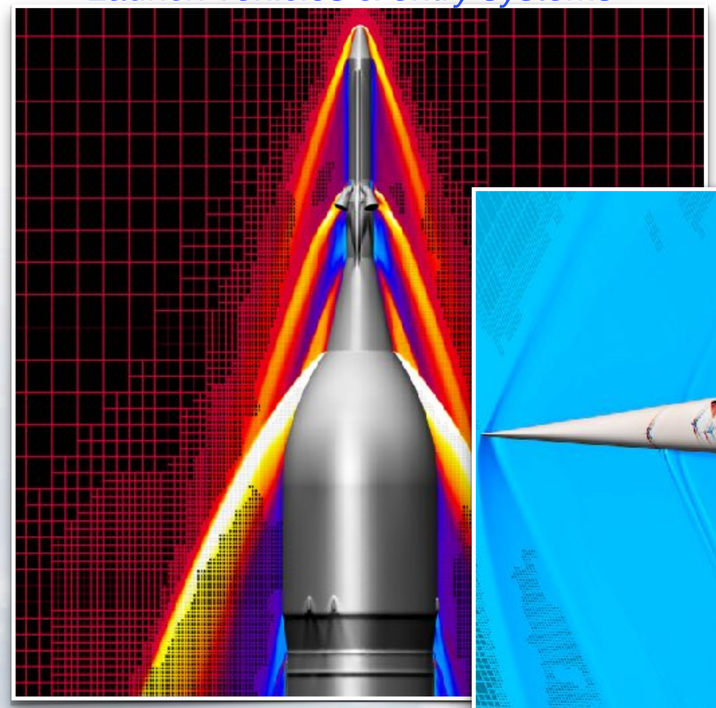
Cart3D Design Framework v1.0

- Full support for ground noise-based design
- Updates for SNOPT v.7.7 with examples
- Include OpenMDAO Components for Cart3D
- Standalone function & gradient eval. for external optimizers (OpenMDAO, ESP/CAPS)

I/O libs – c3dlibs_v1.0

- I/O libs for direct integration
- NASA Open Source release

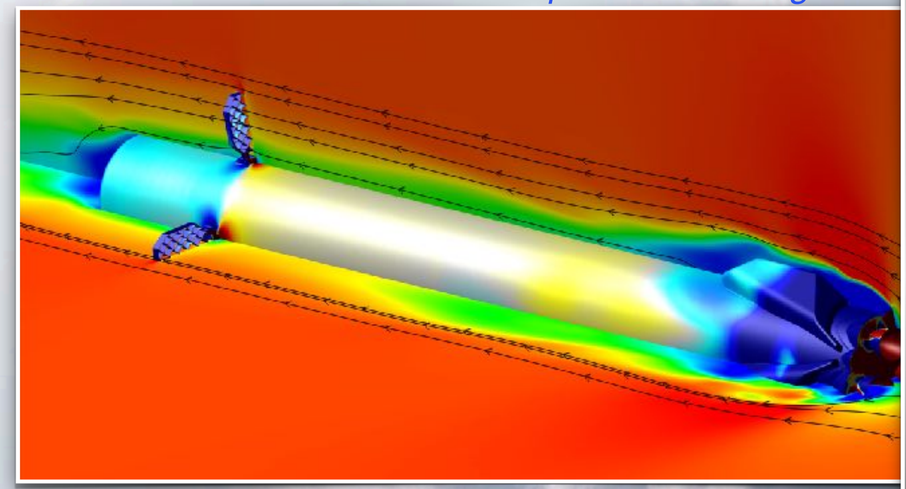
Launch vehicles & entry systems

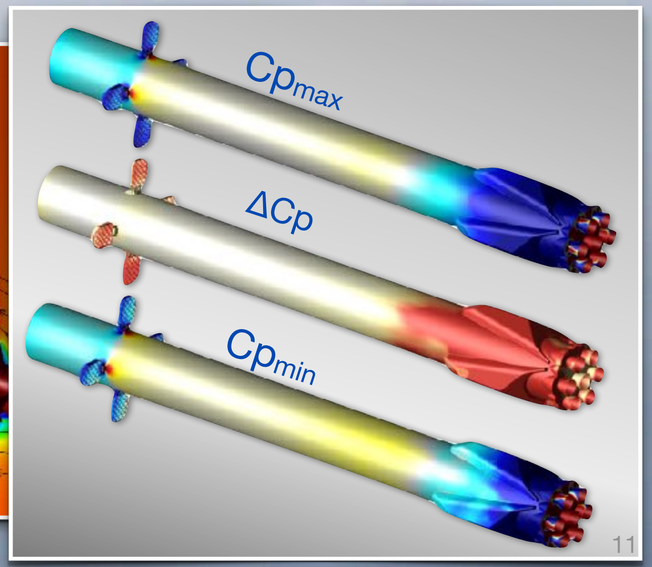


Low boom analysis & design



Booster separation & design



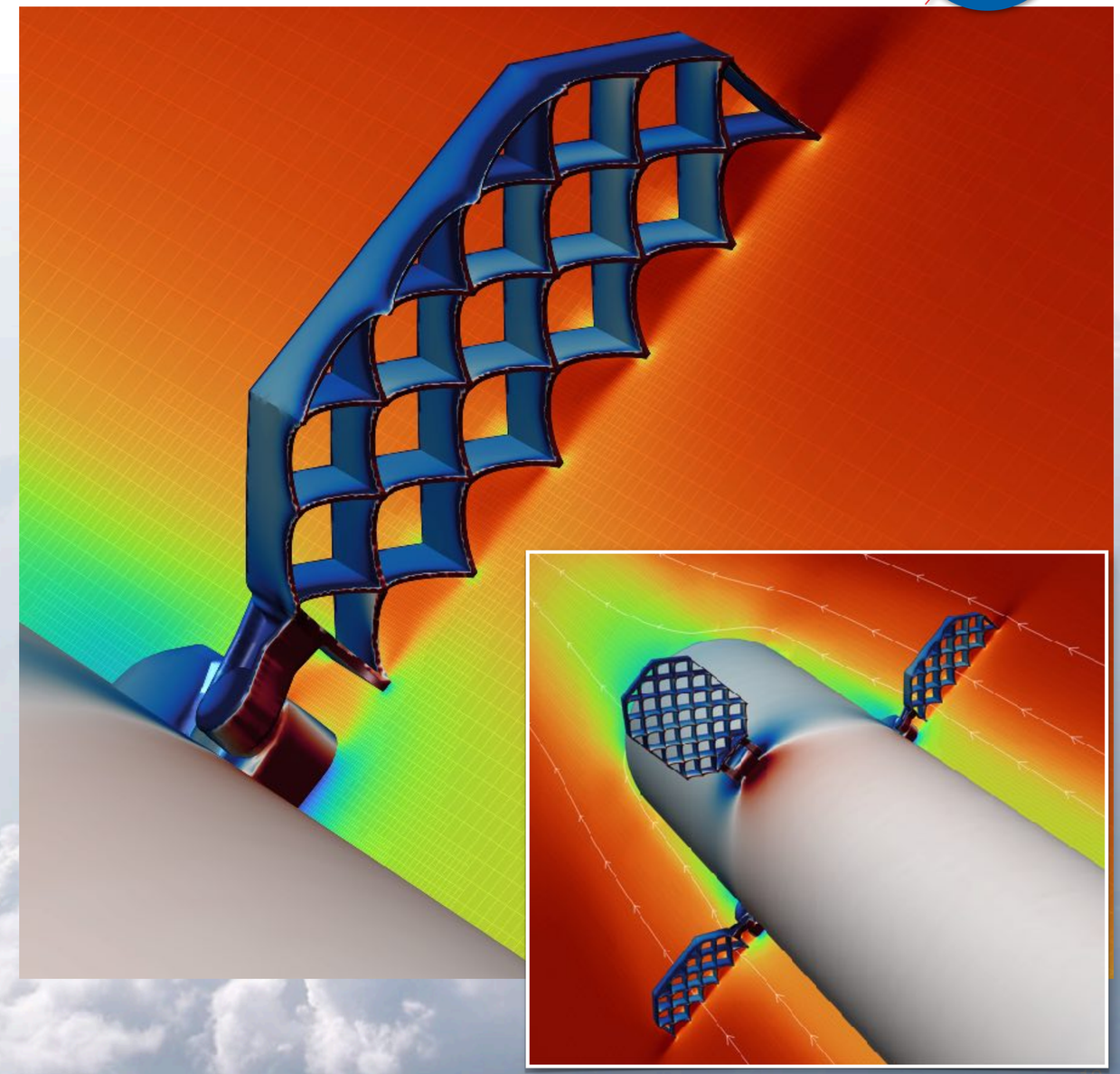


Automation

Fully automated meshing & simulation

Automation requires

- User independence
  - Avoid empirical inputs
    e.g. meshing clustering
  - Avoid reversing the dependency chain
    Only require inputs that are known when they're required
  - Surface triangulation only describes geometry
    The triangulation is decoupled from the solver's mesh
  - At solution
    Only require the computational domain, conditions and goal
- Robustness
- Determinism



Automation

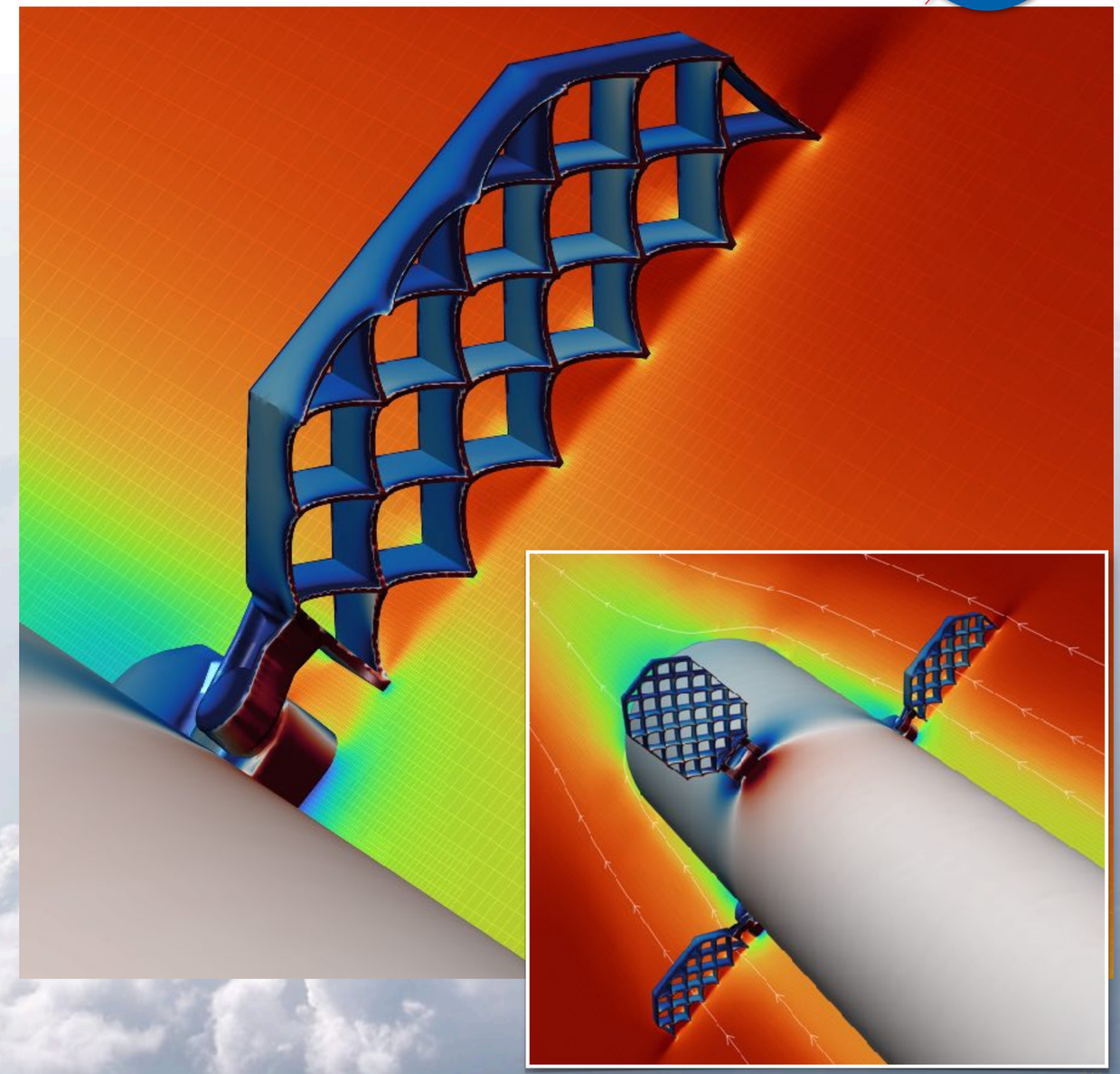
Fully automated meshing & simulation

Automation requires

- User independence
- Robustness
- Determinism

Guaranteed meshing

- Algorithmically robust for watertight geometry
- Robust geometric predicates
- Exact evaluation
  - Topological primitives
  - Intersection testing
- Algorithmic tie breaking
  - See VKI Notes 1997 & AIAA Jol. 36(6)†



*See: Aftosmis, VKI 1997; AIAA J. **36**(6), 1998 & AIAA 2004-1232*

Automation

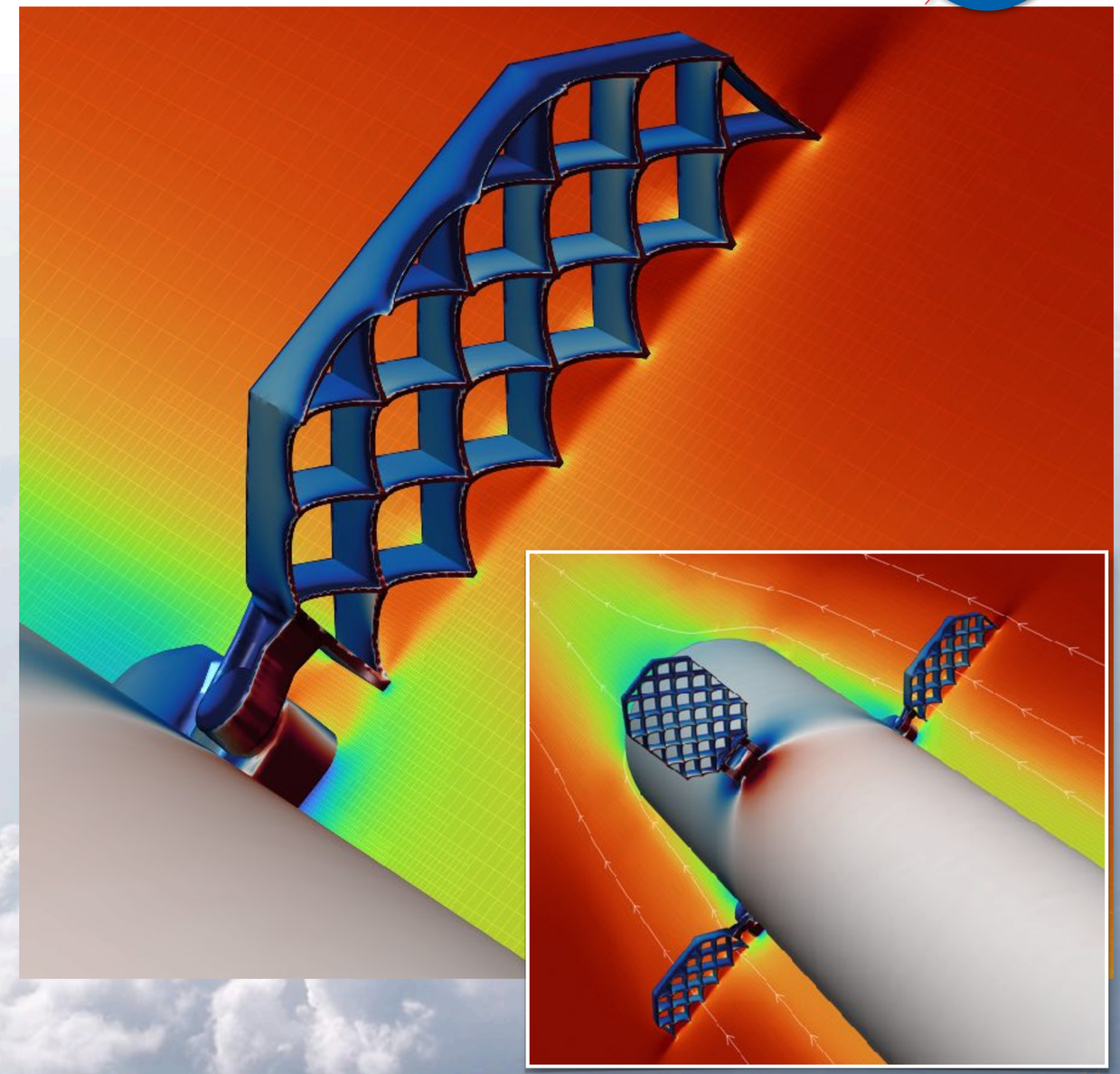
Fully automated meshing & simulation

Automation requires

- User independence
- Robustness
- Determinism

Guaranteed meshing

- Algorithmically robust for watertight geometry
- Robust geometric predicates
- Exact evaluation
- Algorithmic tie breaking†
- Resulting mesher
  - Mesh is unstructured collection cells, uncut: $\mathcal{O}(N^3)$, cut: $\mathcal{O}(N^2)$
  - Extensive use of bit-wise operations & packed integer math
  - Packed integer storage, (96-bits/cell)
  - Linear asymptotic complexity (speed ~1.5-2.5 M cells/sec)
  - Automatic coarsening, SFC ordering for on-the-fly partitioning



*See: Aftosmis, VKI 1997; AIAA J. **36**(6), 1998 & AIAA 2004-1232*

Automation

Fully automated meshing & simulation

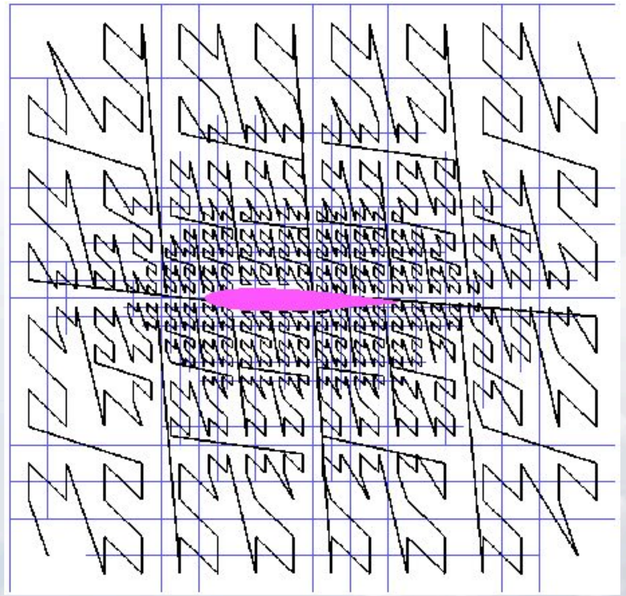
Automation requires

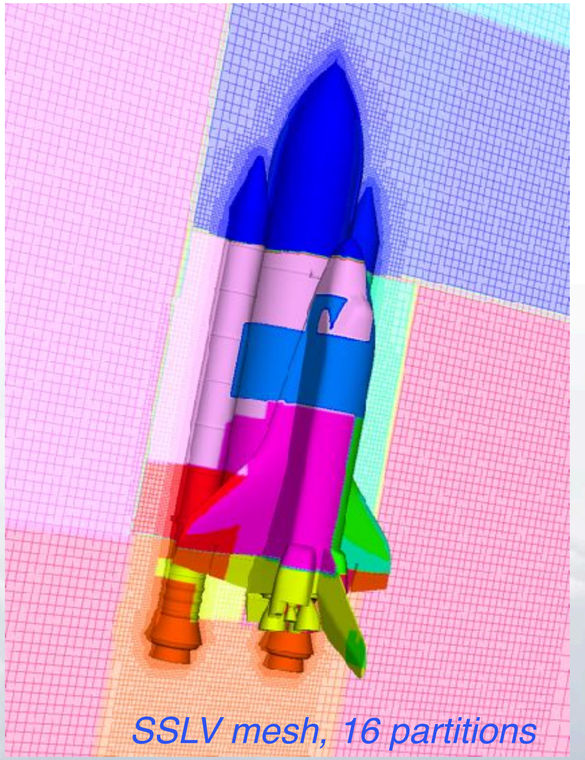
- User independence
- Robustness
- Determinism

Guaranteed meshing

- Algorithmically robust for watertight geometry
- Robust geometric predicates
- Exact evaluation
- Algorithmic tie breaking†
- Resulting mesher
  - Mesh is unstructured collection cells, uncut: $\mathcal{O}(N^3)$, cut: $\mathcal{O}(N^2)$
  - Extensive use of bit-wise operations & packed integer math
  - Packed integer storage, (96-bits/cell)
  - Linear asymptotic complexity (speed ~1.5-2.5 M cells/sec)
  - Automatic coarsening, SFC ordering for on-the-fly partitioning

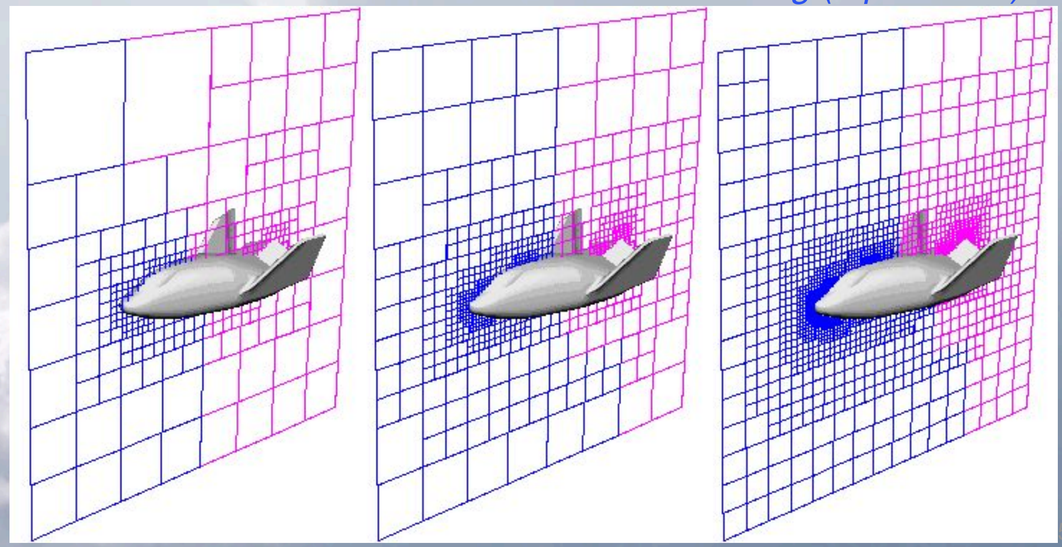
SFC (Morton) for multilevel 2D mesh





SSLV mesh, 16 partitions

Automatic mesh coarsening (2 partitions)



*See: Aftosmis, VKI 1997; AIAA J. **36**(6), 1998 & AIAA 2004-1232*

Automation

Fully automated meshing & simulation

Automation requires

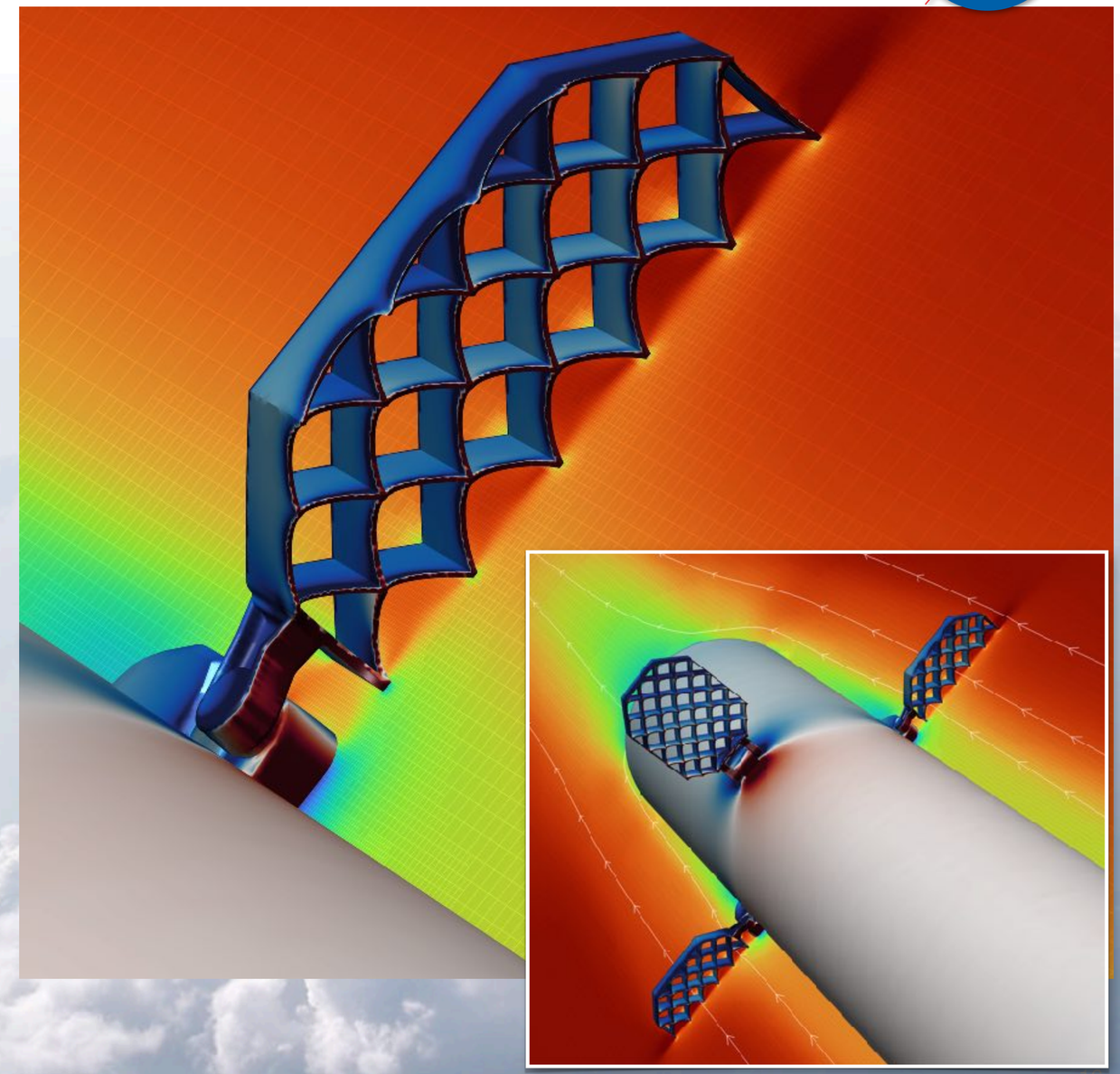
- User independence
- Robustness
- Determinism

Guaranteed meshing

- Algorithmically robust for watertight geometry
- Robust geometric predicates
- Exact evaluation
- Algorithmic tie breaking

Guaranteed Simulation Accuracy

- Engineer supplies simulation goals
- Goal-oriented mesh adaptation
  - Based on method of adjoint-weighted residuals
  - Provides quantified error estimates in outputs of interest
- Every simulation produces a mesh refinement study with quantified error bounds



Automation

Method of adjoint-weighted residuals



- Gives error estimates for a particular objective (functional), $J = C_L$, C_D etc.
- Gives cell-wise indicator for guiding automatic mesh refinement
- Outline
  - Flow Solve: $R(\mathbf{U}_H) = 0$
  - Objective function: $J(\mathbf{U}_H)$
  - Adjoint system: $\frac{\partial \mathbf{R}}{\partial \mathbf{U}_H}^{\mathrm{T}} \psi_H = \frac{\partial J}{\partial \mathbf{U}_H}^{\mathrm{T}}$
  - Estimate of improved functional:

$$J(\mathbf{U}_h) \approx J(\mathbf{U}_h^H) - (\psi_h^H)^{\mathrm{T}}\mathbf{R}(\mathbf{U}_h^H) - (\psi_h - \psi_h^H)^{\mathrm{T}}\mathbf{R}(\mathbf{U}_h^H)$$

Adjoint Correction — Remaining Error

See: Nemec et al.: AIAA 2007-4187, AIAA 2008-0725 & NASA/TP 2016-219422

Automation

Method of adjoint-weighted residuals

$$J(\mathbf{U}_h) \approx J(\mathbf{U}_h^H) - (\psi_h^H)^{\mathrm{T}}\mathbf{R}(\mathbf{U}_h^H) - (\psi_h - \psi_h^H)^{\mathrm{T}}\mathbf{R}(\mathbf{U}_h^H)$$

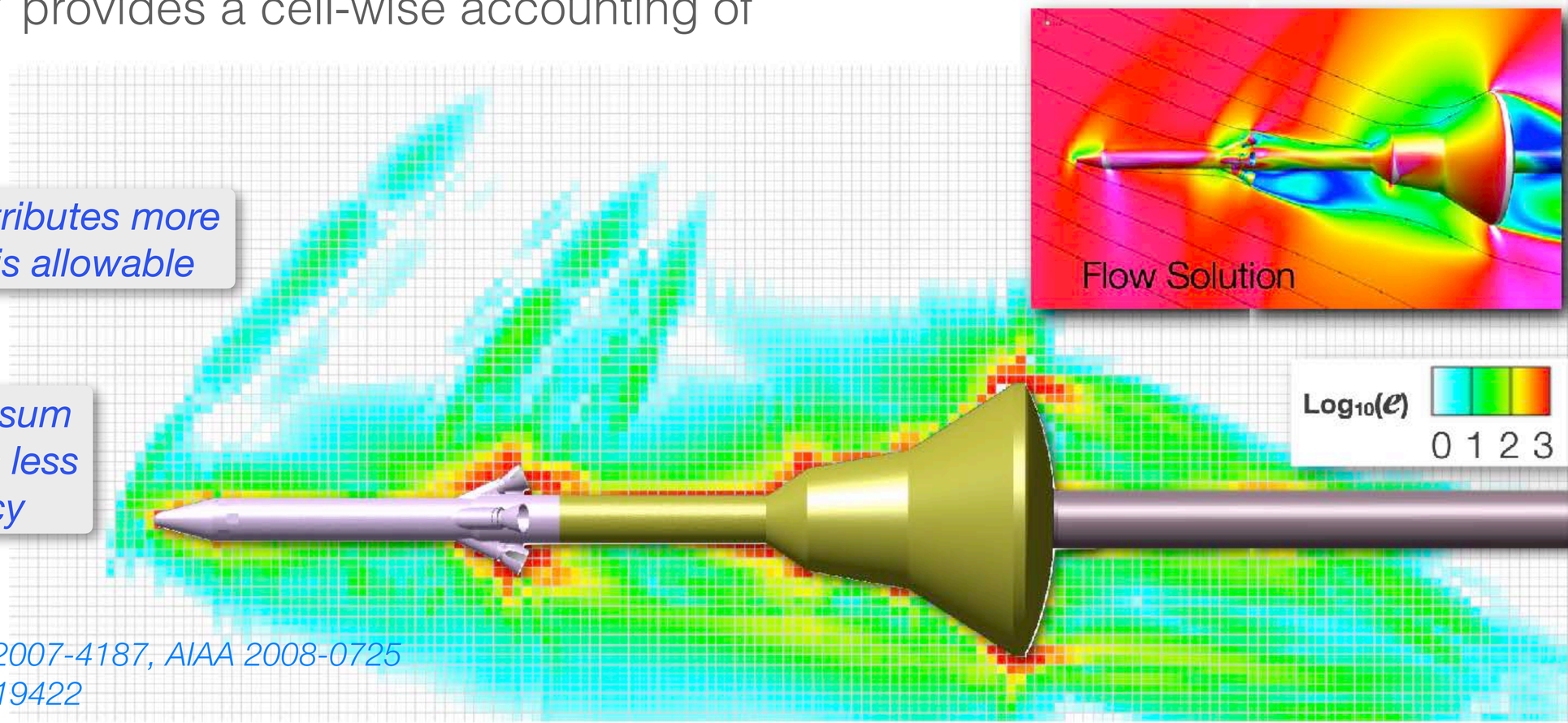
Adjoint Correction

Remaining Error

"Remaining-error" provides a cell-wise accounting of mesh deficiency

Adapt any cell that contributes more to the functional than is allowable

Stop refining when the sum of the cell-wise errors is less than desired accuracy



See: Nemec et al.: AIAA 2007-4187, AIAA 2008-0725 & NASA/TP 2016-219422

Automation

Method of adjoint-weighted residuals

$$J(\mathbf{U}_h) \approx J(\mathbf{U}_h^H) - (\psi_h^H)^{\mathrm{T}}\mathbf{R}(\mathbf{U}_h^H) - (\psi_h - \psi_h^H)^{\mathrm{T}}\mathbf{R}(\mathbf{U}_h^H)$$

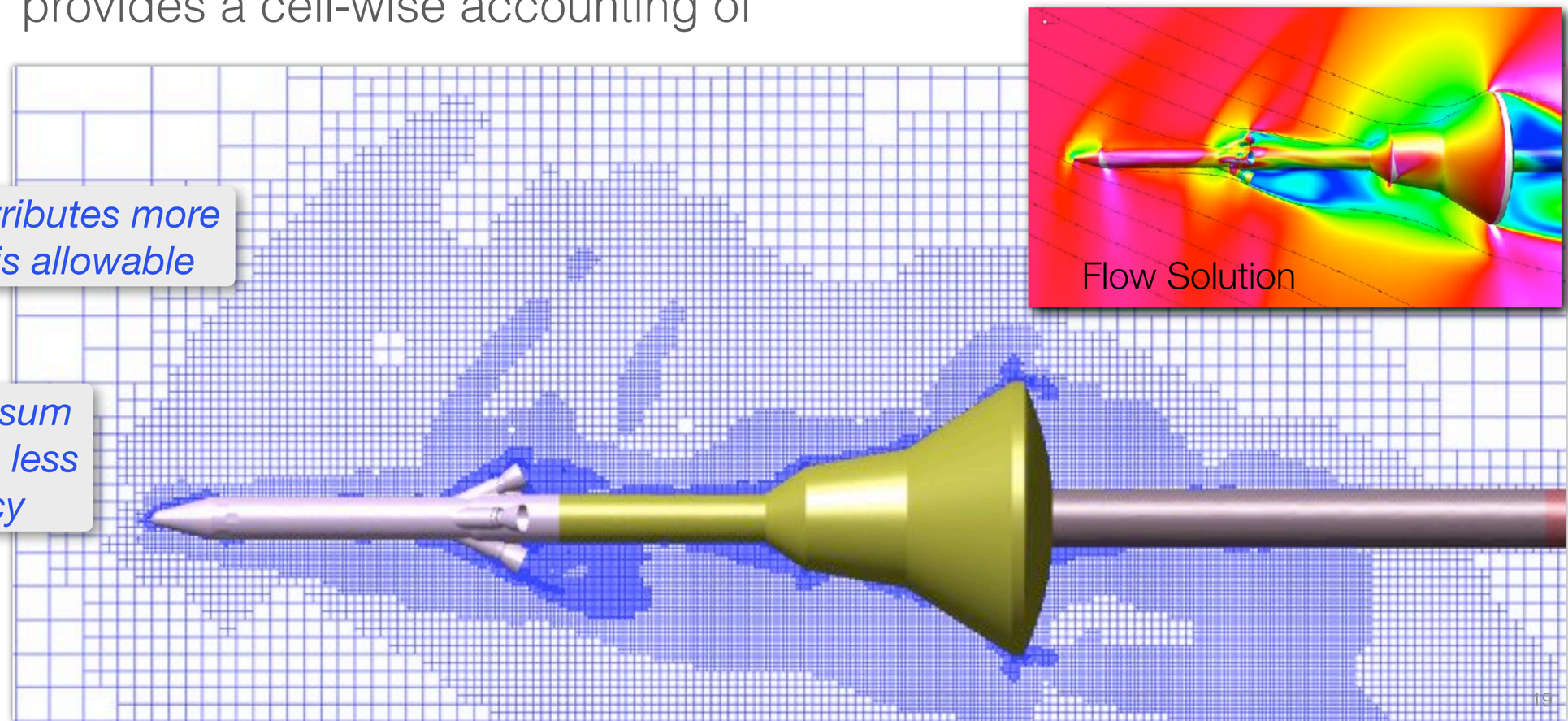
Adjoint Correction

Remaining Error

"Remaining-error" provides a cell-wise accounting of mesh deficiency

Adapt any cell that contributes more to the functional than is allowable

Stop refining when the sum of the cell-wise errors is less than desired accuracy



Simulation Example

Computational Challenge: Euler Solution for Ellipses

Thomas H. Pulliam*
NASA Ames Research Center, Moffett Field, California

Abstract

THIS paper presents a difficult flow problem for the numerical solution of the Euler equations: the inviscid flow past an ellipse. The basic result obtained here is a lifting solution for any combination of grid and/or angle of attack which is nonsymmetric. The purpose of this paper is to present this flow as a challenge to the computational fluid dynamics community, where the hope is that someone can explain this unusual behavior.

I. Introduction

The purpose of this paper is to introduce a flow problem for the Euler equations that should be relatively simple to solve numerically, but turns out to be very difficult. The problem is inviscid subcritical flow past an elliptical two-dimensional surface at angle of attack. In particular, a 6:1 ellipse at $M_\infty = 0.2$, $\alpha = 5$ deg is considered, where conventional finite-difference or finite-volume schemes are employed. Assuming initial and boundary conditions which are irrotational and contain no circulation, one would expect that the inviscid flow at any angle of attack would remain irrotational, and not generate any circulation. In practice, every numerical solution obtained to date by this author and many others has produced results with nonzero lift. The results obtained are very sensitive to algorithm parameters, mesh definition, and algorithm type. Even on the same mesh, various codes produce a wide scatter of lift values all of which are nonzero. It can be shown, however, that the solutions obtained are equivalent to potential flow past an ellipse with added circulation defined by the lifting numerical solution. This suggests that the numerical solutions obtained are reasonable solutions to the Euler equations with some mechanism which sets the lift. The mechanism responsible for the circulation generation is not understood at this time, and this paper stands as a challenge for other researchers to define the mechanism or to produce numerical results which are nonlifting for this class of problems.

II. Potential and Euler Solutions

Theoretically, the inviscid irrotational flow (i.e., potential flow) past an ellipse or cylinder is unique up to specification of the circulation or equivalently, the location of the stagnation points on the body. By setting the circulation or stagnation point locations, a one-parameter family of flowfield solutions can be obtained.

Two exact potential solutions are given below. In both cases, $M_\infty = 0.2$, $\alpha = 5$ deg and the solution is plotted on an "O" grid of 129×49 grid points. The ellipse has a major to minor axis ratio of 6:1. Figure 1 shows pressure contours and coefficient of pressure for a nonlifting case ($C_l = 0.0$) and for a lifting case ($C_l = 1.545$), which will be a useful choice in the later discussions. In the case of no lift, as one would expect, stagnation occurs at the front below the leading edge and at the rear antisymmetrically at the top. In the lifting case, stagnation occurs below the leading edge at the front and below the trailing edge at back; see Fig. 1.

This is all straightforward and can be found in any reference on potential flow, e.g., Ref. 1. The question that will be posed here is: What is the Euler solution to this problem? In particular, what is the numerical Euler solution, since a closed-form solution to the nonlinear equations is unknown?

Any procedure is affected by errors such as truncation, added terms (artificial dissipation), insufficient mesh resolution, and approximations in boundary conditions. As a computational experiment, the numerical solution on the preceding mesh was obtained using the Euler code, ARC2D.[2] Details of the various numerical experiments applied to this problem are presented in the original AIAA paper[3] and (due to space limitations) will not be repeated here.

The computations were performed at the preceding conditions. All residuals were driven to machine zero to assure stability of the converged solution. The basic numerical algorithm employs central differencing with added artificial dissipation, $\kappa^{(4)}$. The artificial dissipation coefficients were chosen at their nominal values for the results shown in Fig. 2. Pressure contours and coefficient of pressure are shown in Figs. 2a and 2b for this case. The contour levels for pressure were chosen to be the same for all plots presented here.

The converged value of lift coefficient for this case is $C_l = 1.545$, which corresponds to the lifting potential solution (Fig. 1). In fact, the two solutions are almost identical. The convergence history for the preceding case is shown in Figs. 2c and 2d. This is a very curious result; the initial solution has no circulation associated with it and the final solution, one would have assumed, should have zero lift. A nonlifting result can be obtained only if the oncoming flow is directly aligned with the grid line of upper and lower symmetry. In general, whenever the flow is not exactly aligned with a mesh line of symmetry, a lifting result is obtained.

It is remarkable that the numerical solution and the potential solution at the same lift compare so well. This implies that the numerical solution is a solution to the Euler equations (since potential solutions also satisfy the Euler equations for cases where there are no shocks). The question now posed is: What causes the resulting circulation and what determines the final value of lift? Various numerical experiments show that many different final solutions can be obtained for the same physical problem, either by changing some of the algorithm parameters, the grid, or the differencing scheme. In all cases, some converged, very stable solution is obtained and there is no explanation of the mechanism which produces the final results.

Sensitivity to initial conditions can be one indication of nonuniqueness. For the preceding solution, various initial conditions were used ranging from an impulsive start from freestream flow to using the potential solution as initial conditions. The numerical time integration was also extensively modified, where time accurate and non-time accurate paths were taken to convergence. In all tests, for a given mesh, M_∞, α, and $\kappa^{(4)}$, the final steady-state result was the same as the preceding; i.e., $C_l = 1.545$.

Some of the numerical parameters which may influence the results include mesh definition, distribution, and refinement.

Received March 1, 1989; Synoptic received Oct. 10, 1989. Full paper available from National Technical Information Service, Springfield, VA 22151, at the standard price (available upon request). Copyright © 1989 by the American Institute of Aeronautics and Astronautics, Inc. No copyright is asserted in the United States under Title 17, U.S. Code. The U.S. Government has a royalty-free license to exercise all rights under the copyright claimed herein for Governmental purposes. All other rights are reserved by the copyright owner.

*Section Head, Computational Fluids Division, Computational Fluid Dynamics Branch. Member AIAA.

*Pulliam, AIAA J., **28**(10) 1990*

Simulation Example

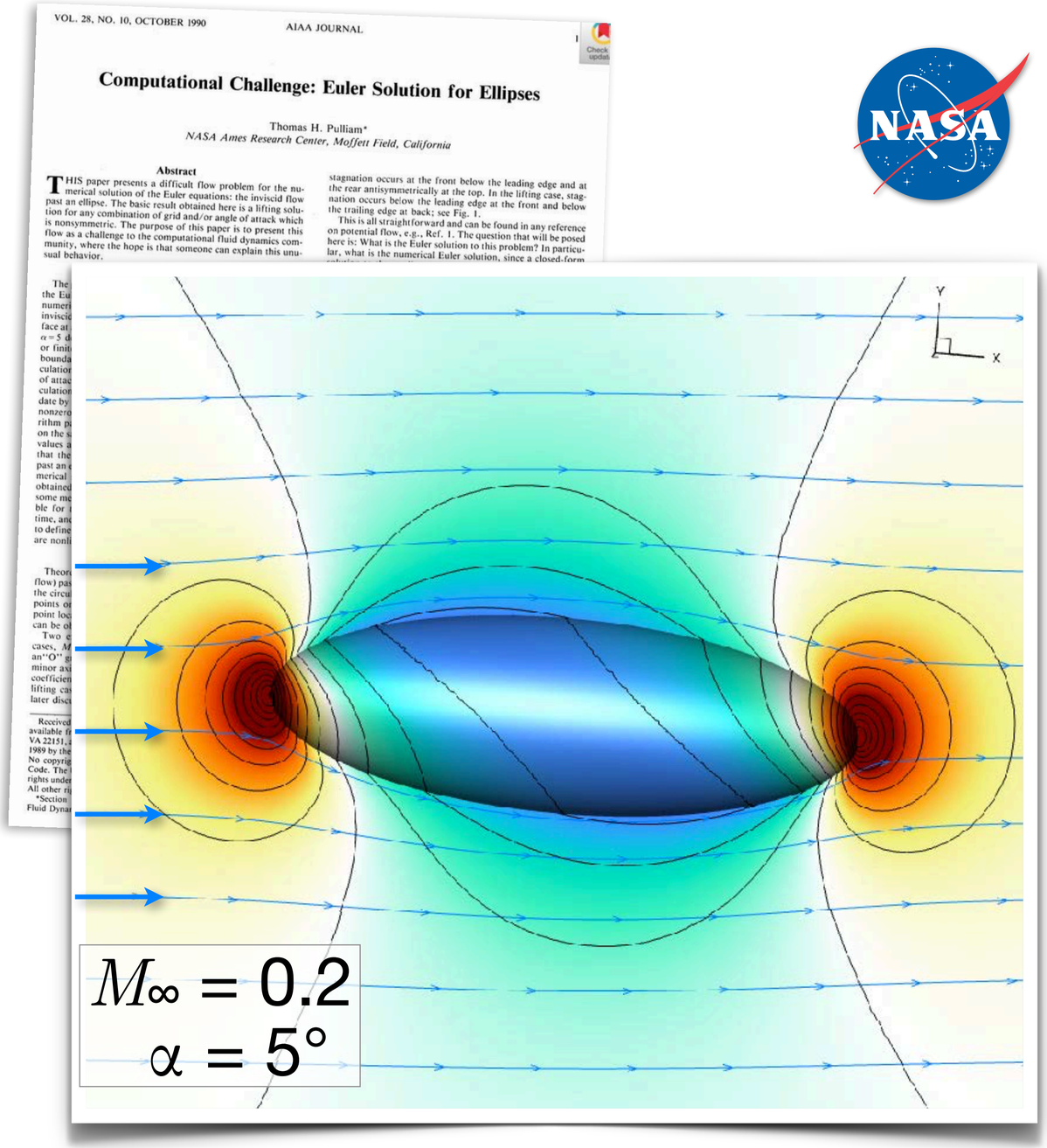
Subcritical ellipsoid w/ exact solution

Inviscid flow over 3D ellipsoid

- 3D version of Pulliam's "Computational Challenge" of 1990†
- Subcritical flow over ellipsoid at angle of attack
- Theoretical results are $C_L = C_D = 0$

Simulation

- $M_\infty = 0.2$, AoA = 5°
- Adapt mesh to minimize error in functional $J = C_L + C_D$
- Since $J_{Exact} = 0$ know exact error on any mesh
- Any $J_H \neq 0$ is identically error in the discrete solution
- Can directly quantify discretization error in lift & drag

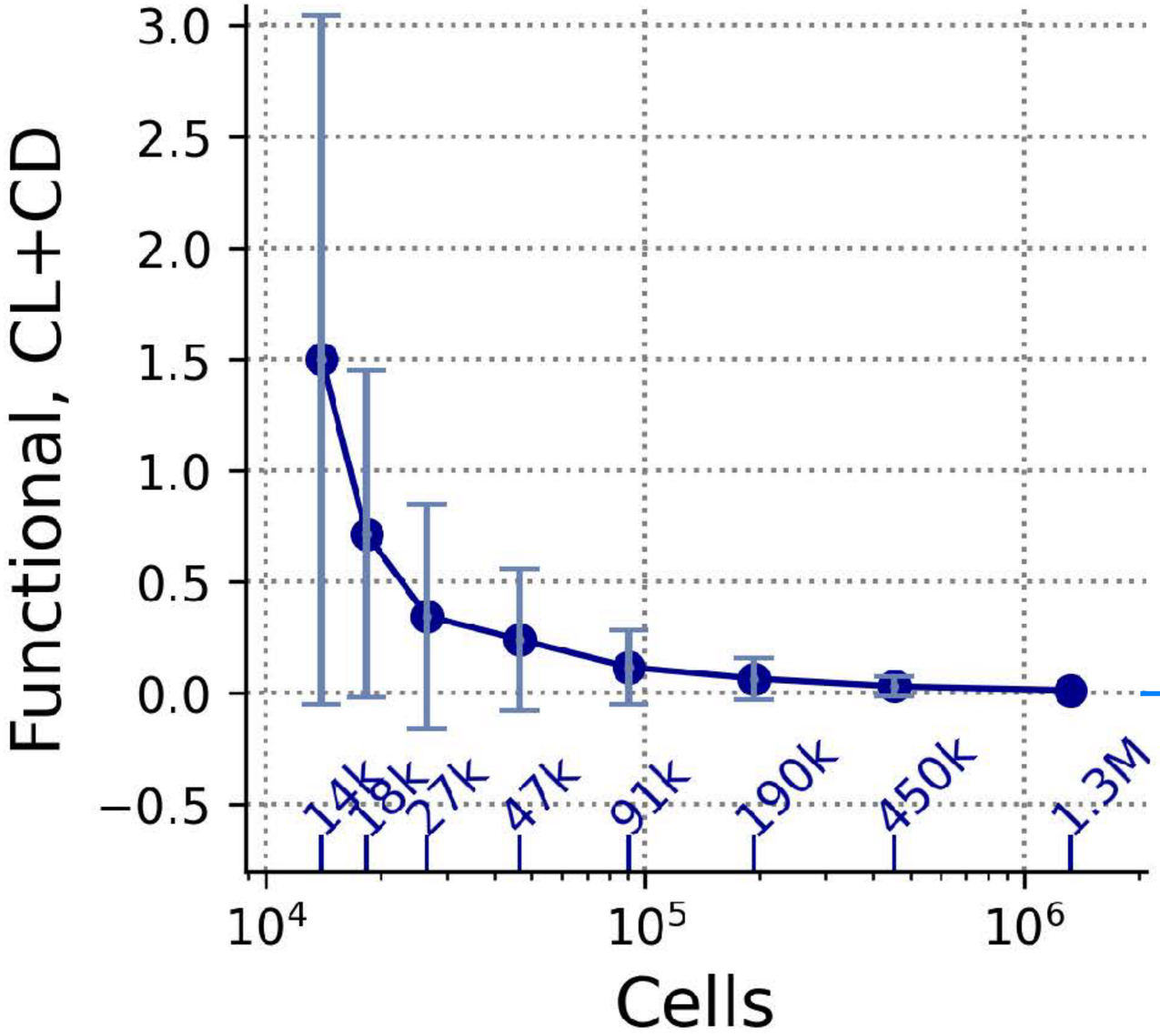


Adapt mesh to minimize error in $J = C_L + C_D$

† *Pulliam, "Computational Challenge: Euler Solution for Ellipses" AIAA J., **28**(10) 1990*

Subcritical ellipsoid

Mesh convergence



- Every adaptive case automatically generates a plot of mesh convergence of discrete functional, J_h
- Successive J_h monotonically and asymptotically approach J_{Exact}
- Adjoint based error estimate shown with error bars

Observations

- Functional value is identically discretization error
- Error bars on J_h are credible when they encompass the exact solution for all finer meshes & are tightening at a constant rate

$J_{Exact} = 0$

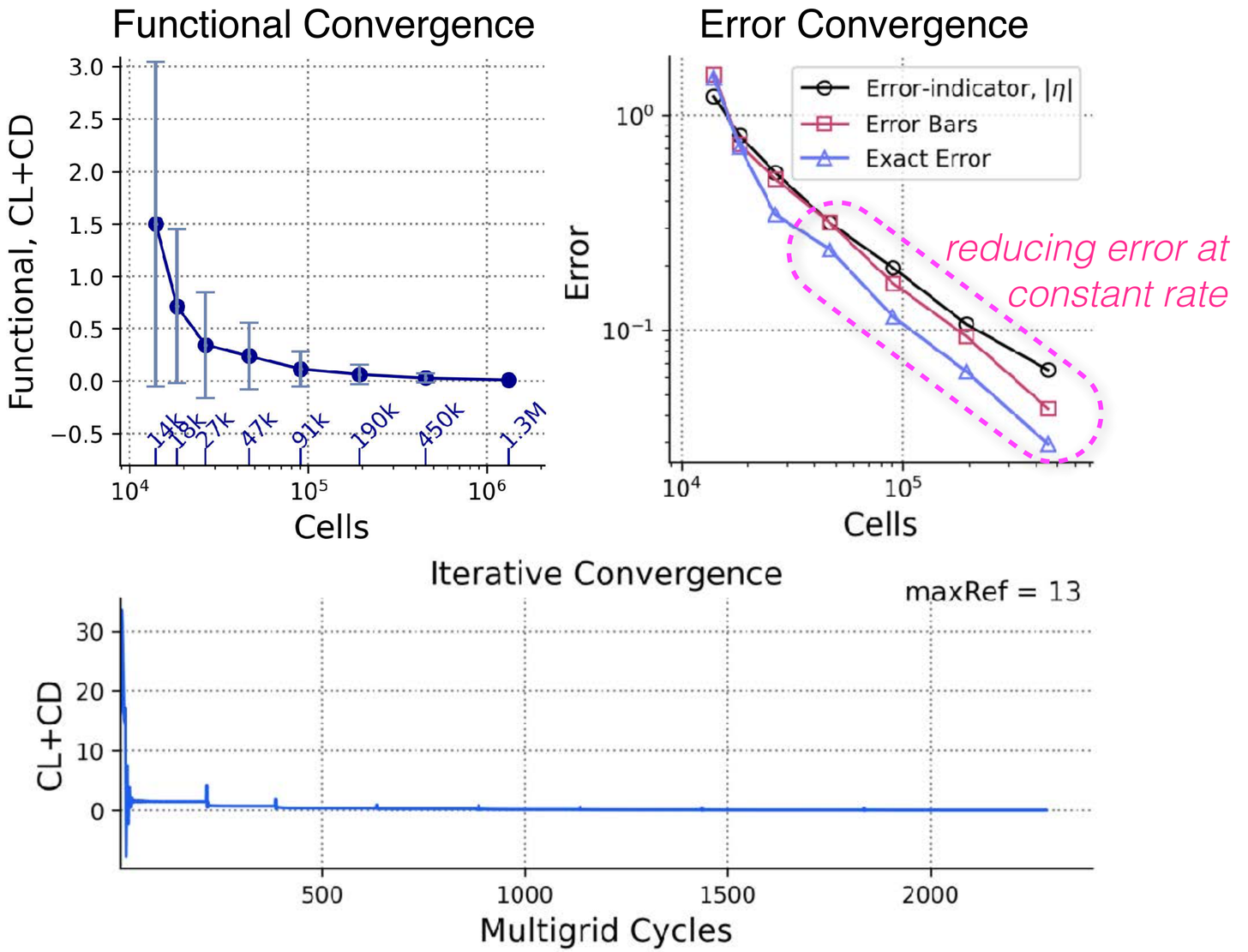
Subcritical ellipsoid

Mesh convergence

- Mesh convergence plot can be auto-matically produced for any adaptive solution
- Directly shows elimination of discretization error (mesh convergence)
- In this case, since $J_{Exact} = 0$, J_h is also the exact error
- Linear convergence of error (on log-log paper), shows error is being reduced at a constant rate
- Note that the adjoint correction also gives an accurate (and conservative) estimate of the exact error

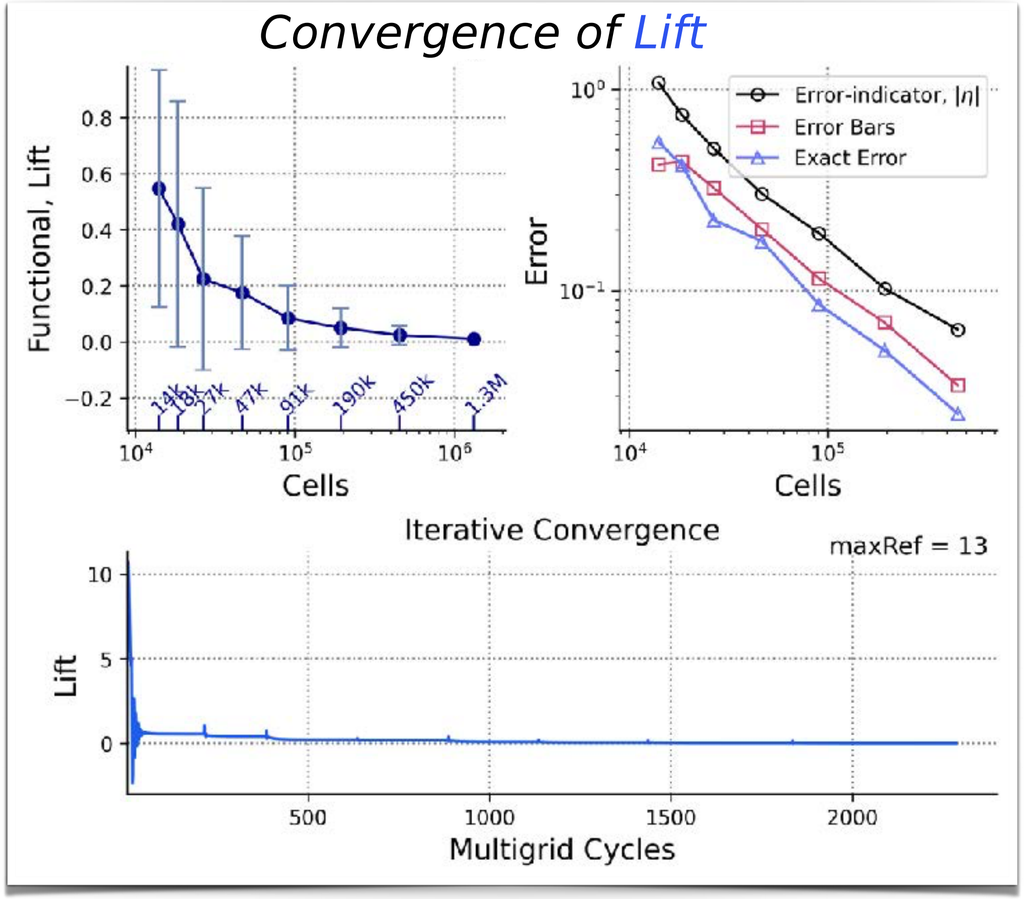
With 7 adapt cycles, Cart3D v1.6.0 took ~4 mins on 2022 laptop, takes ~75 s on a current linux workstation

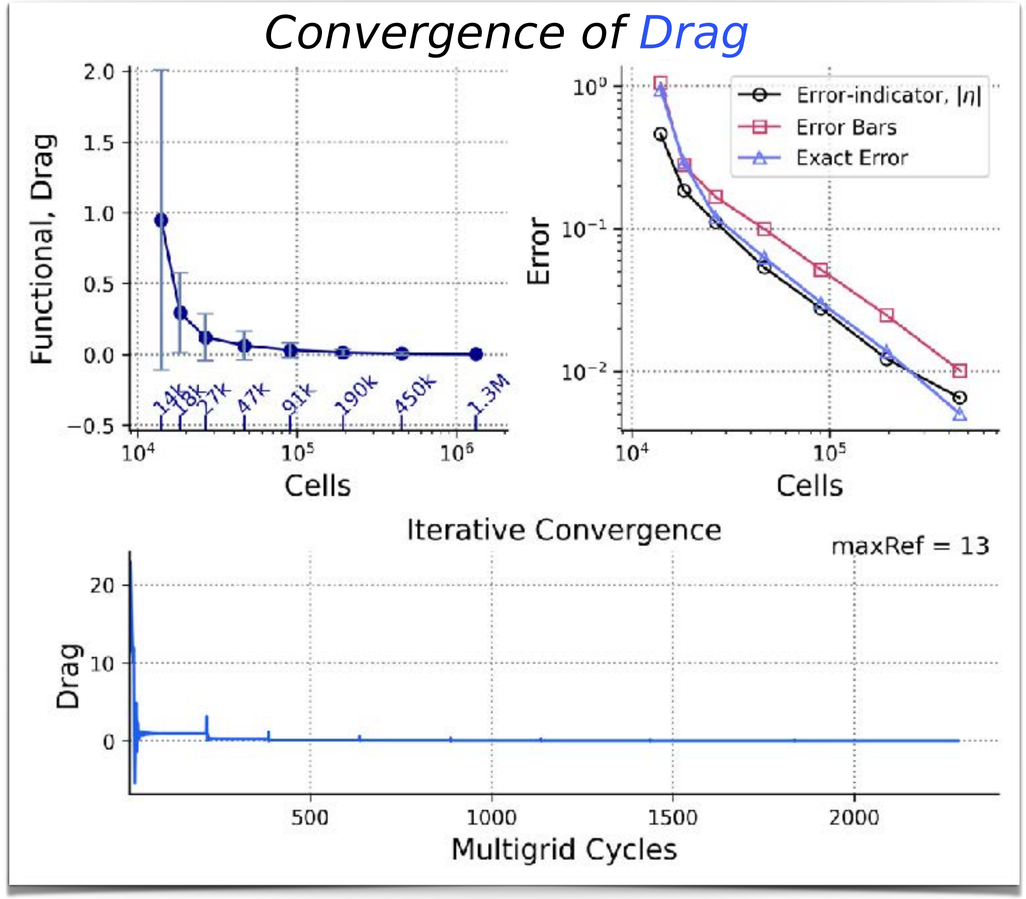
Mesh convergence



Subcritical ellipsoid

Mesh convergence

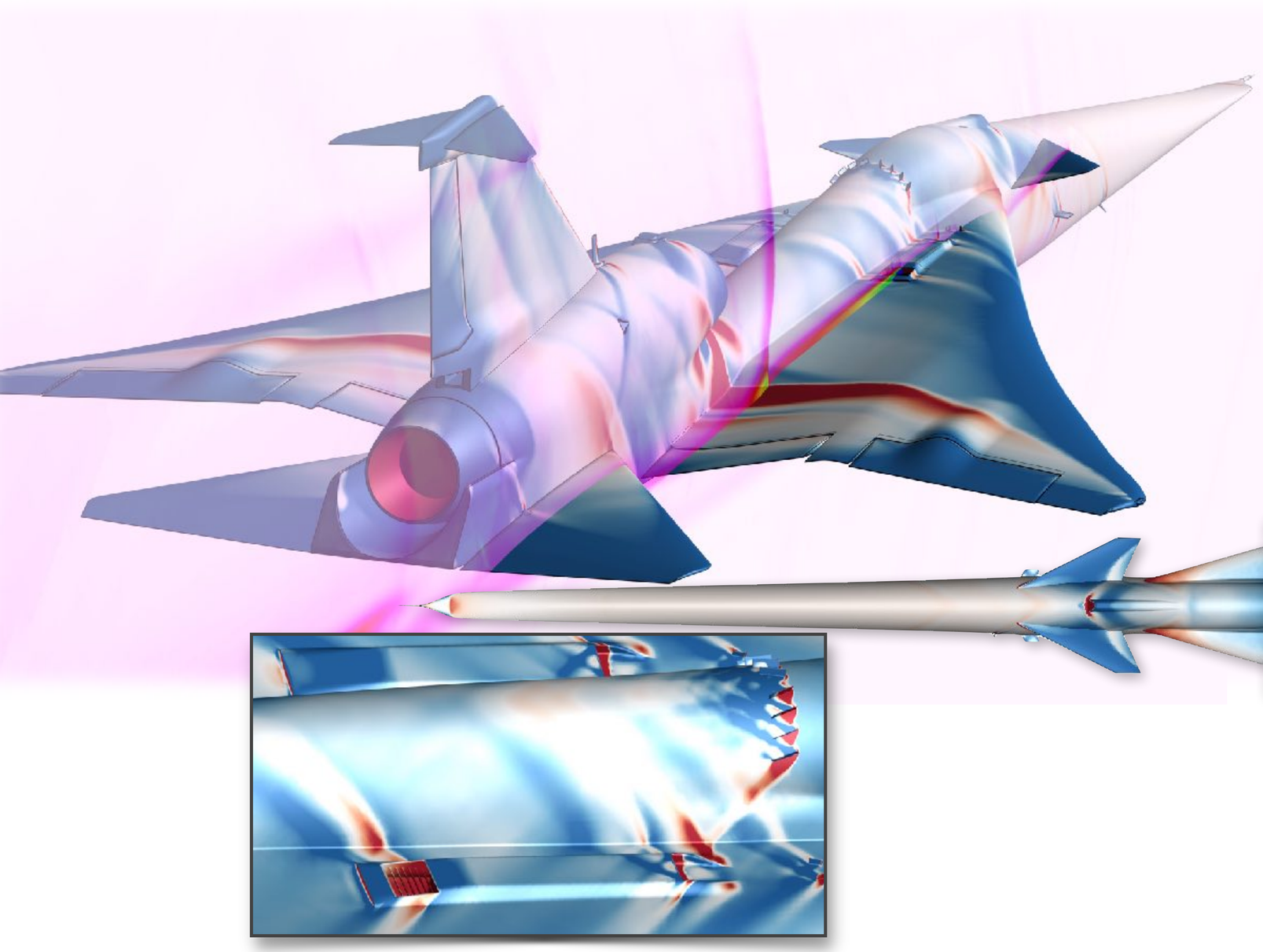


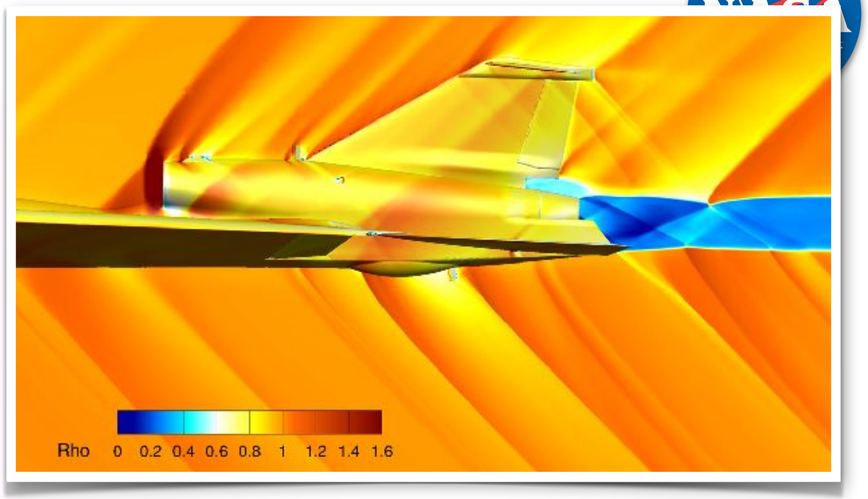


- Can solve additional adjoints to estimate error in additional functionals
- Can independently monitor convergence of C_L and C_D
- Error bars are conservative, convergence of both is asymptotic after about 20k cells

Simulation example:

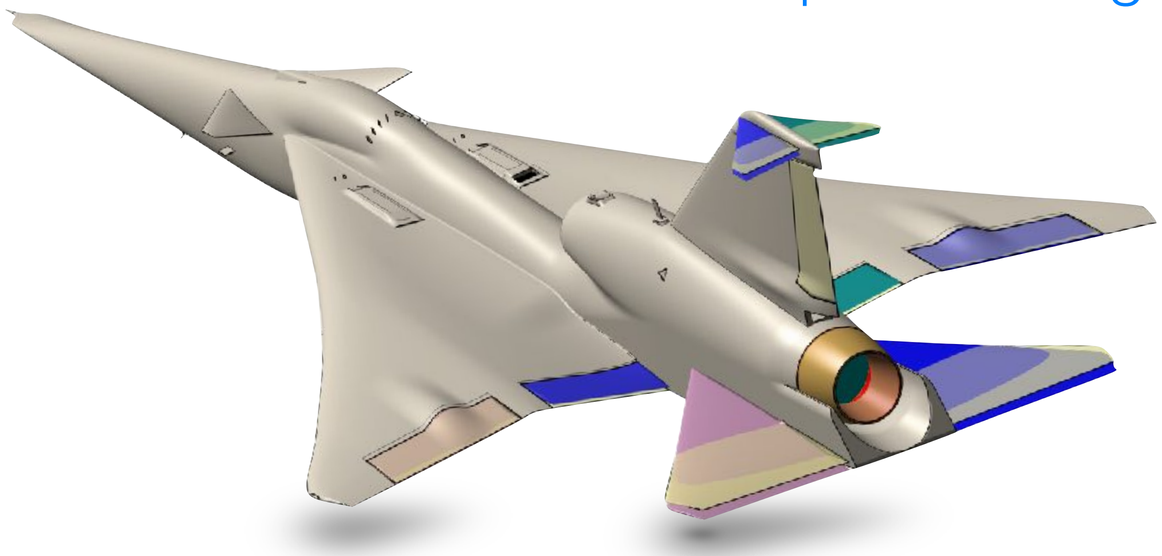
Powered X-59 at supersonic cruise

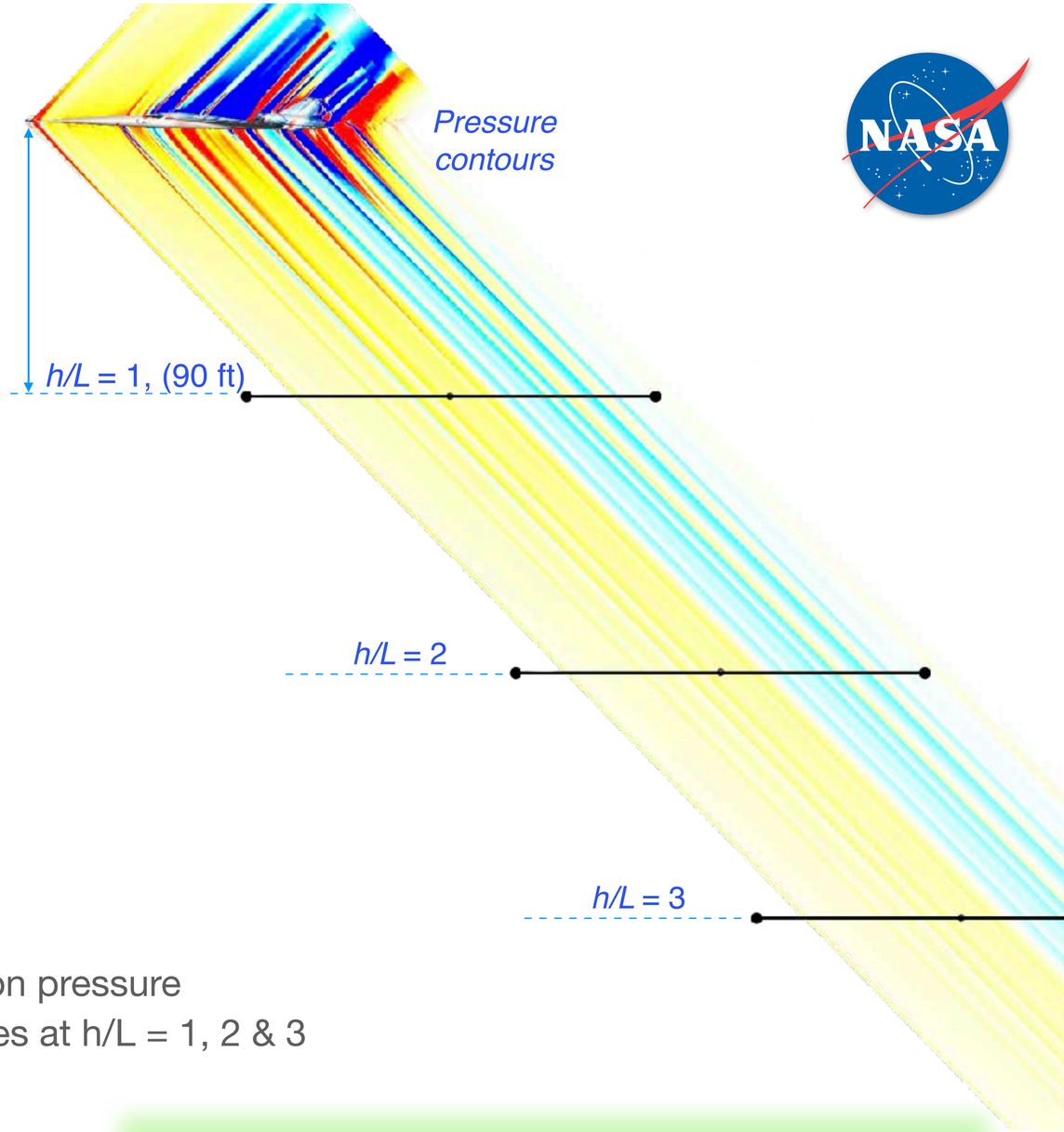




Powered X-59

Minimize error in on-track pressure signature





Realistic model of X-59 at Mach 1.4, Alt. ~53 kft

- Many length scales, small probes, complex small ducts
- 6 independently articulated control surfaces & 11 Power BC's

Output of interest

- Pressure signatures ($\Delta p/p_\infty$) at h/L = 1, 2 & 3
- Need ~0.1Pa accuracy 270ft below aircraft = ~5-6 digits of accuracy on pressure
- Adaptation functional is weighted sum of integrated pressure signatures at h/L = 1, 2 & 3

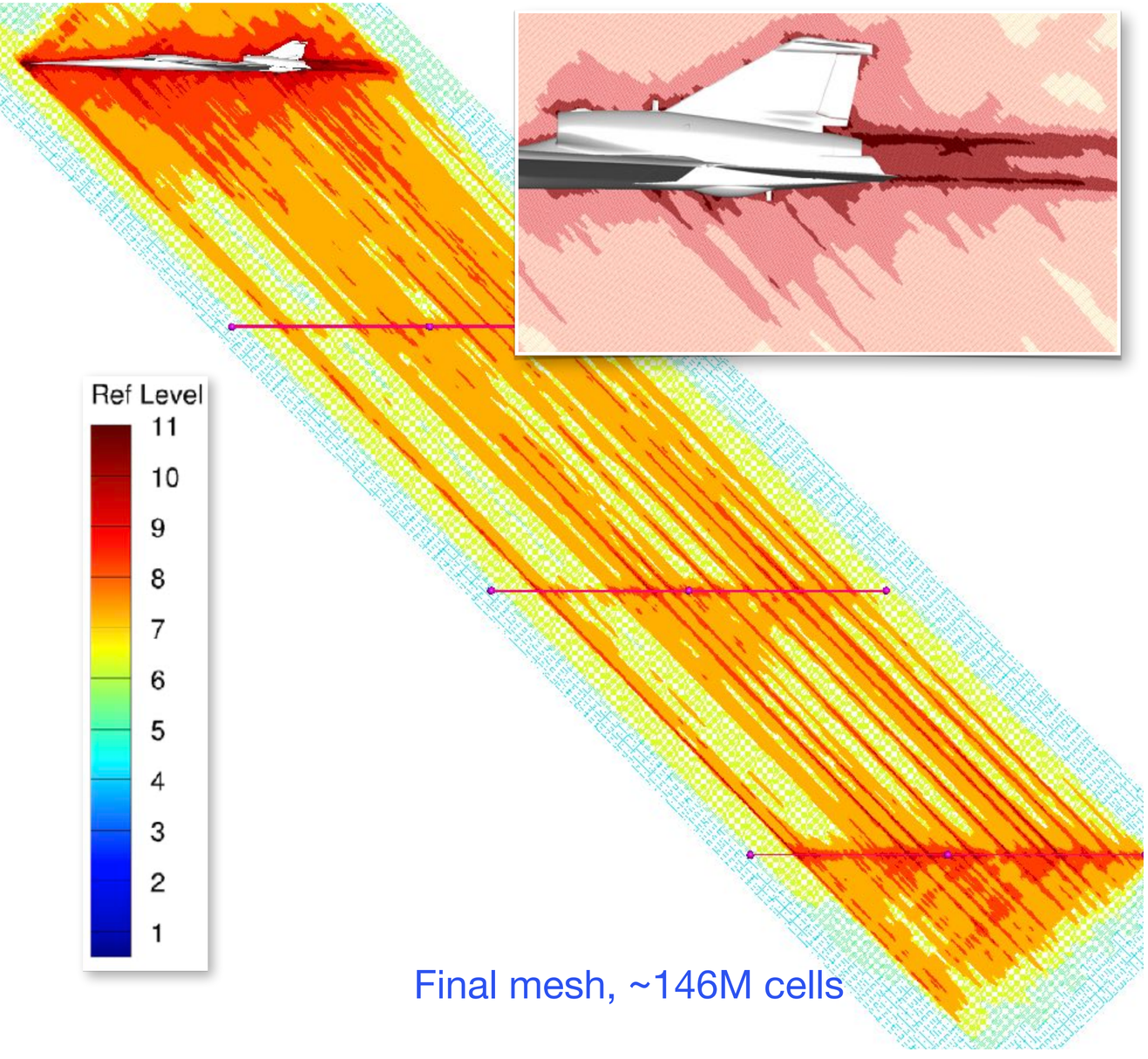
Features

- Complex geometry and simulation
- Very high accuracy requirements
- Solution is non-smooth, and gov. eqs. are non-homogeneous

Ideally suited for automated meshing & output-based mesh adaptation

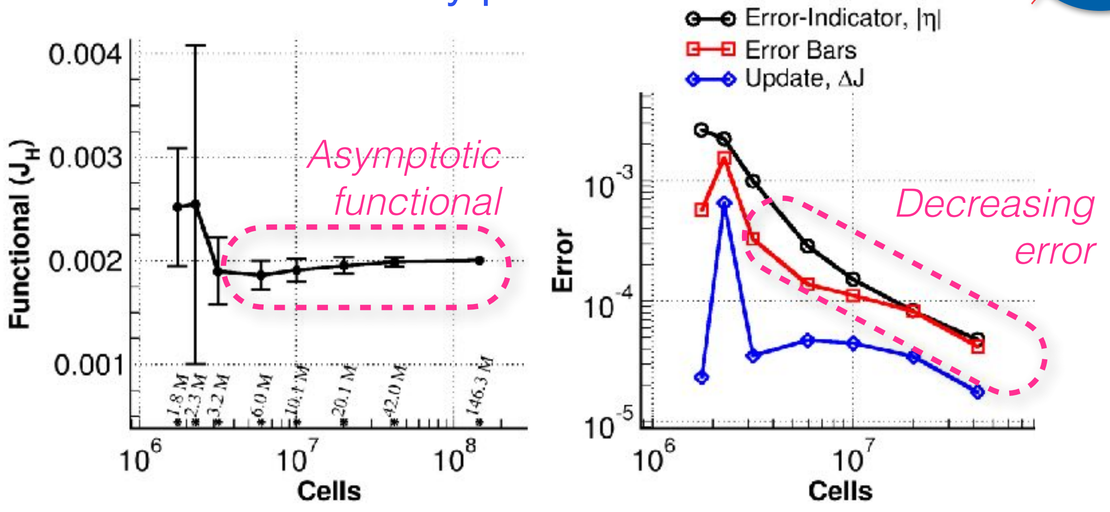
Powered X-59

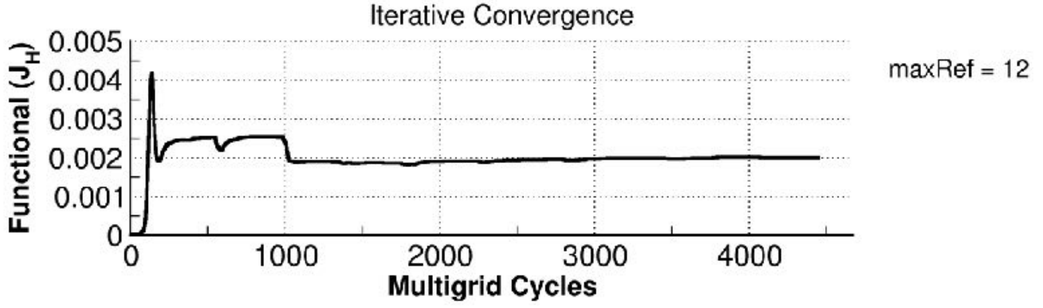
Mesh convergence of pressure functional



Final mesh, ~146M cells

Off-body pressure sensors



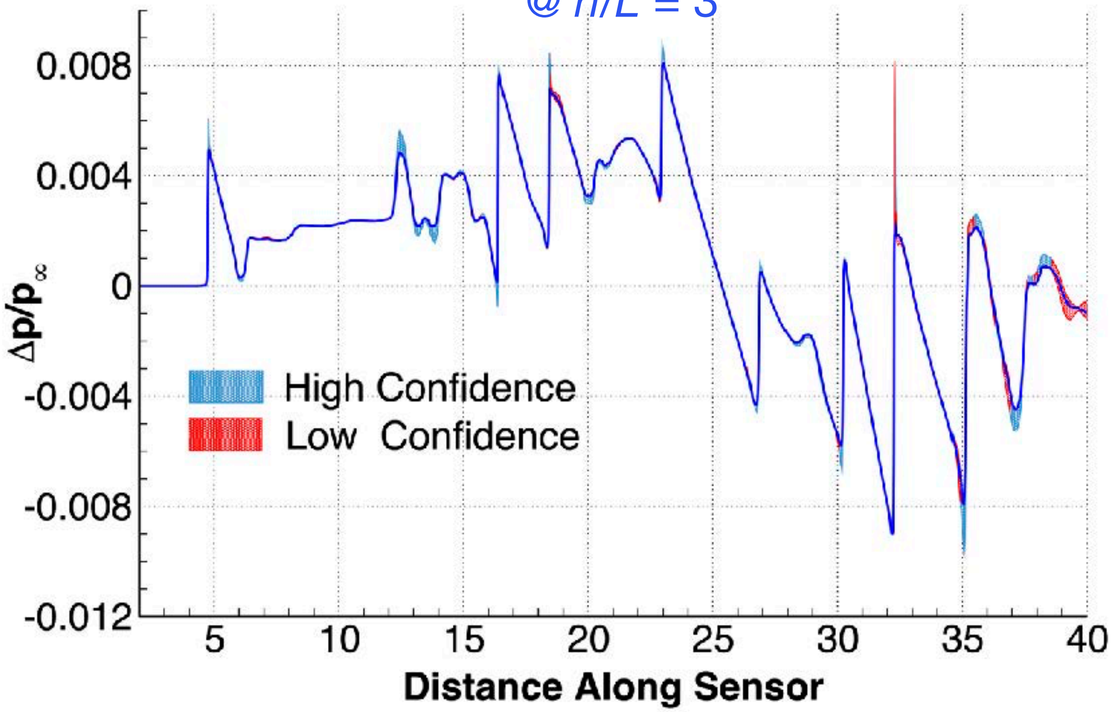


- Functional is converging asymptotically with credible error bounds
- Error decreasing at constant rate
- Essentially textbook behavior, despite real-world complexity

Powered X-59

Mesh convergence of pressure functional

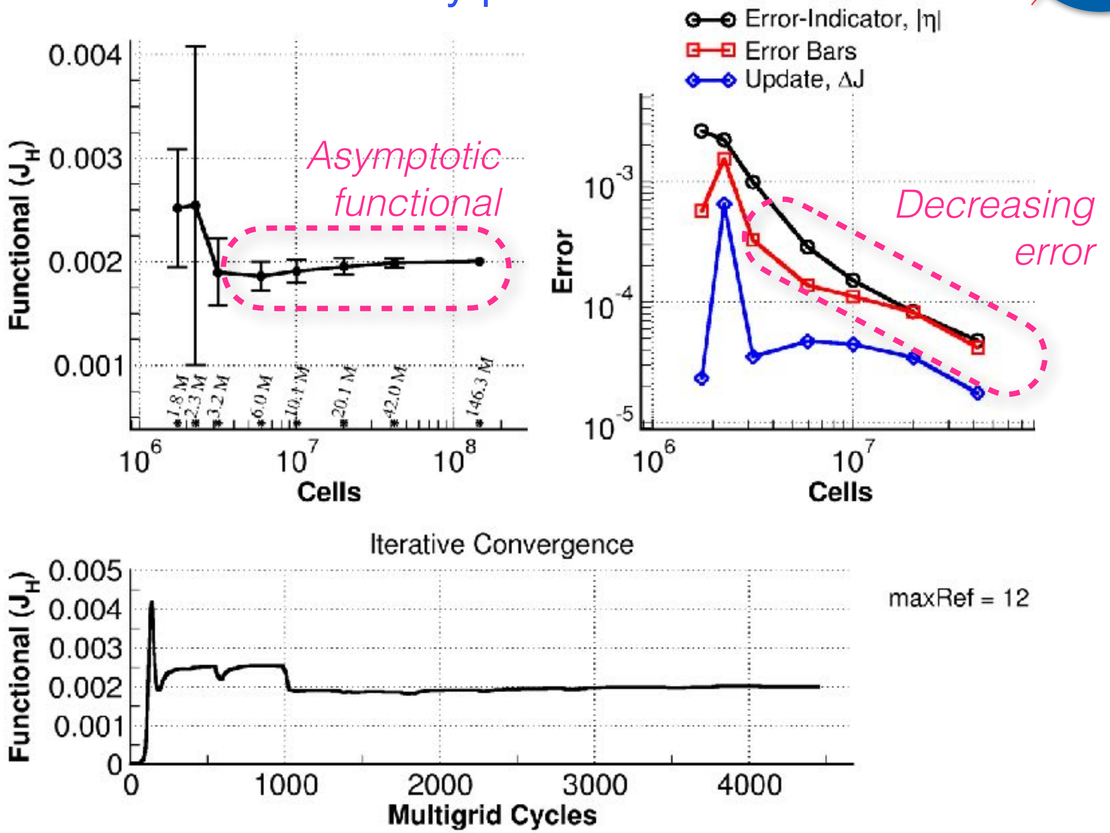
Pressure along sensor with localized error estimate, @ $h/L = 3$



- Mesh sequence also allows use of Richardson-extrapolation to localize discretization error along pressure sensor‡.

‡ *JoA* ***56****(3):1–16, 2018 (Anderson, Aftosmis & Nemec)*

Off-body pressure sensors



- Functional is converging asymptotically with credible error bounds
- Error decreasing at constant rate
- Essentially textbook behavior, despite real-world complexity and non-smooth solution

Outline

Cart3D Overview

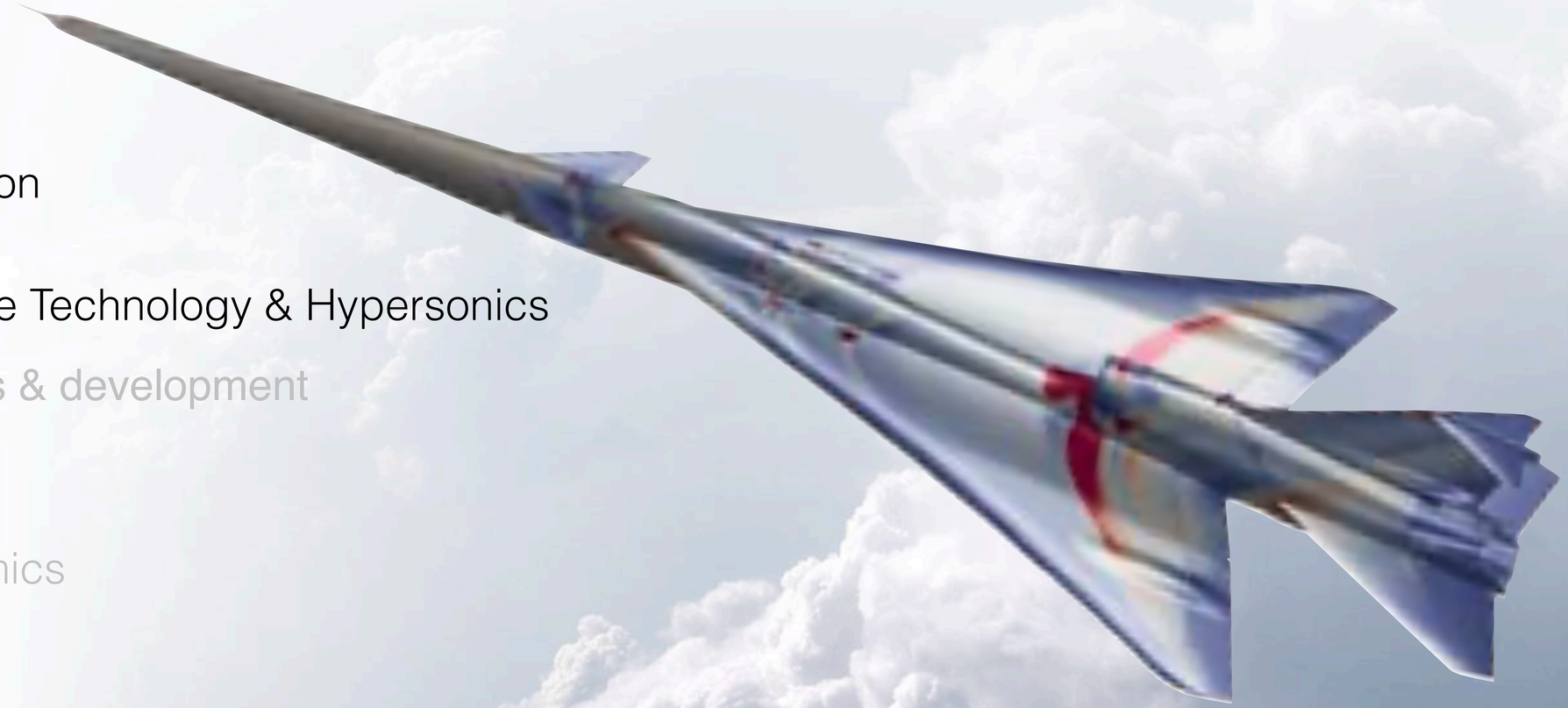
- Usage & application areas
- Current release
- Automation

Recent highlights

- Aeronautics Mission
- Science Mission
- Exploration, Space Technology & Hypersonics

Near term opportunities & development

- OpenMDAO
- Equilibrium Gas
- Aerothermodynamics



Recent Highlights

Cart3D development for mission support

Aeronautics Mission

- CST: Error control in coupled nearfield-farfield simulations (Cart3D + sBOOM)
- CST: Ground noise-based design for low boom
- CST & LBFD: X-59 nearfield “dry runs”, flight test support and point-cloud sensors
- CST: Coupling with LAVA Space Marching solver
- TTT: OpenMDAO support
- TTT: Strong solvers

Science Mission

- ATAP: Long distance blast propagation for asteroid entry
- MWG: Lead “hazards” element developing the National Near-Earth Object Preparedness Strategy and Action Plan
- Massively parallel unsteady mesh adaptation

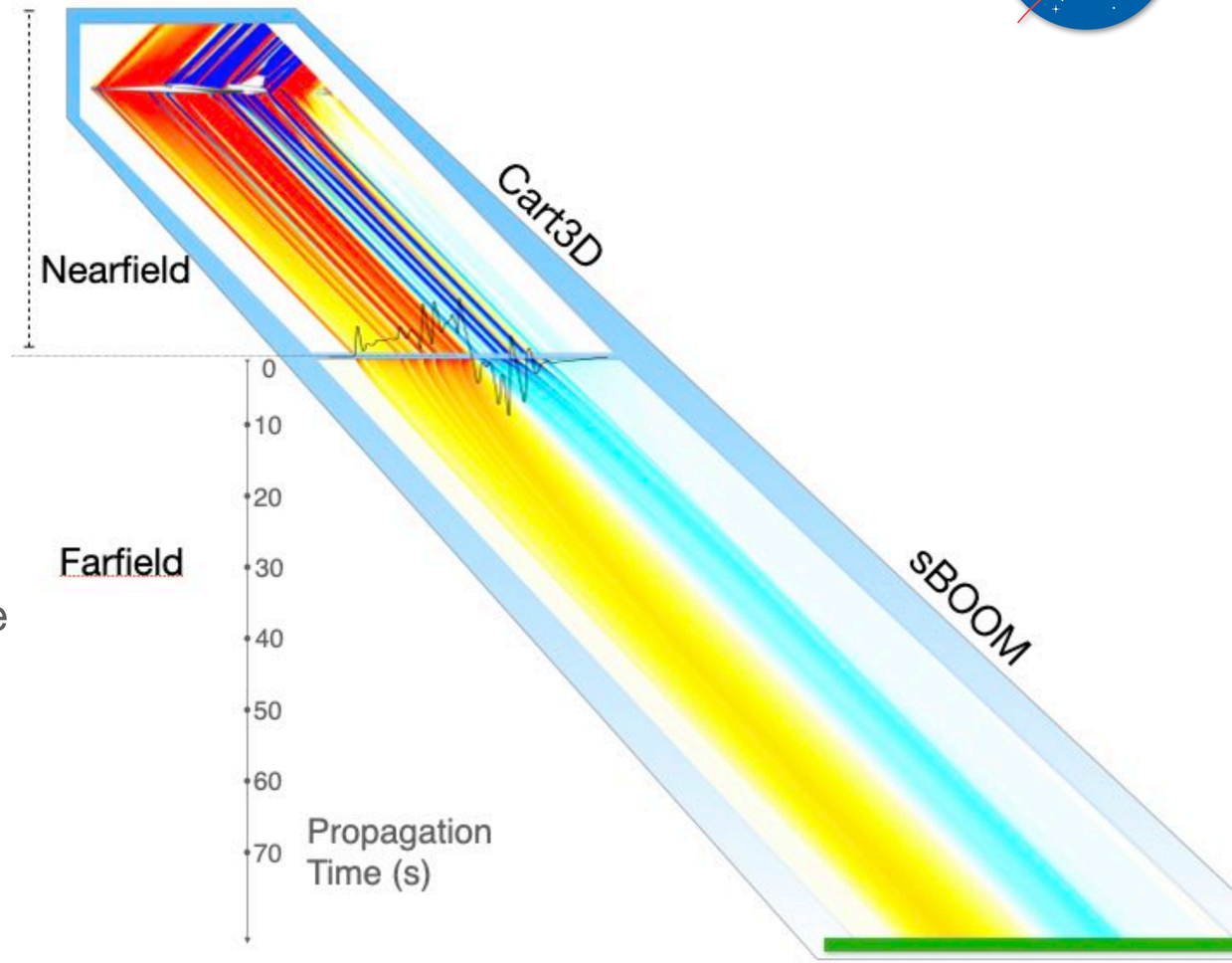
Exploration, Space Technology & Hypersonics

- Commercial launch vehicles and re/entry
- Coupled Cart3D-CBAero simulations for aerothermal outputs
- Functionals for hypersonics
- Updated equilibrium gas models for Earth and beyond

ARMD: Commercial Supersonics

Error control in coupled nearfield-farfield simulations (Cart3D + sBOOM)

- Combine adjoints of Cart3D and sBOOM to determine sensitivity of ground-noise functionals to the nearfield simulation. Multi-physics coupling enables:
  - Direct ground-noise based low-boom design
  - Ground-noise driven mesh adaptation
  - Quantitative prediction of error in ground noise metrics
- Coupling of nearfield and atmospheric solvers:
  - *AIAA 2022-4085 (Nemec, Aftosmis & Rallabhandi)*
- Improved accuracy of sBOOM adjoints, addressed these in 2024
  - *AIAA 2024-4669 (Rallabhandi, Nemec & Aftosmis)*
- Upgraded sBOOM and ground-noise outputs for Cart3D were released in 2024
  - Cart3D v1.6.0 & Cart3D Design v1.0
  - sBOOM v2.9.1

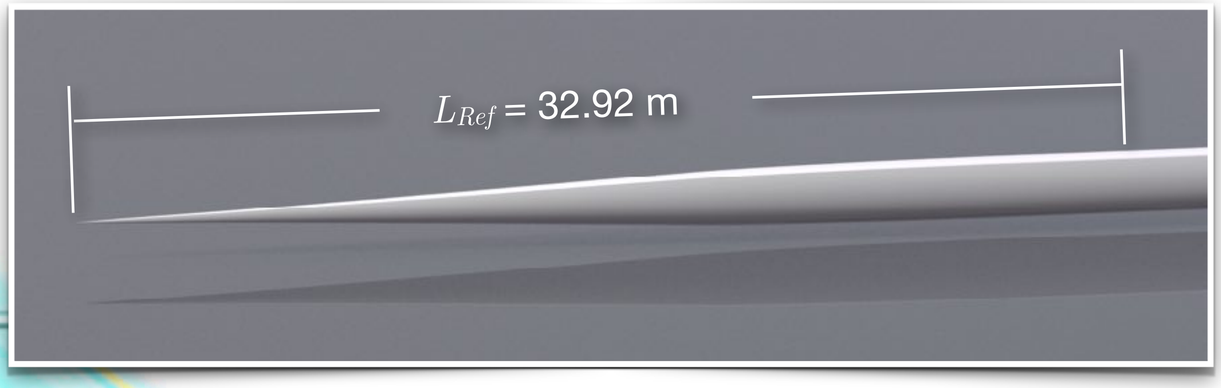


ARMD: Commercial Supersonics

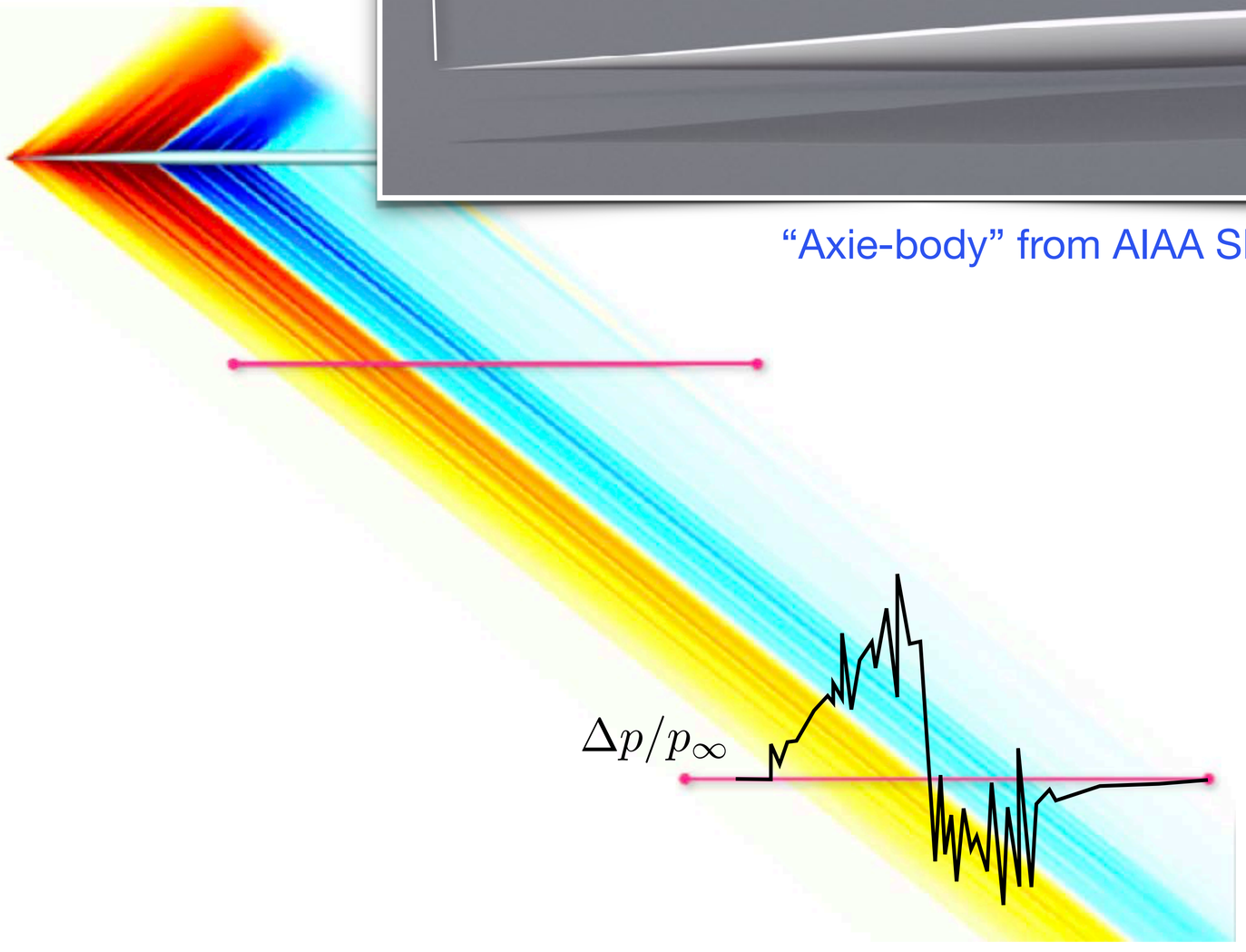
Ground-noise based mesh adaptation and error estimation

- Prior work on adaptive meshing for low-boom focused on minimizing the error in of nearfield pressure outputs

M_∞ = 1.6
L_{ref} = 32.92 m
h/L = 3
Alt. = 15.76 km



"Axie-body" from AIAA SBPW2

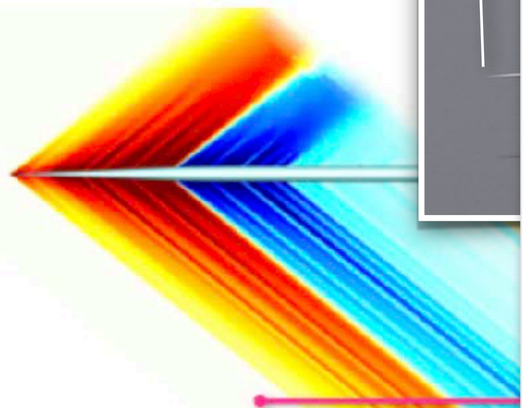


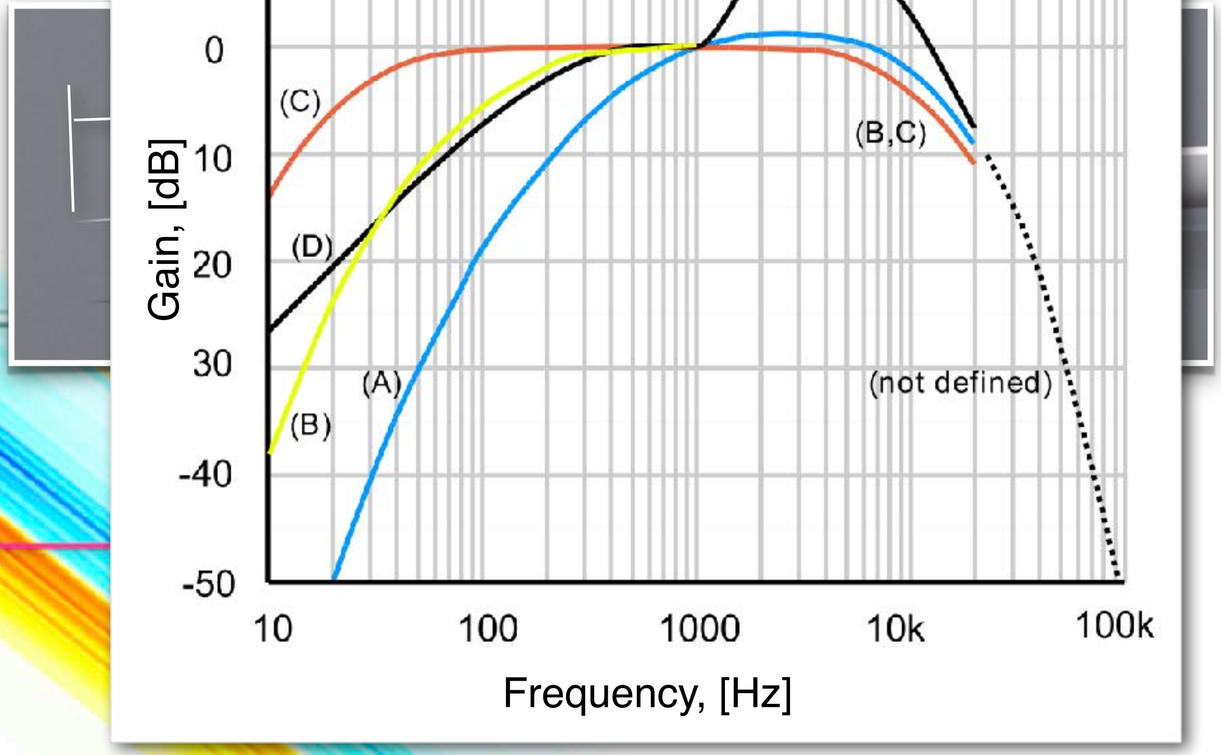
ARMD: Commercial Supersonics

Ground-noise based mesh adaptation and err

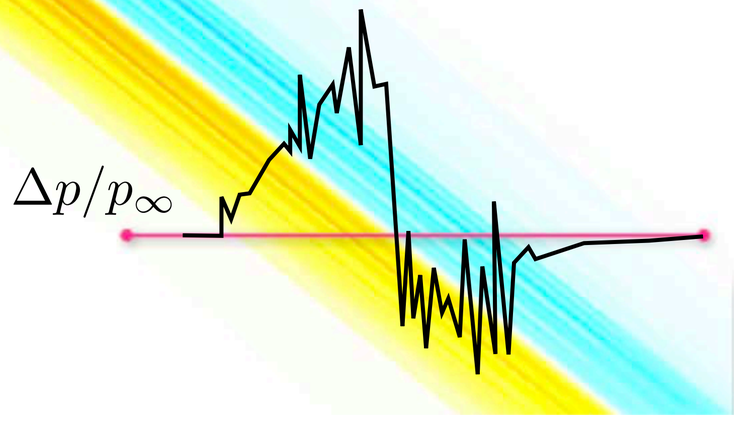
- Prior work on adaptive meshing for low-boom focused on minimizing the error in of nearfield pressure outputs

$M_\infty = 1.6$
$L_{ref} = 32.92$ m
$h/L = 3$
$\mathrm{Alt.} = 15.76$ km



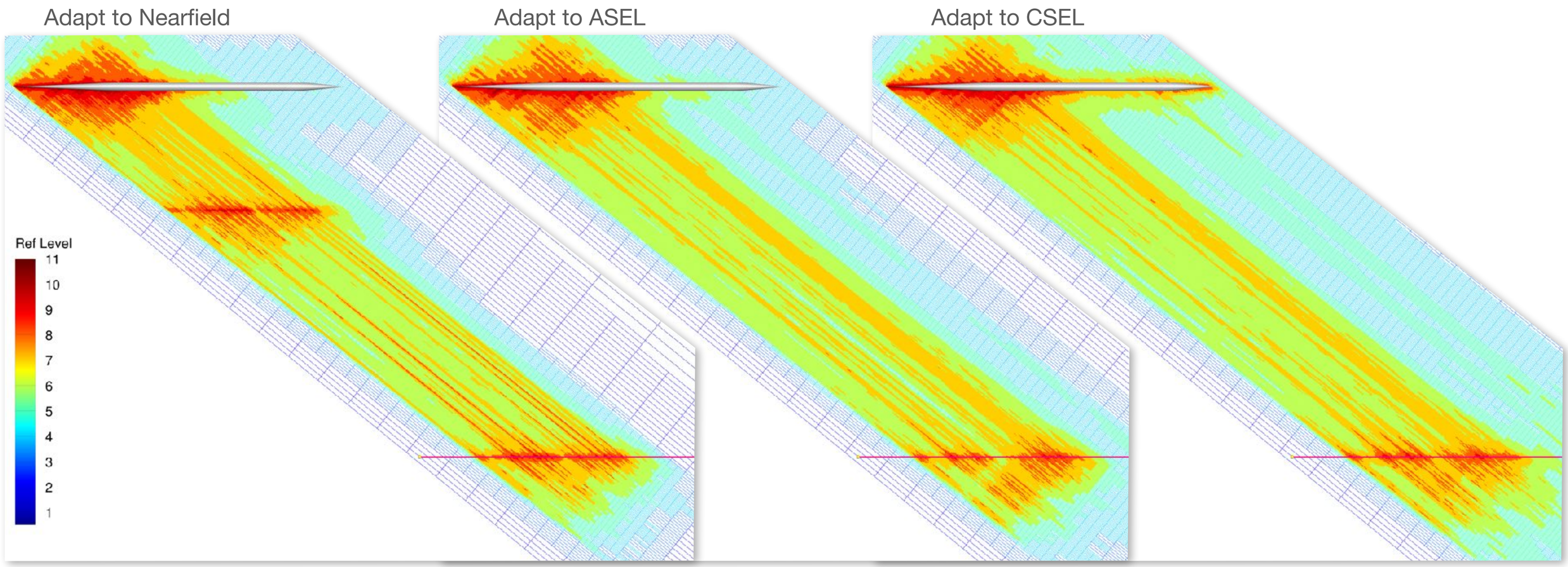


- *How effective is this at minimizing error in the ground pressure signal?*
- *How effective is it at minimizing error in the ground sound exposure level? (e.g. metrics like A/B/C-SEL)*
- *How accurate (in decibels) are computed values of the ground noise metrics?*



Ground-noise based mesh adaptation and error estimation

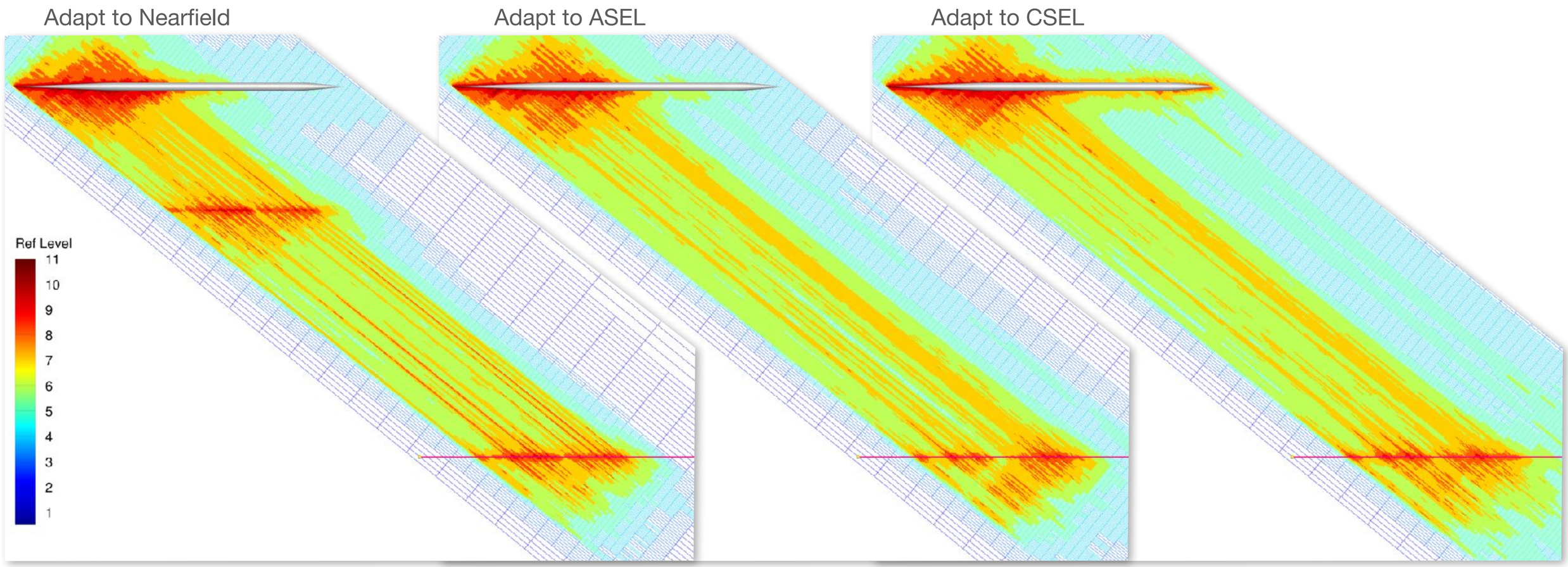
ARMD/CST



- Mesh adaptation to reduce error in nearfield signal or ground-based outputs (e.g. A-SEL or C-SEL)
- Can monitor the error in any other output. *e.g*. adapt to NF but estimate error in A-SEL

Ground-noise based mesh adaptation and error estimation

ARMD/CST

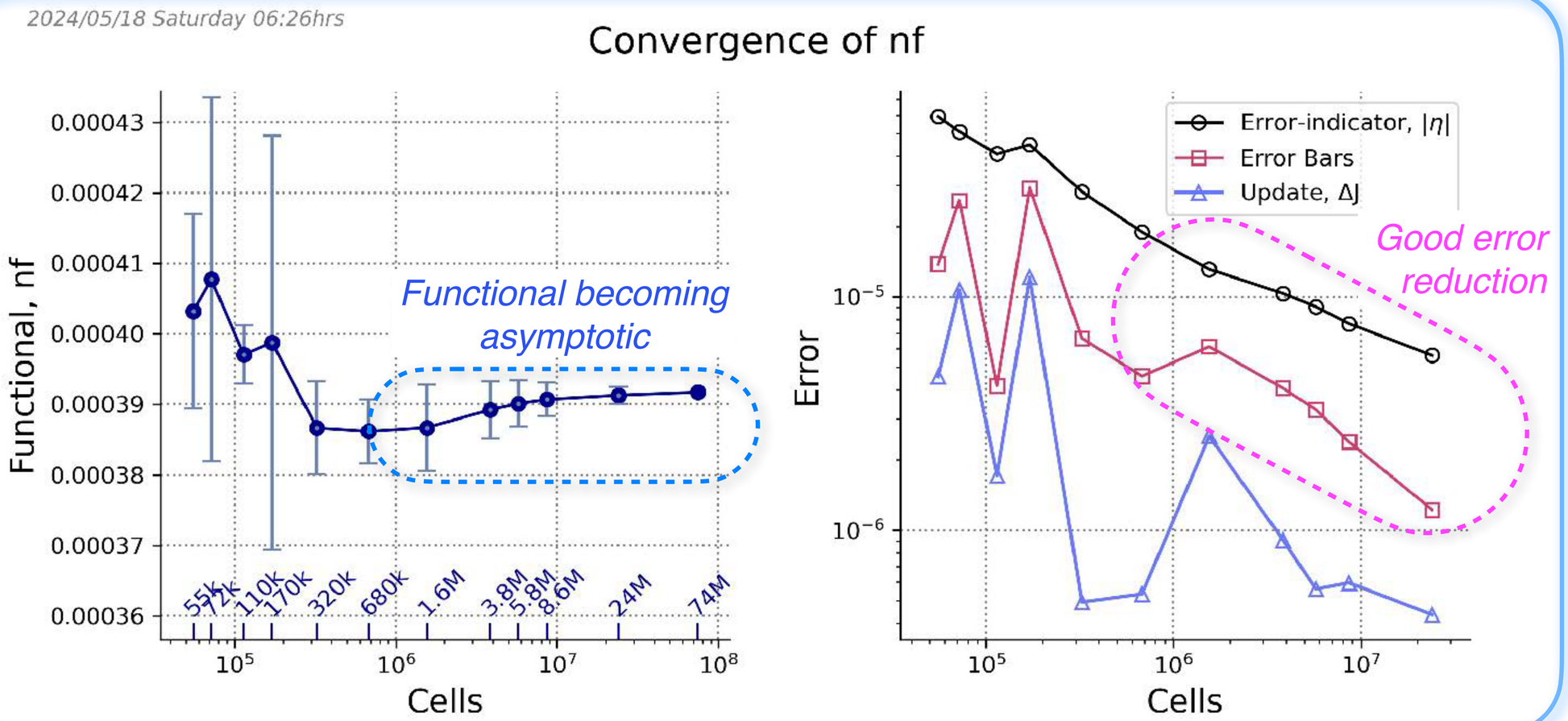


How good is adapting to signal at h/L = 3 at reducing error in A/B/CSEL ground noise?

Ground-noise based mesh adaptation and error estimation

ARMD/CST

Adapt to Nearfield

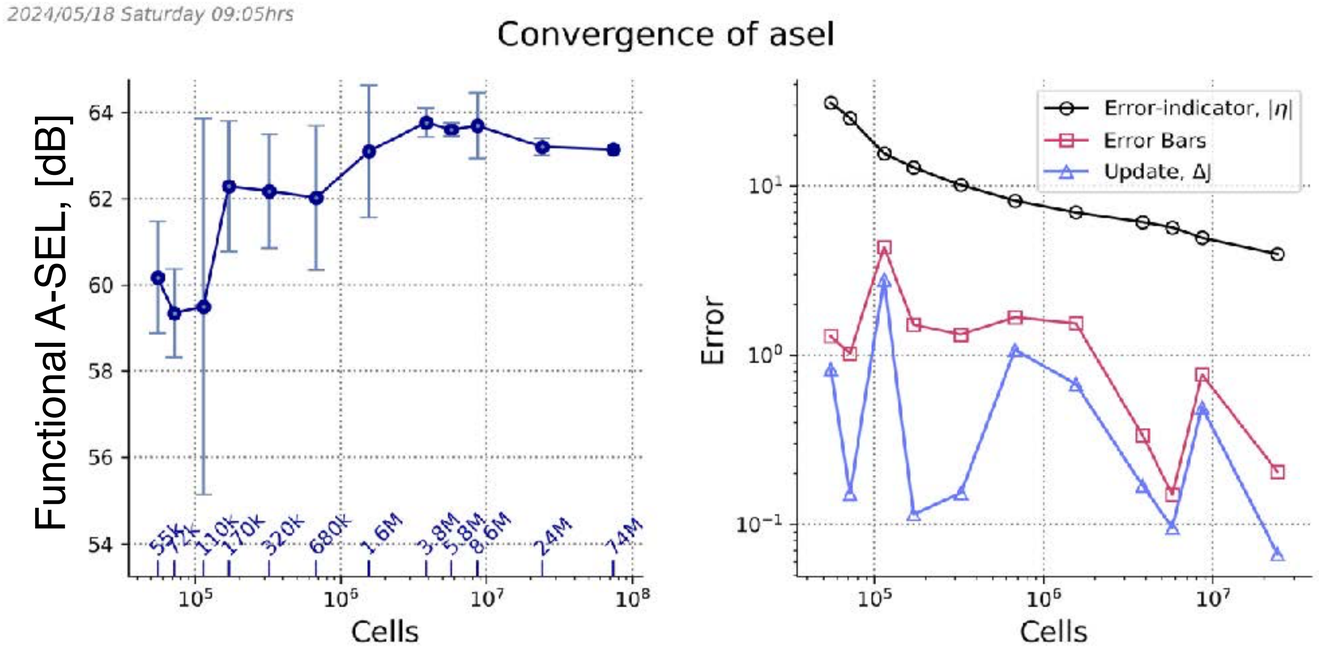


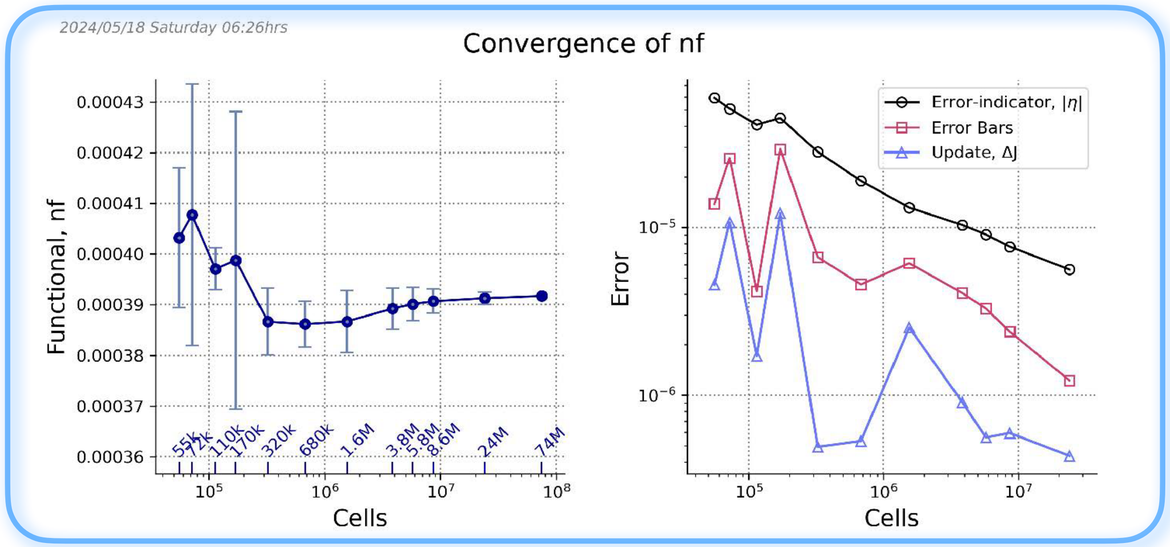
Objective Function

Ground-noise based mesh adaptation and error estimation

ARMD/CST

Adapt to Nearfield, *monitor error in ASEL, [dB]*



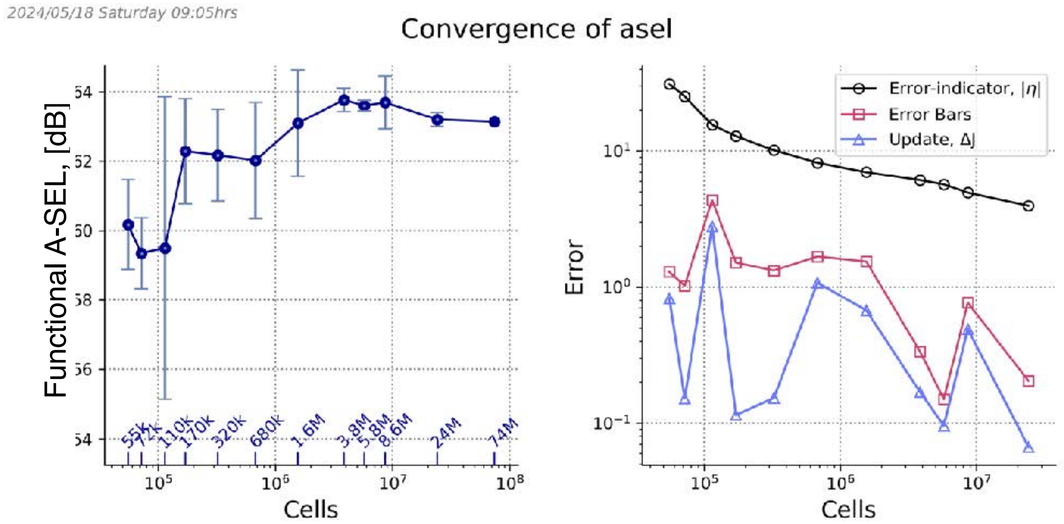


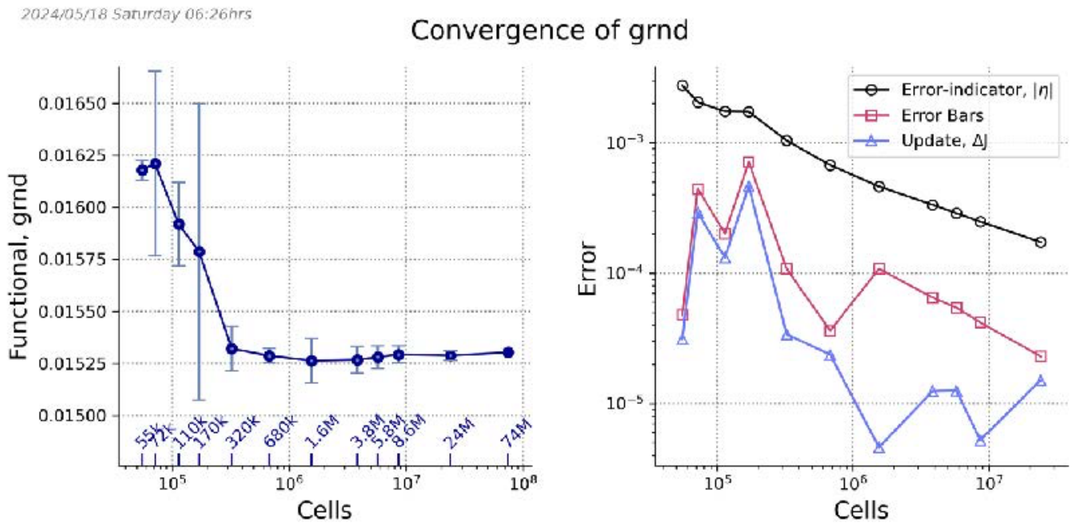
Objective Function

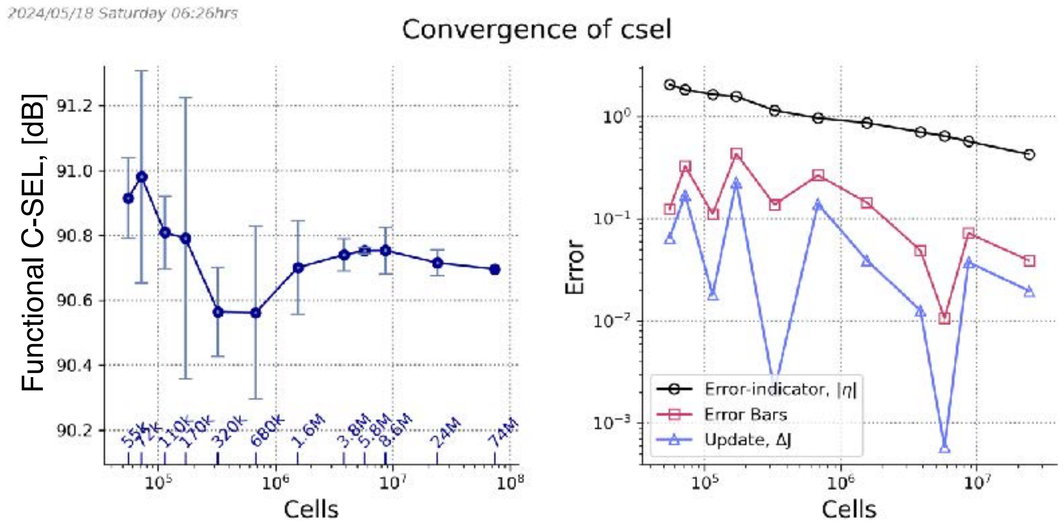
Ground-noise based mesh adaptation and error estimation

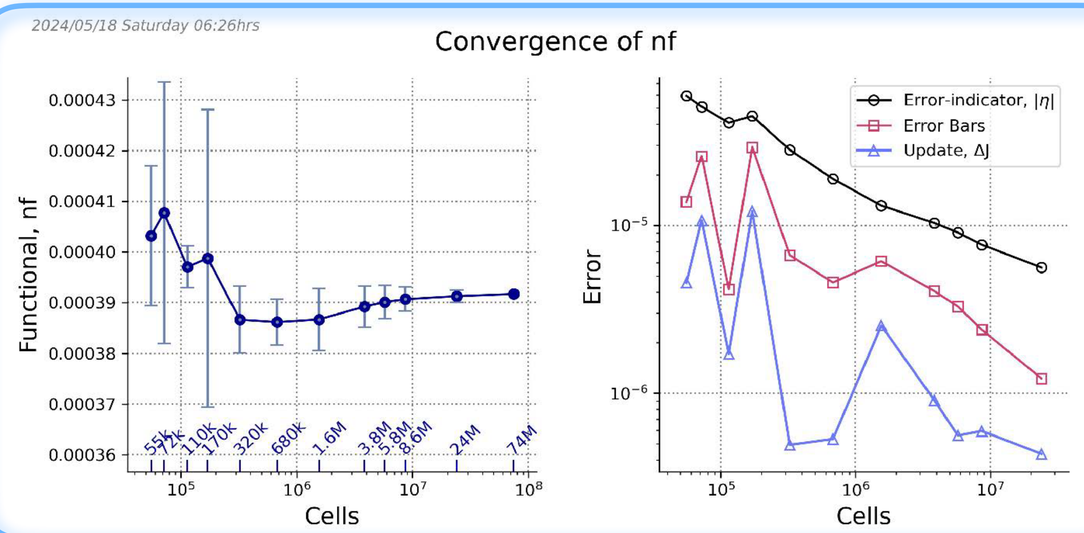
ARMD/CST

***Adapt to Nearfield**, monitor error in A/C-SEL, [dB] & ground signal*







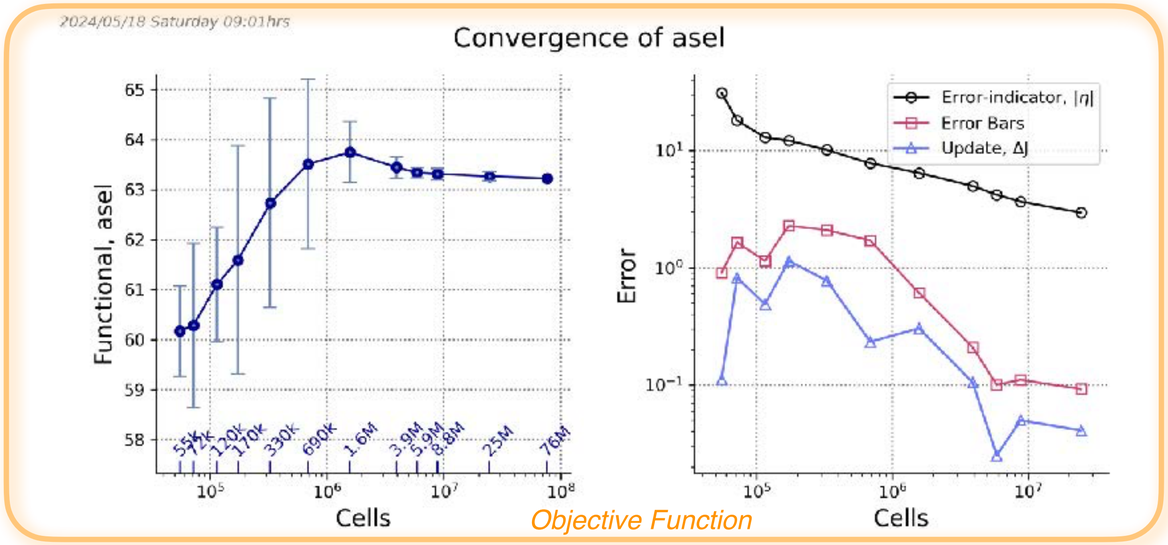


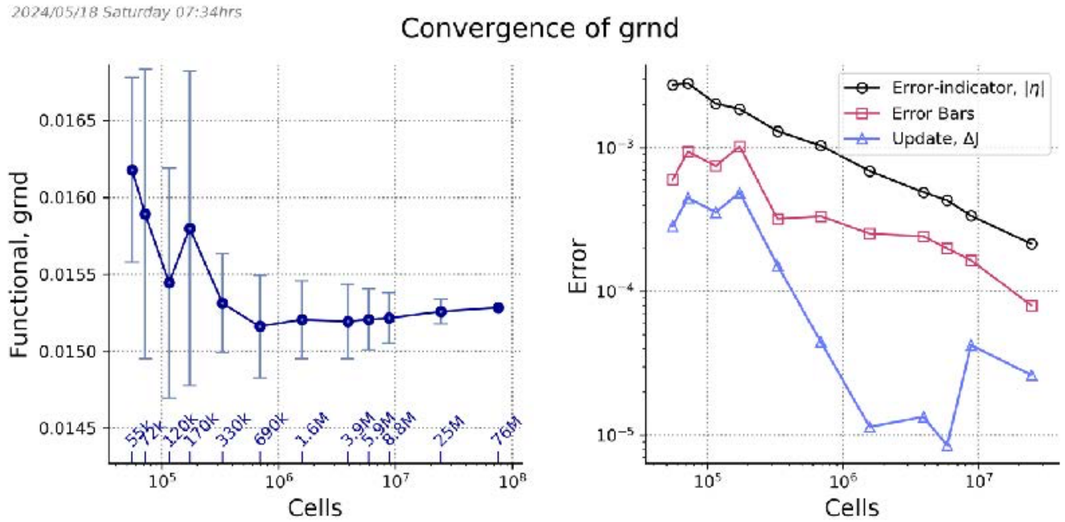
Objective Function

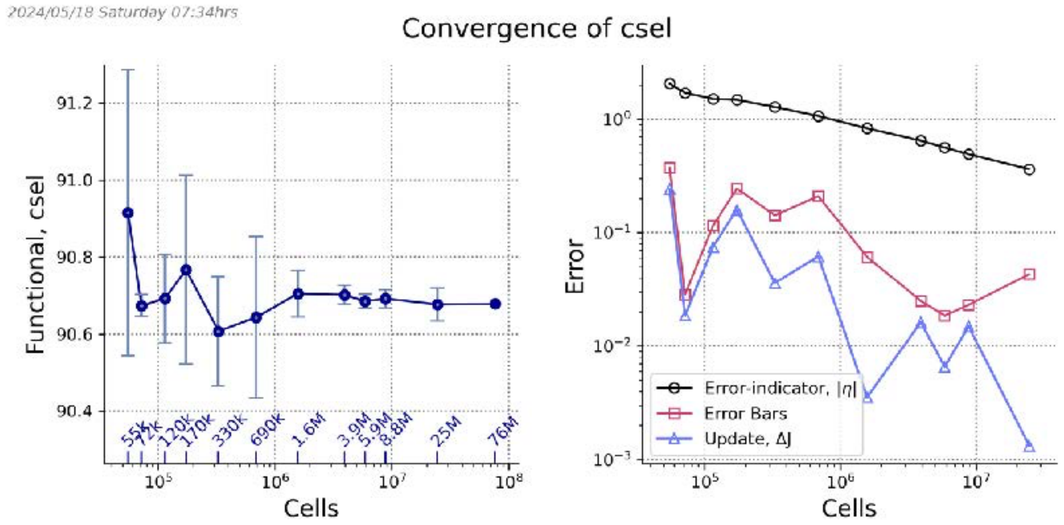
Ground-noise based mesh adaptation and error estimation

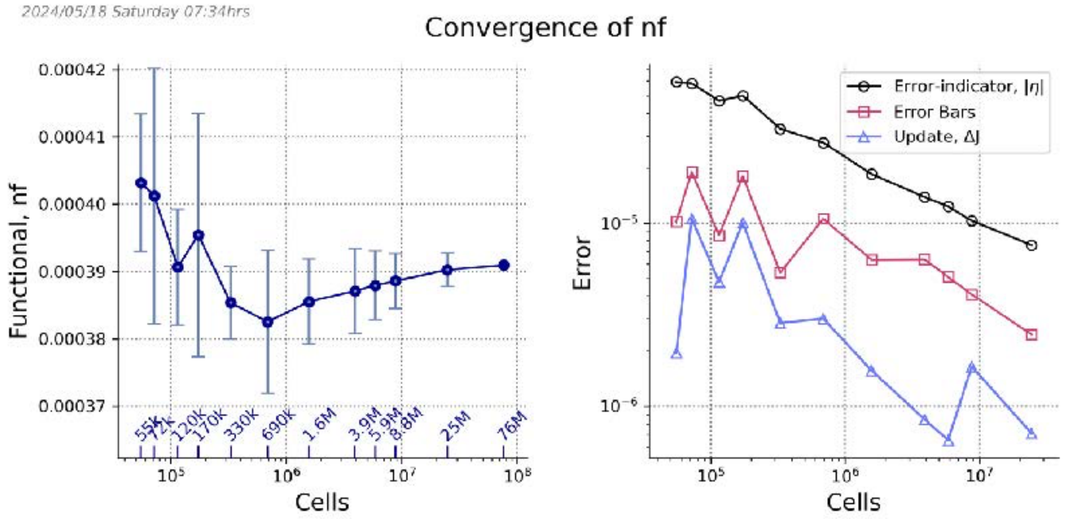
ARMD/CST

Adapt to A-SEL, *monitor error in C-SEL, ground signal & nearfield*





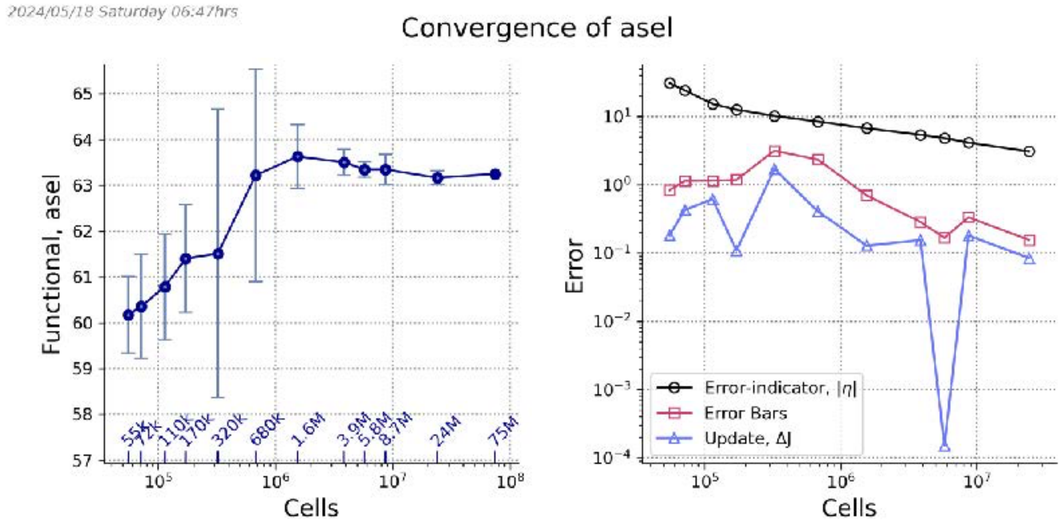


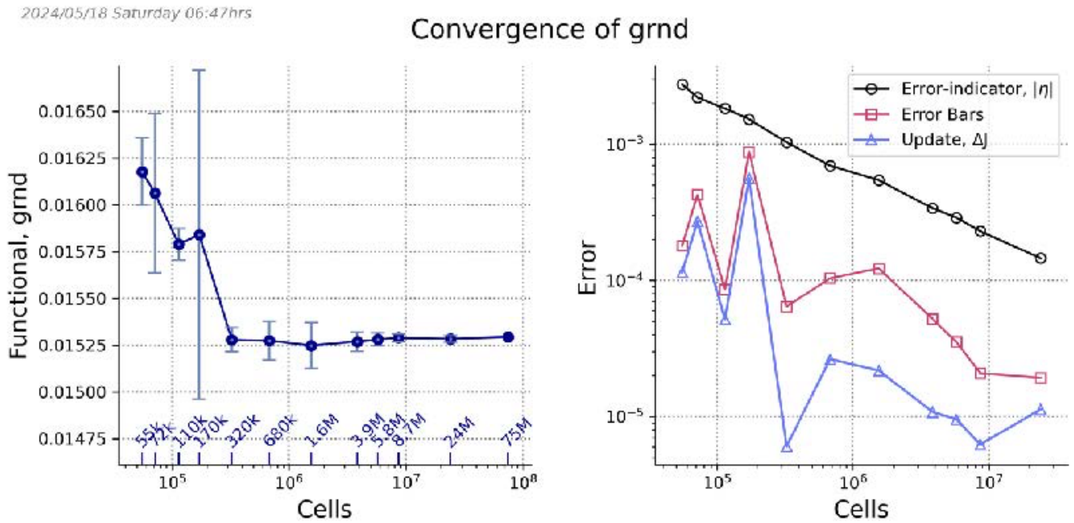


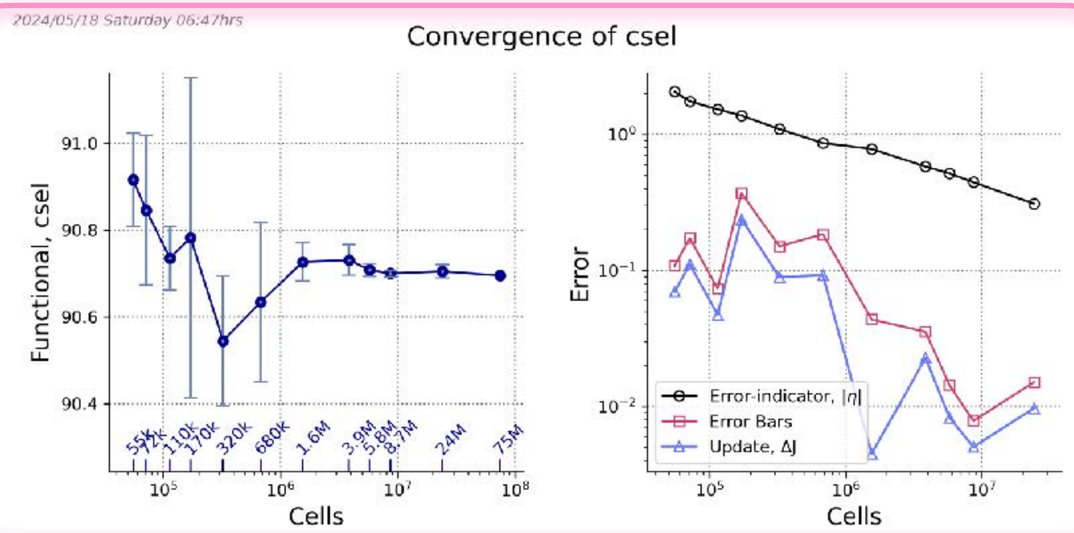
Ground-noise based mesh adaptation and error estimation

ARMD/CST

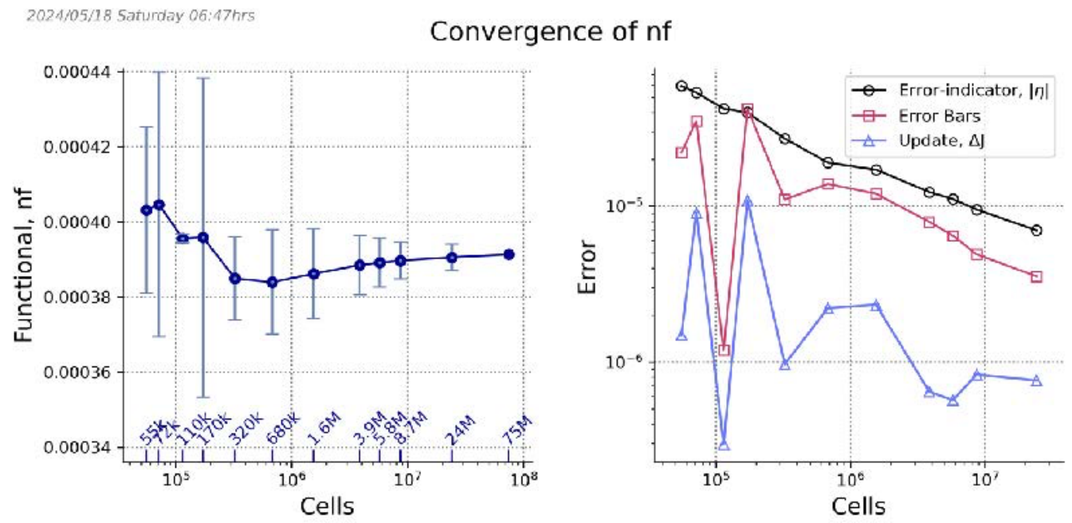
Adapt to C-SEL, *monitor error in A-SEL, ground signal & nearfield*







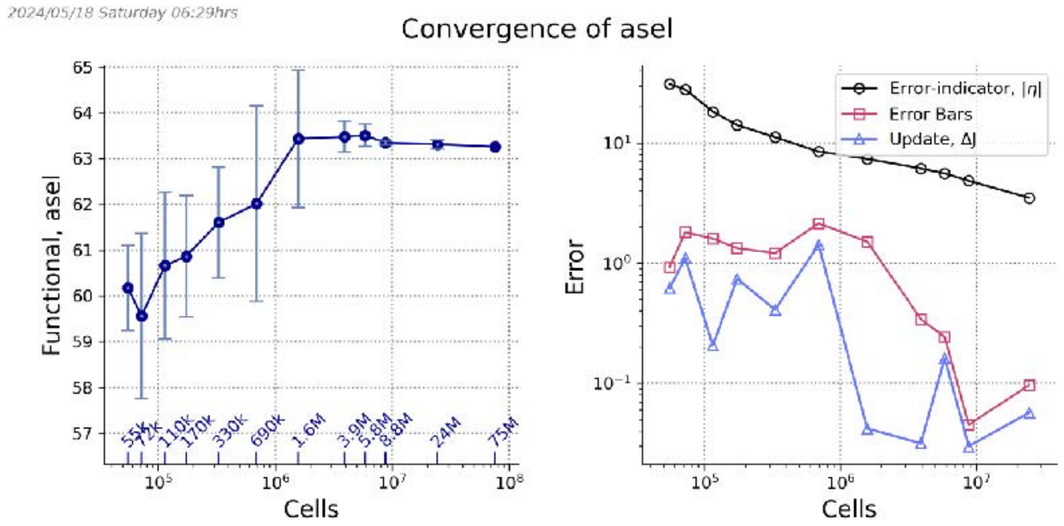
Objective Function

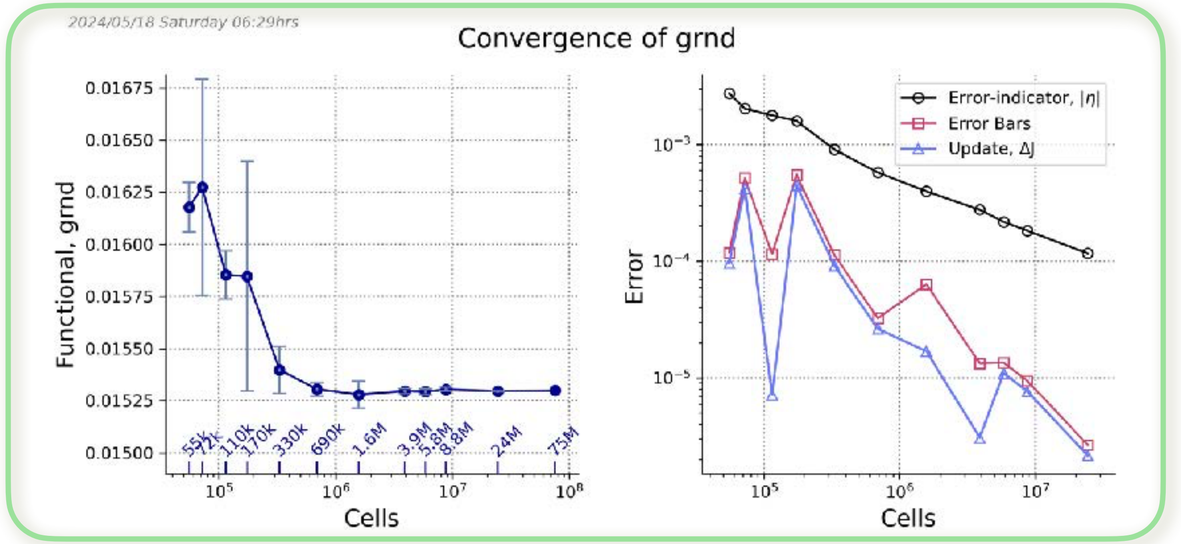


Ground-noise based mesh adaptation and error estimation

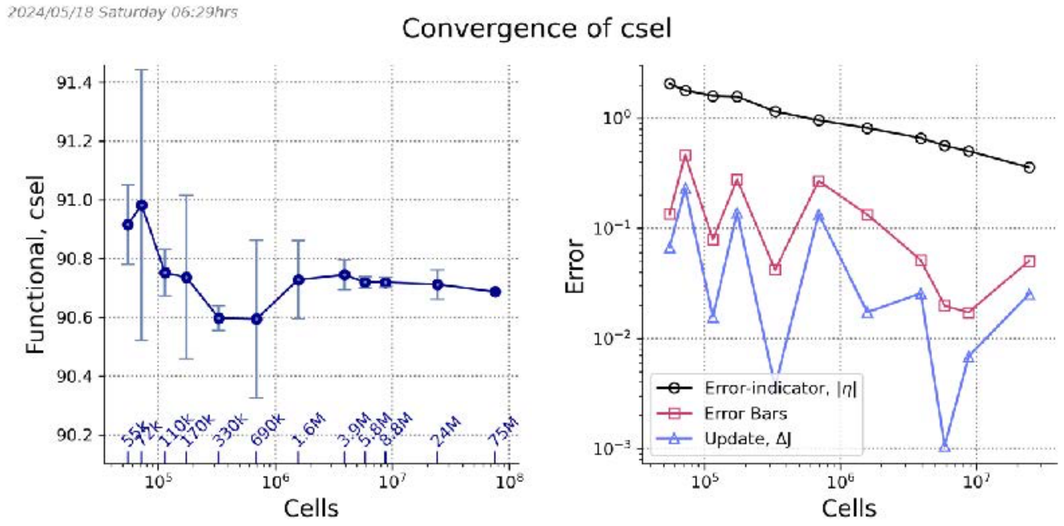
ARMD/CST

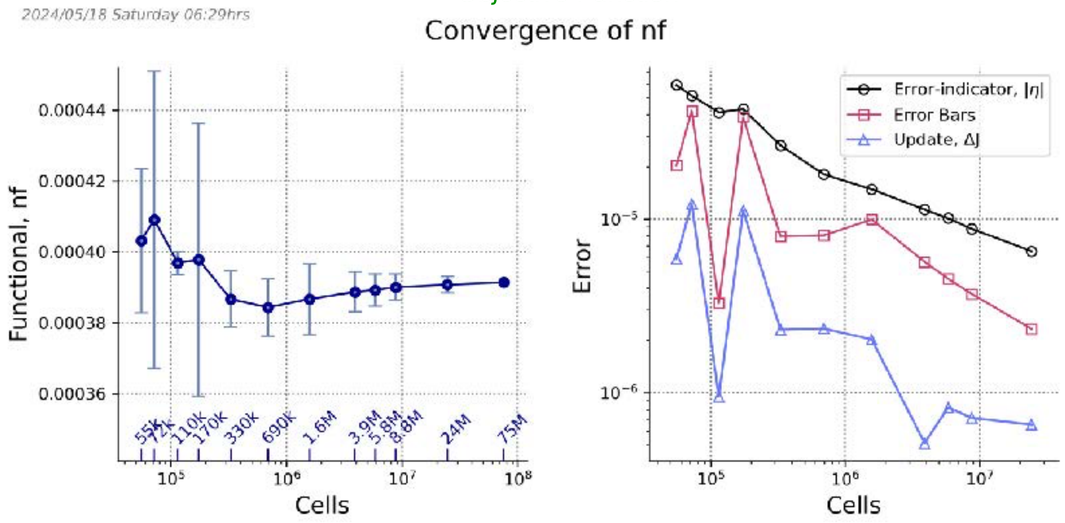
Adapt to ground signal, monitor error in A-SEL, C-SEL & nearfield





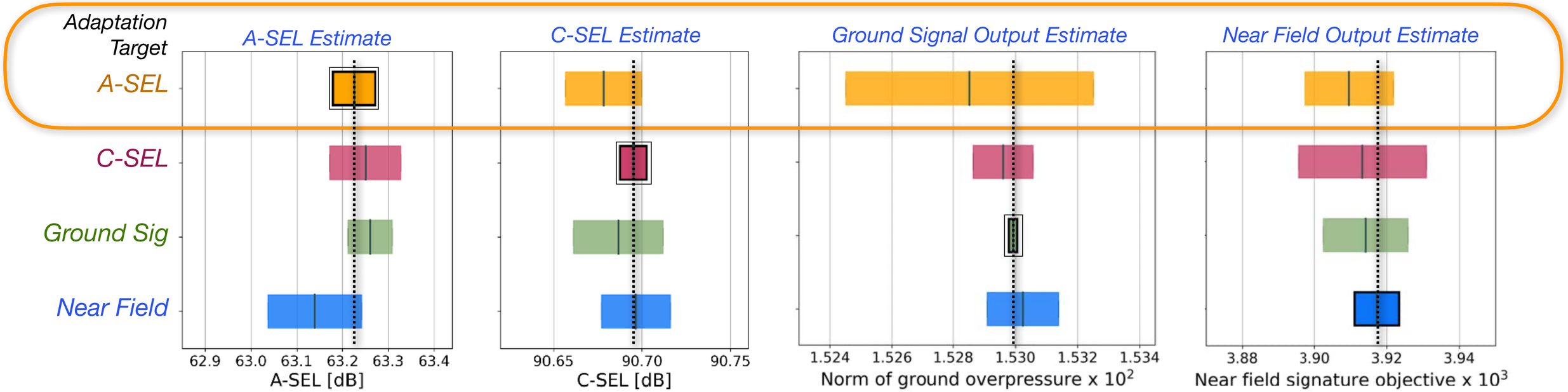
Objective Function





Ground-noise based mesh adaptation and error estimation

ARMD/CST

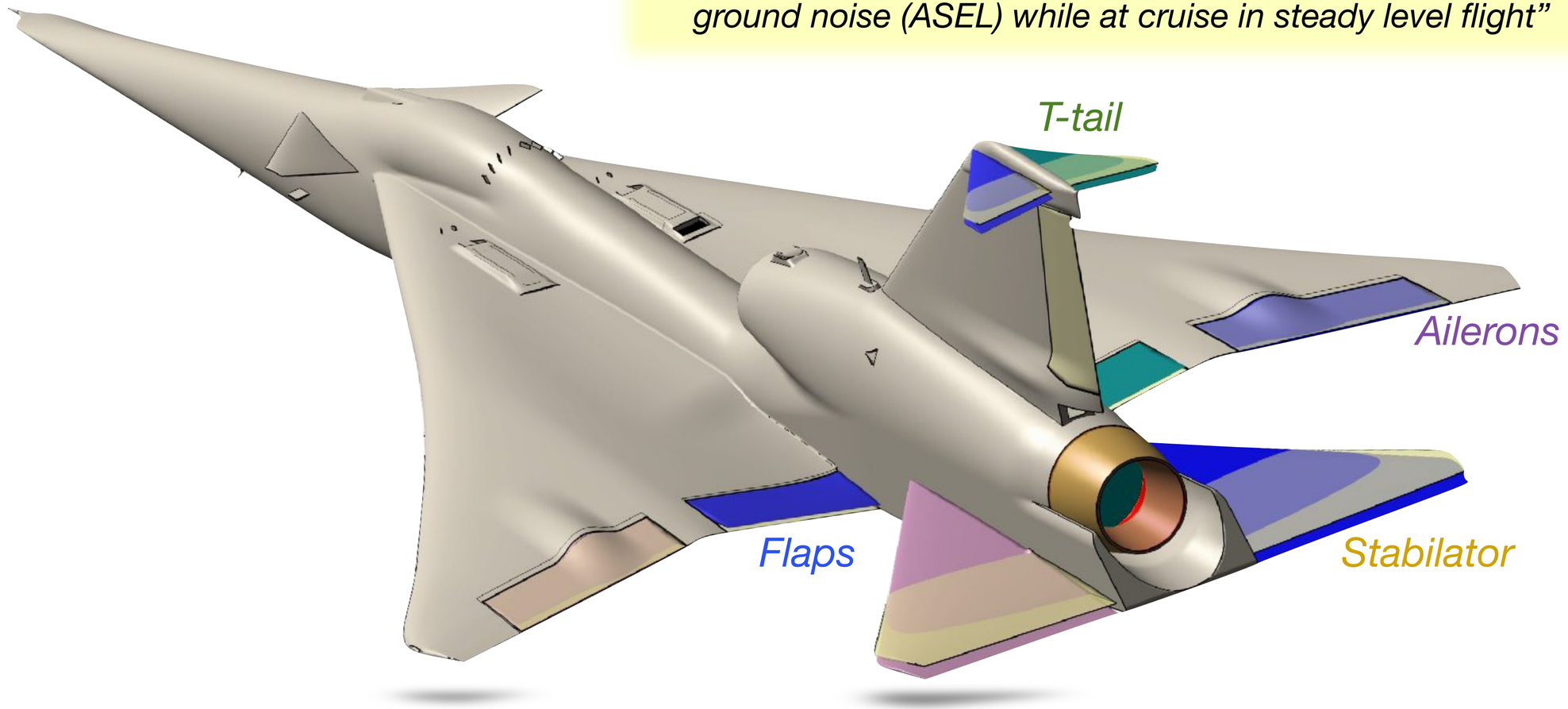


- Error bars for noise metrics are quantitative and are in dB
- 4-8 times more accurate than reported in 2022 (AIAA 2022-4085)
- Adapt for for particular output results in lowest error in that same output
- Error bars overlap for all outputs — shows error estimate is accurate

Ground-noise driven shape design for supersonic flight

ARMD/CST - Cart3D + sBOOM coupling

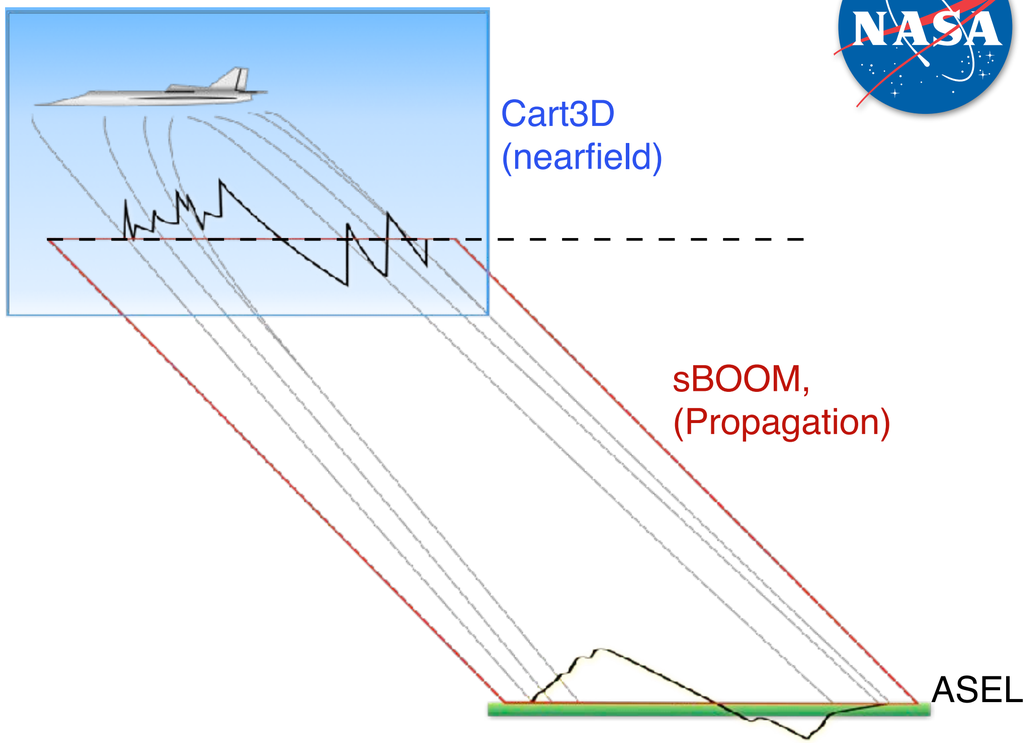
"Use control surface deflection and flight altitude to minimize ground noise (ASEL) while at cruise in steady level flight"



See: AIAA 2025-0772, Rodriguez, Aftosmis, Nemec & Rallabhandi

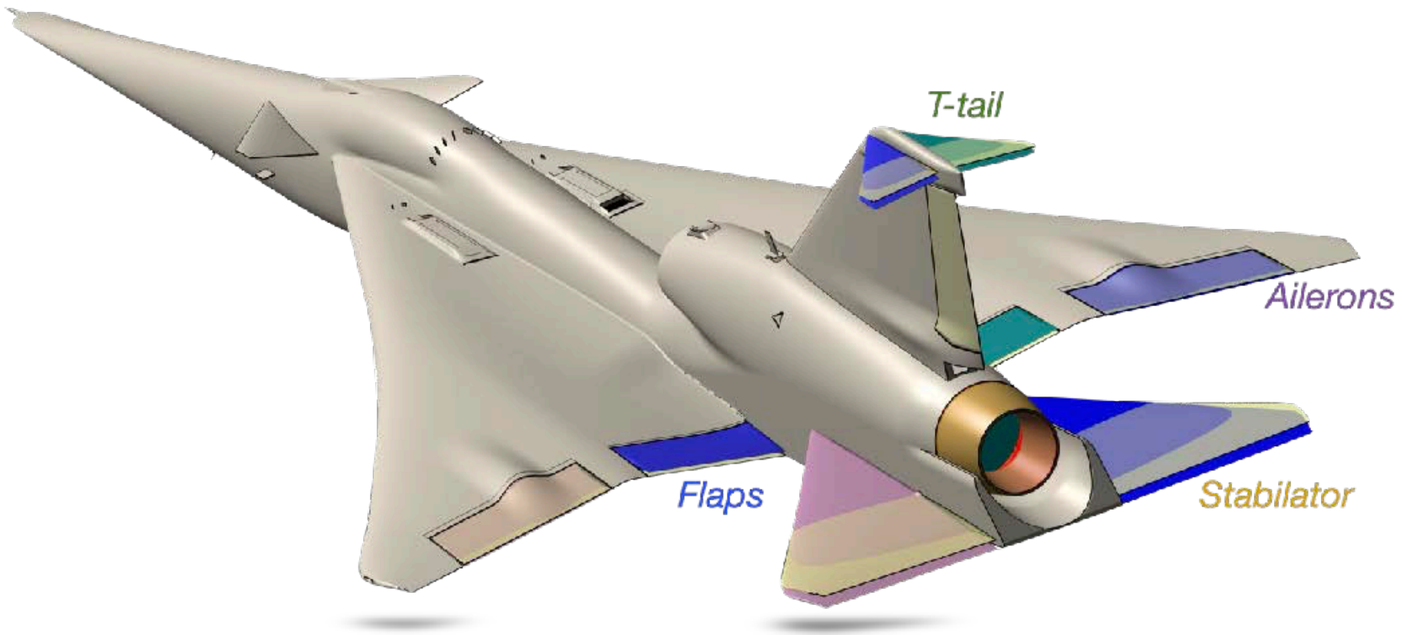
Ground-noise based low-boom shape design

ARMD/CST - Cart3D + sBOOM coupling



Design of full aircraft with power

- **Objective:** Minimize ground noise (ASEL) of full X-59 in steady level cruise
- **Design Variables:** 6 total: four control surfaces, cruise altitude & angle-of-attack
- **Constraints:** Pitching moment & dimensional lift
- Coupled adjoints of Cart3D, atmospheric propagation (sBOOM) and noise metric evaluation†



$$
\begin{aligned}
\text{minimize:} \quad & ASEL\,(\alpha, \delta_f, \delta_a, \delta_s, \delta_t, h) \\
\text{subject to:} \quad & L\,(\alpha, \delta_f, \delta_a, \delta_s, \delta_t, h) = L_{cruise} \\
& C_M\,(\alpha, \delta_f, \delta_a, \delta_s, \delta_t, h) = 0 \\
& \delta_{f,min} \le \delta_f \le \delta_{f,max} \\
& \delta_{a,min} \le \delta_a \le \delta_{a,max} \\
& \delta_{s,min} \le \delta_s \le \delta_{s,max} \\
& \delta_{t,min} \le \delta_t \le \delta_{t,max} \\
& h_{min} \le h \le h_{max}
\end{aligned}
$$

† *See: AIAA 2022-4085 (Nemec, Aftosmis, Rallabhandi & Rodriguez)*

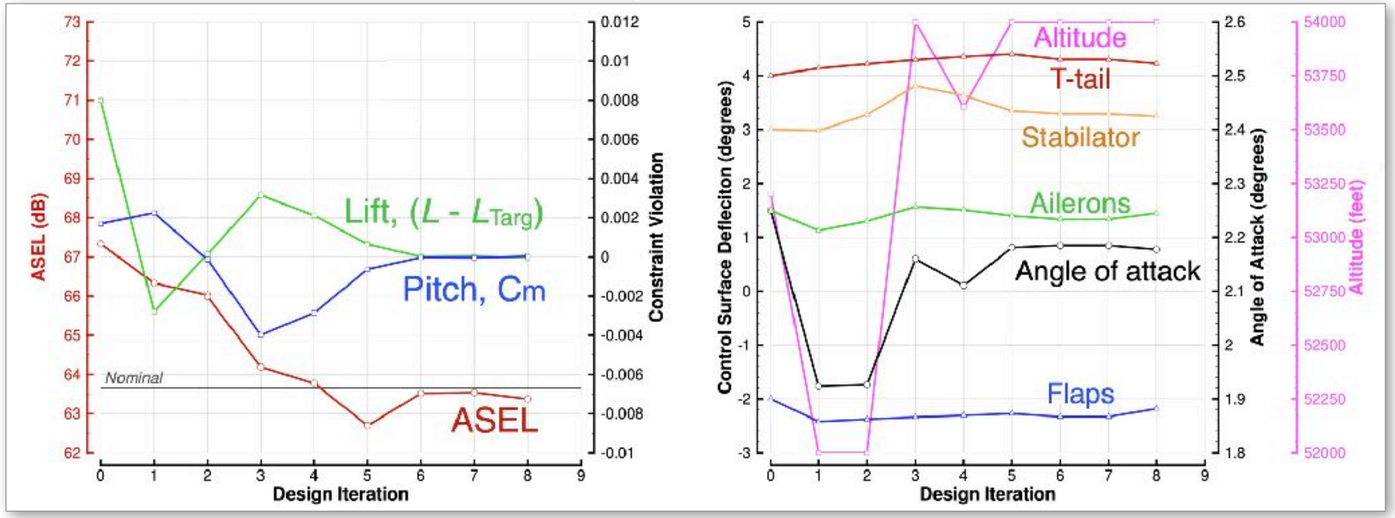
Ground-noise based low-boom shape design

ARMD/CST - Cart3D + sBOOM coupling

Design of full aircraft with power

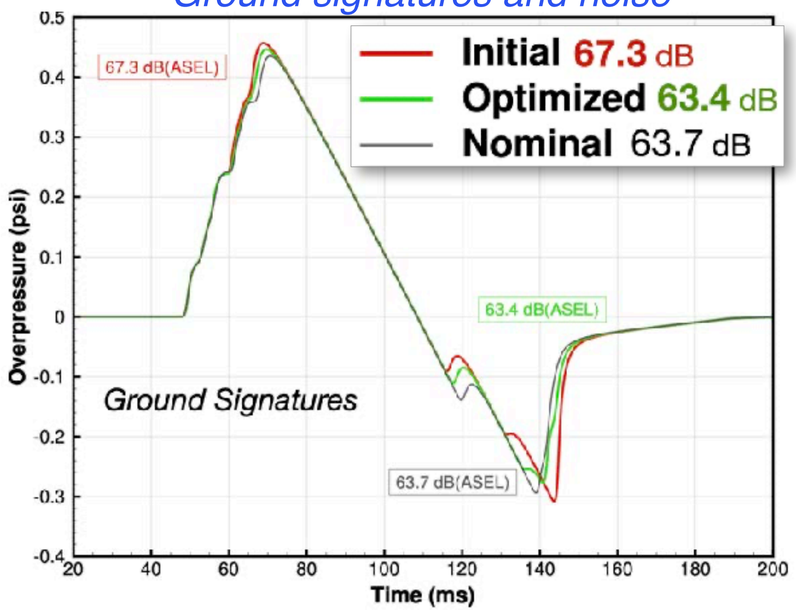
- **Objective:** Minimize ground noise (ASEL) of full X-59 in steady level cruise
- **Design Variables:** 6 total: four control surfaces, cruise altitude & angle-of-attack
- **Constraints:** Pitching moment & dimensional lift
- Coupled adjoints of Cart3D, atmospheric propagation (sBOOM) and noise metric evaluation.

Design evolution



- David presented results in *AIAA 2025-0772* “Sonic boom ground noise minimization via the adjoint method” (J. manuscript in-press)
  - Demonstrated on simple bodies of revolution & verified accuracy of coupled gradients
  - Reduced noise by ~4 dBA & improved upon “Nominal” cruise state
  - Demonstrated on control surface optimization problem for full X-59 aircraft in realistic powered flight for numerous objectives including both noise minimization and specific noise targets

Ground signatures and noise

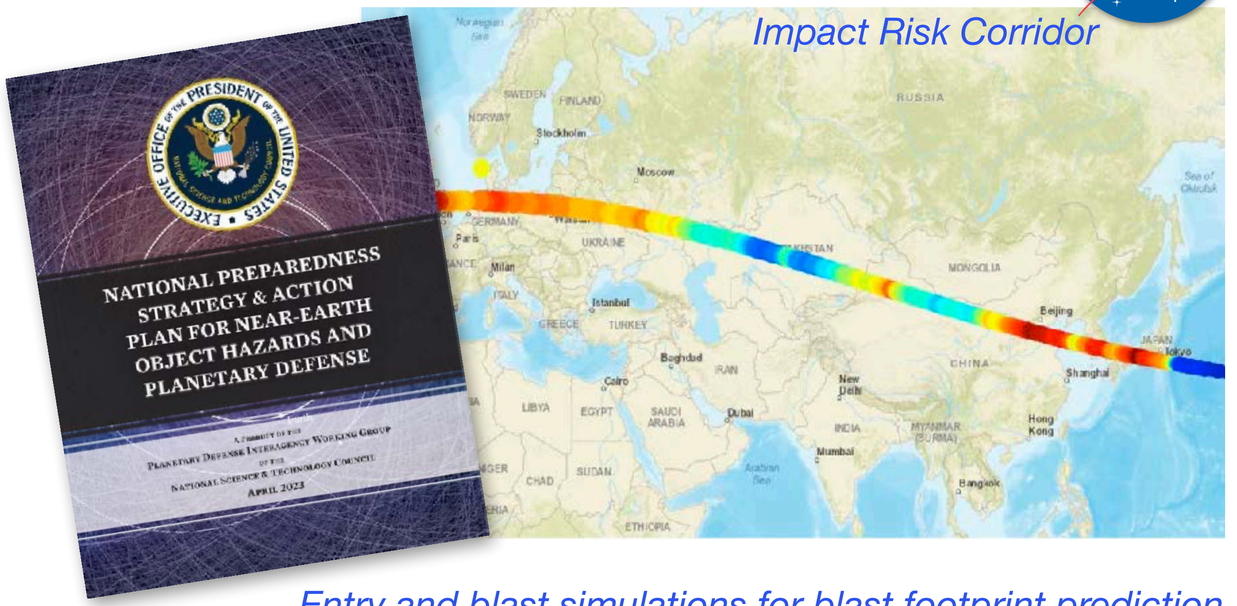


SMD: Planetary Defense

Hazards modeling for the Asteroid Threat Assessment Project

ATAP Hazards task:

- Blast propagation & ground footprint prediction, tsunami, thermal, global effects, etc..
- Tools: Cart3D, ALE3D, HERA, GeoClaw and others
- Perform basic research to develop fast-running tools for risk assessment and threat prediction
- V&V effort against ground truth (Chelyabinsk, Tunguska, etc.)
- Planetary Defense exercises, table top exercises (TTX) with other agencies, etc..
- Respond to threat objects, Bering sea, 2024YR4

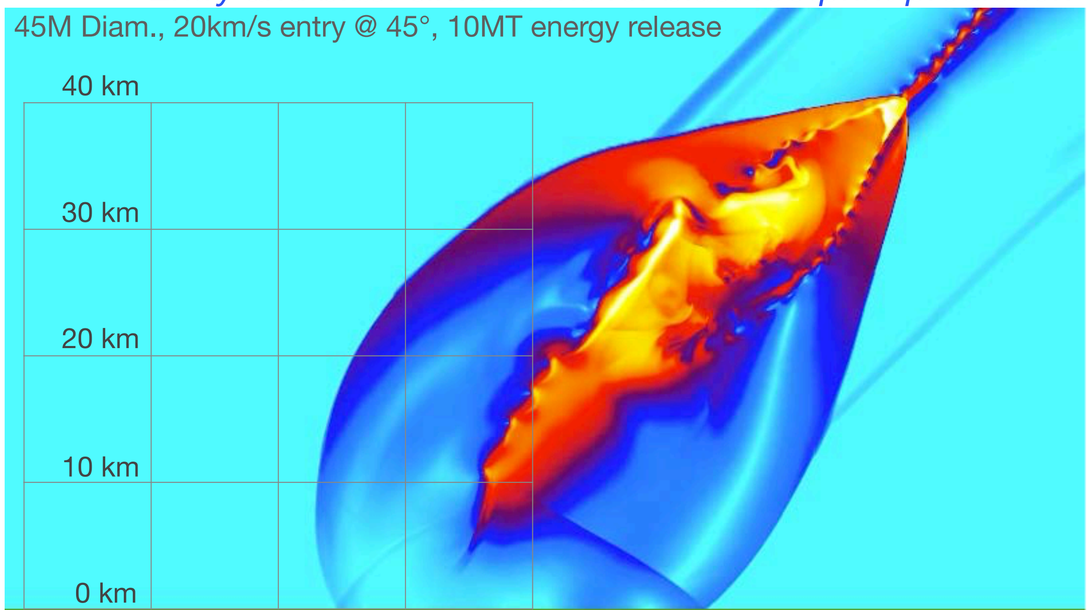


Impact Risk Corridor

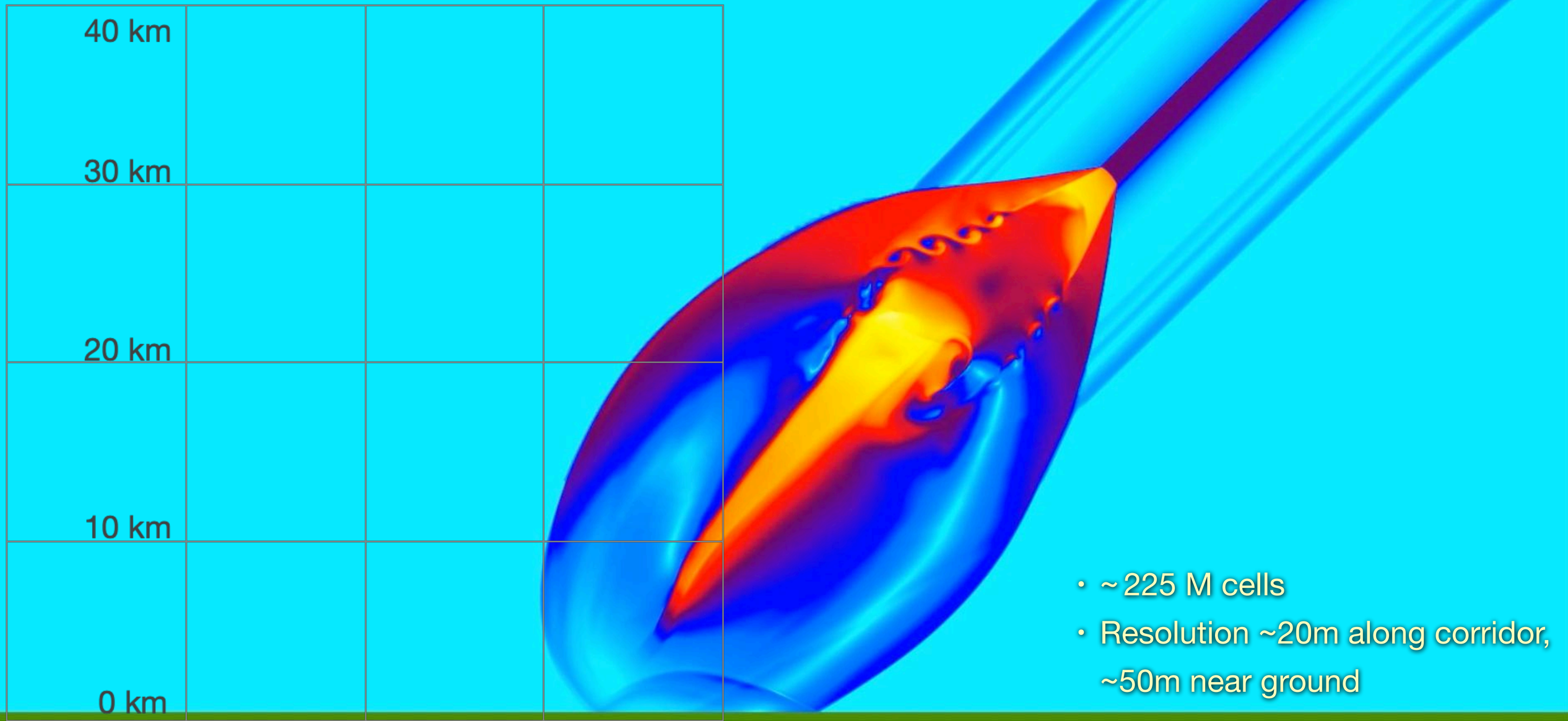
Modeling Working Group (MWG):

- Hazards lead for: *National Near-Earth Object Preparedness Strategy and Action Plan Modeling Working Group (MGW)*
- MWG includes NASA, DoE and others
- Focus: Improving NEO modeling, prediction and information integration
- Develop assessment strategy and plan for NEO impacts

Entry and blast simulations for blast footprint prediction



Mach Contours



- ~225 M cells
- Resolution ~20m along corridor, ~50m near ground

Asteroid entry blast and tsunami modeling

SMD/ATAP

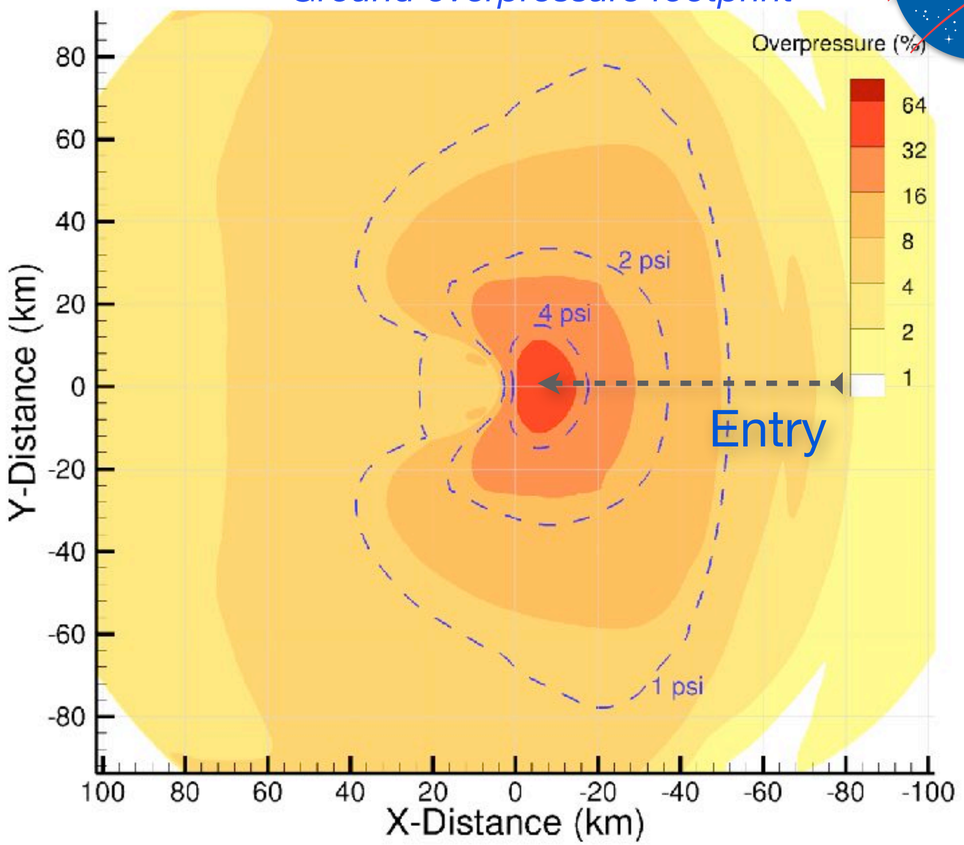
Long range blast blast propagation with Cart3D

- Capture ground overpressure footprints, damage metrics & statistics
- Huge range of length and time-scales
- Large, unsteady 3D simulations, blasts typically ~20-60 mins of real time. 4000-16000 cores x 8-24 hrs
- High-fidelity parametric studies to improve fast running models for risk assessment

Tsunami prediction with GeoClaw

- Extend shallow water-based tsunami simulations to improve predictions of deep-water waves from both airburst & water impact
  - Collaborating with M. Berger (Flatiron Inst.) and R. LeVeque (U.Wash)
- Airwave driven “global tsunami”

Ground overpressure footprint

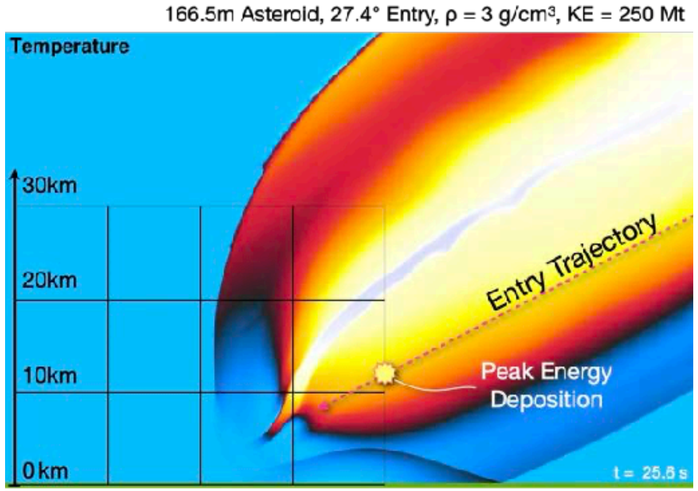


Cart3D development work

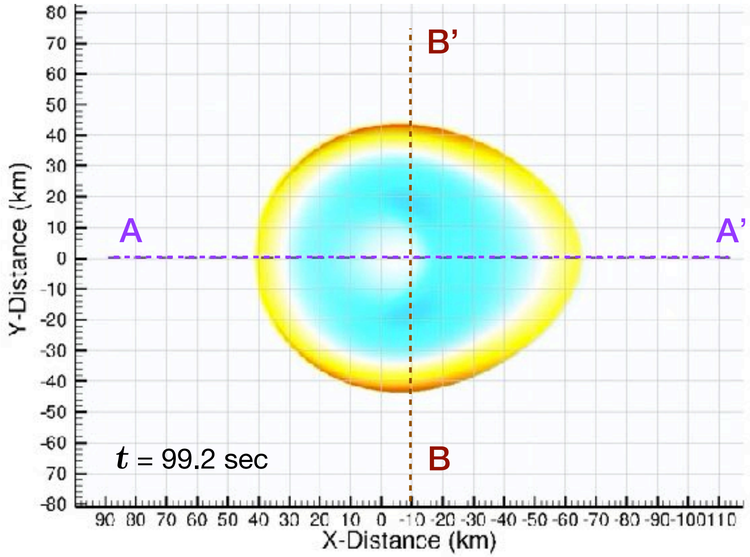
- Massively parallel mesh adaptation for blast simulations to better resolve small (human sized) length scales near the ground
- Boundary conditions for large atmospheric domains
- Understand transition of theater-scale blast to onset of global atmospheric disturbances which can trigger Lamb-wave driven tsunamis anywhere on the globe

Asteroid entry ground overpressure footprint prediction

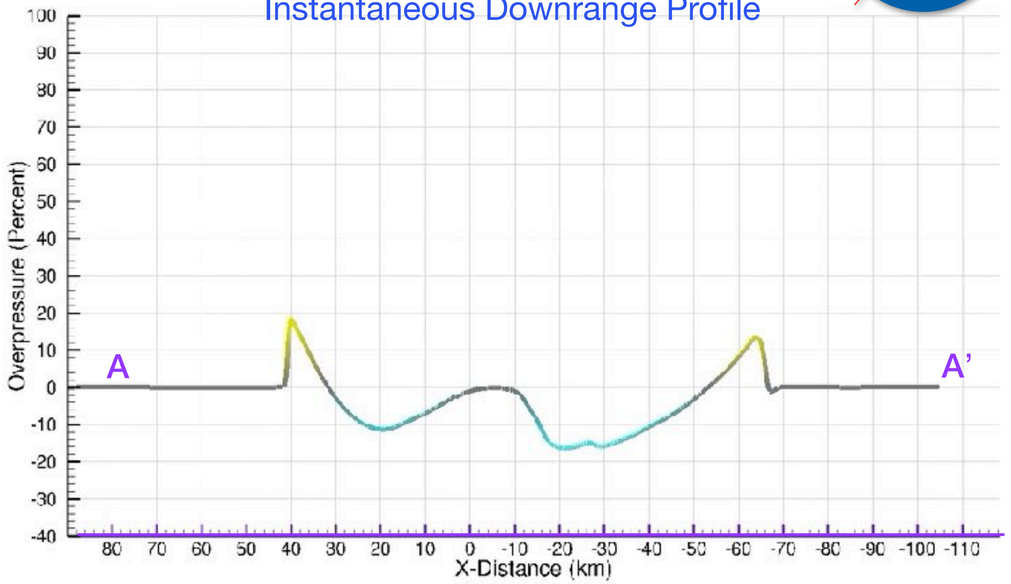
SMD/ATAP



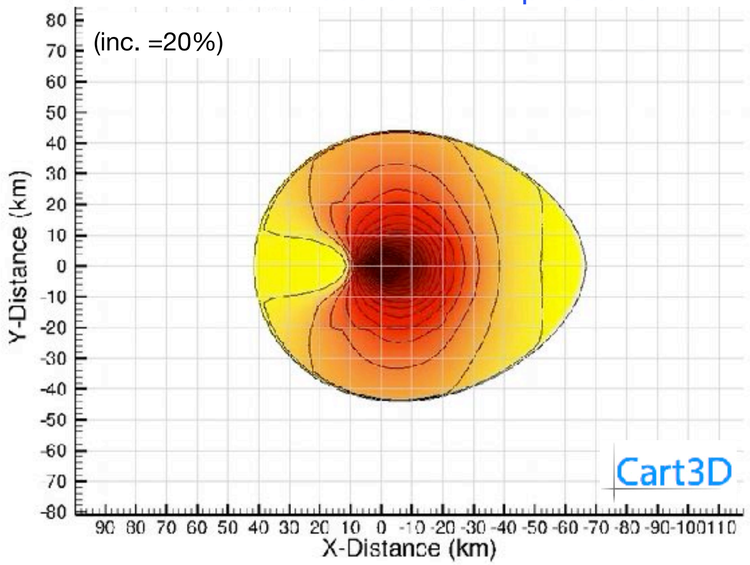
Instantaneous Pressure Profile



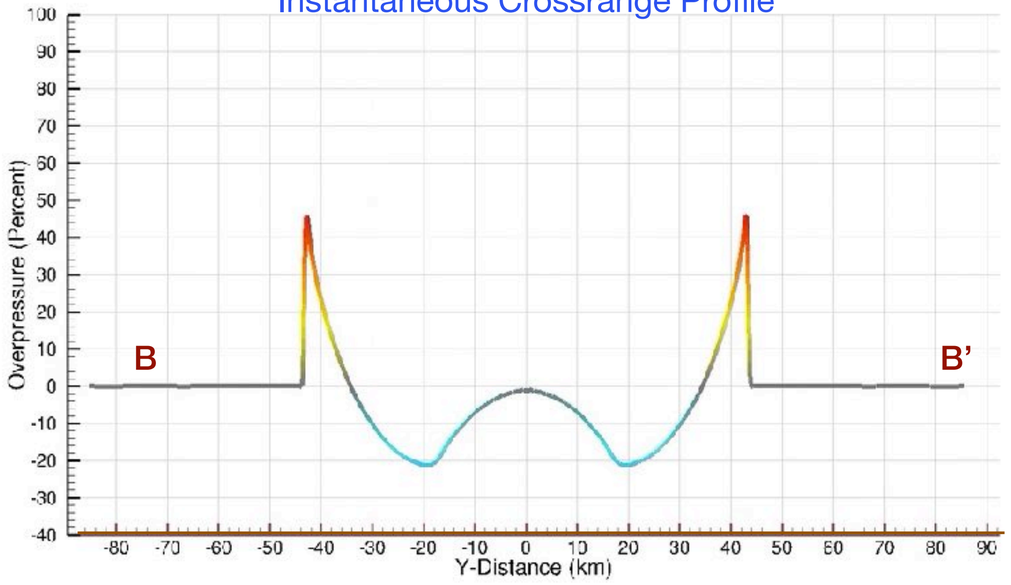
Instantaneous Downrange Profile



Peak Recorded Overpressure

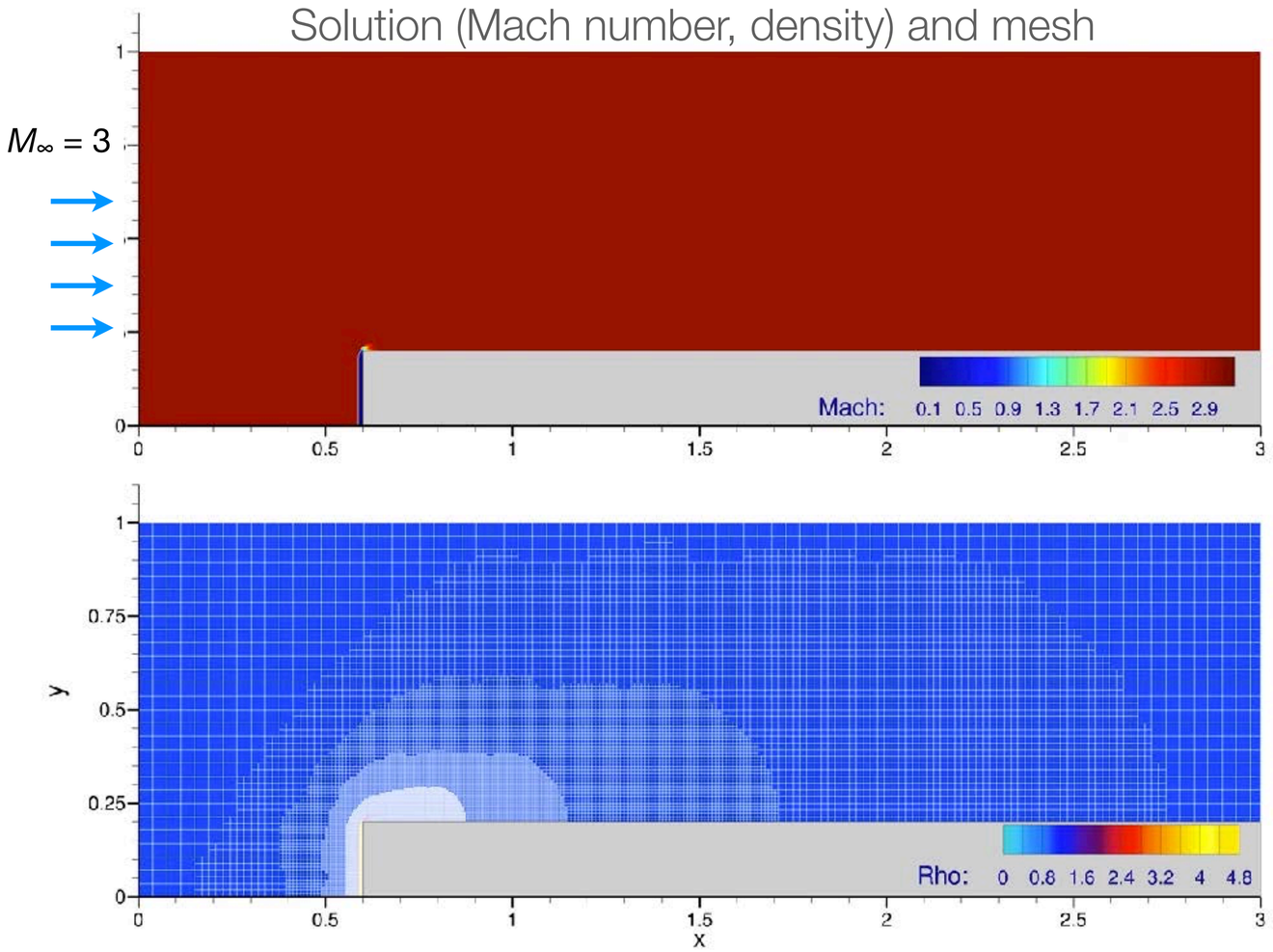


Instantaneous Crossrange Profile

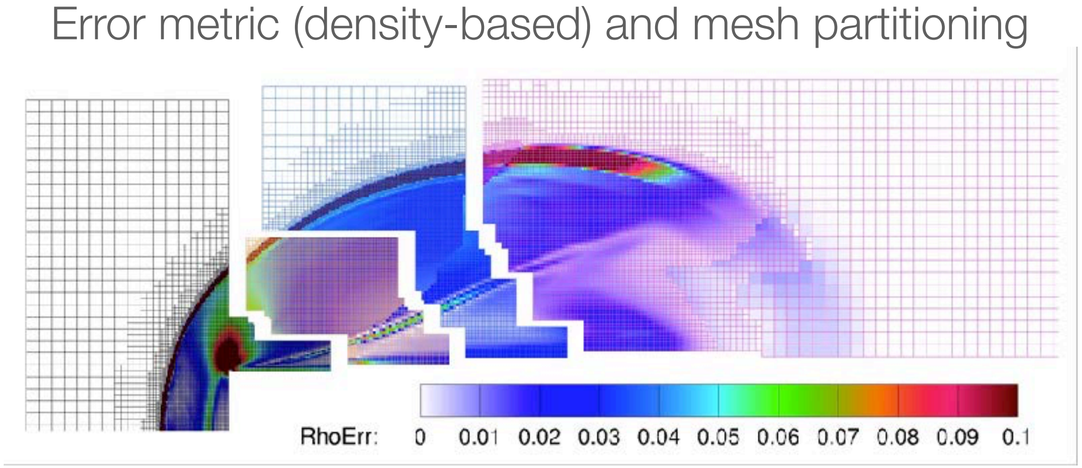


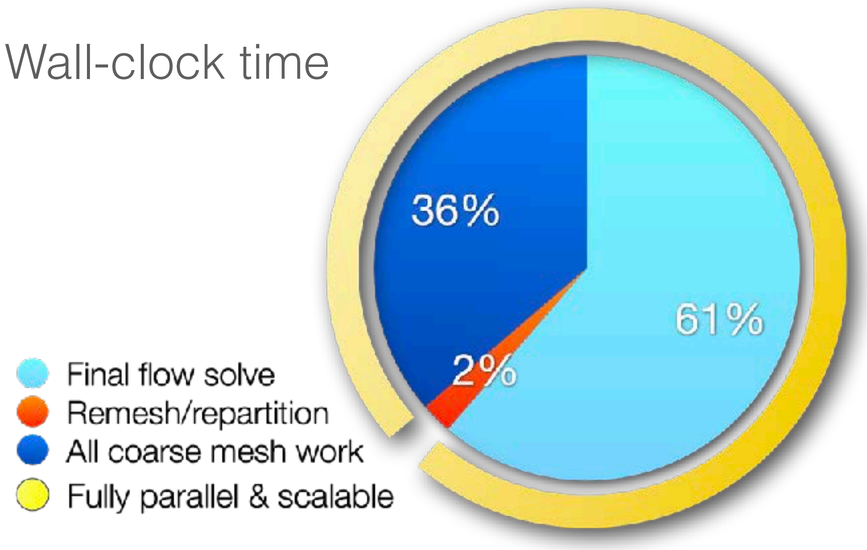
Scalable mesh adaptation for unsteady blast simulations

SMD/ATAP



Unsteady 2D step (model blast problem)



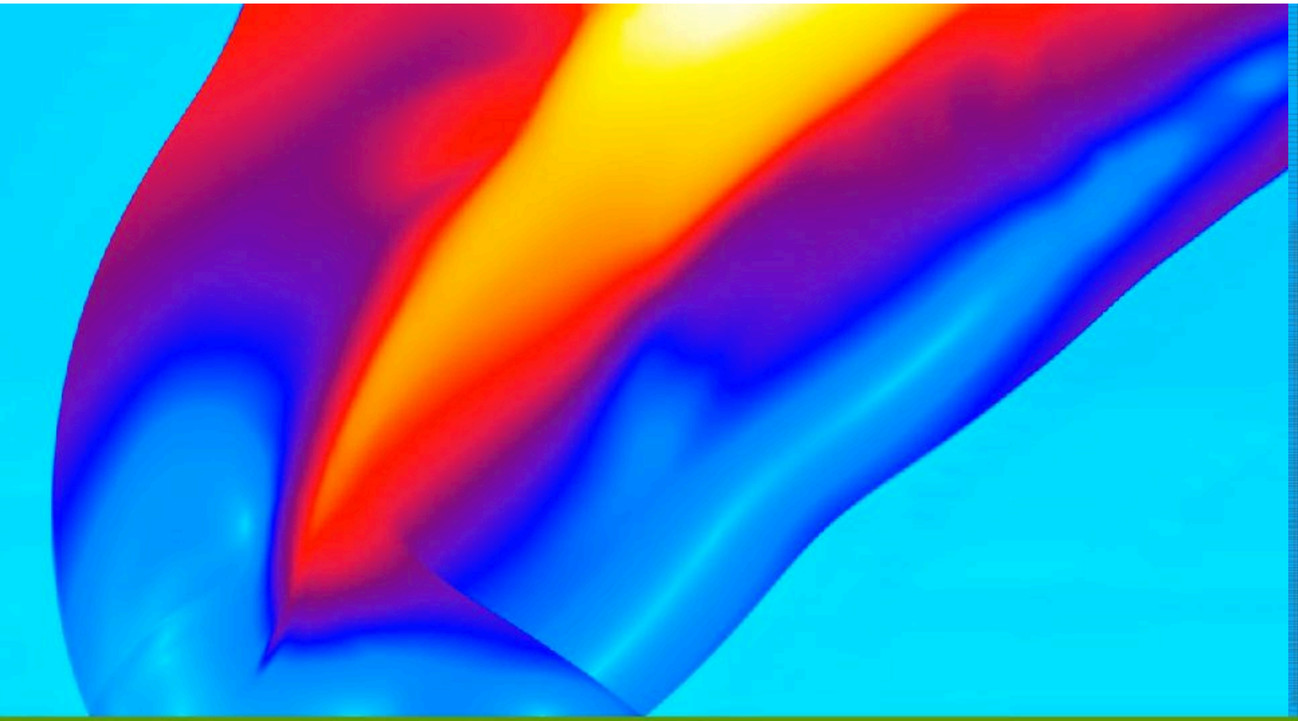


Scalable mesh adaptation for unsteady blast simulations

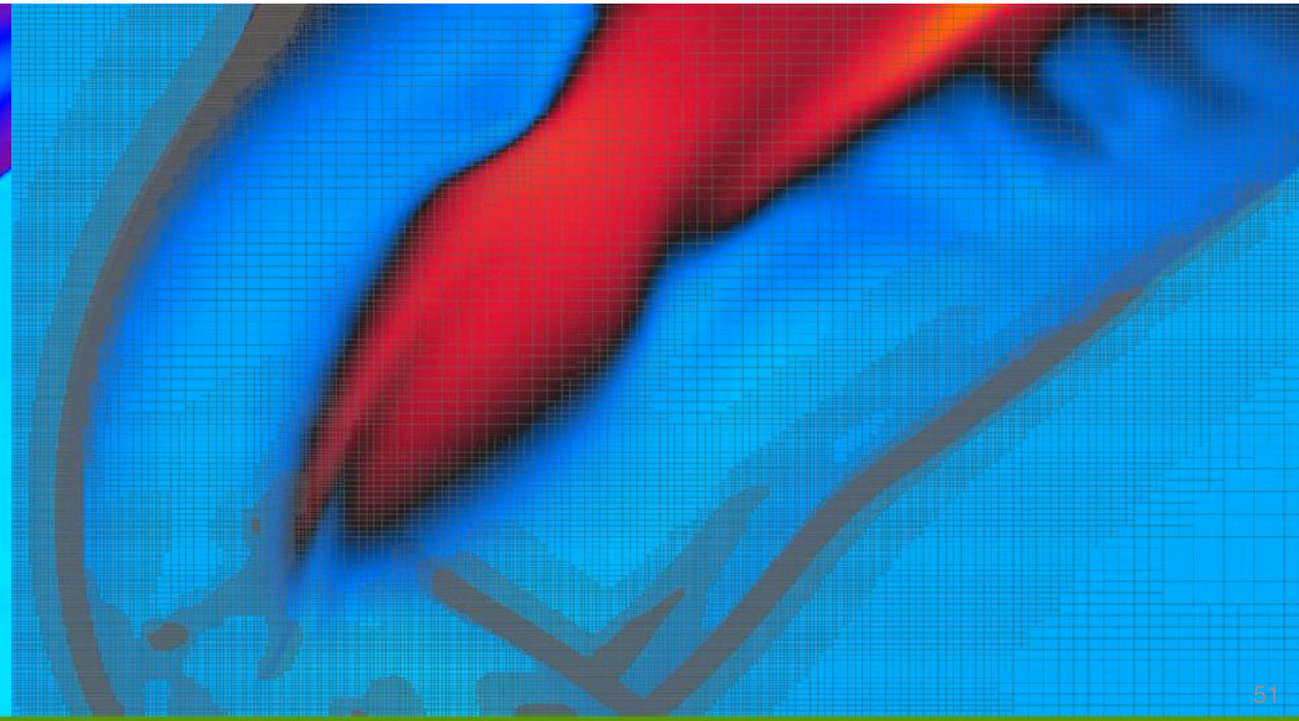
SMD/ATAP

- Use multiple passes through the simulation, see: *AIAA 2023-1792* (Spurlock, Aftosmis, Chiew & Nemec)
- Track space-time error metric during simulation & collect into many time windows
- Simultaneously adapt mesh for all windows (embarrassingly parallel)
- Architecture leverages of many existing adaptation modules in Cart3D package
- Final flow solve dominates wall & CPU time
- Meshing and partitioning small fraction of wall time (typically under 2%)

Mach contours

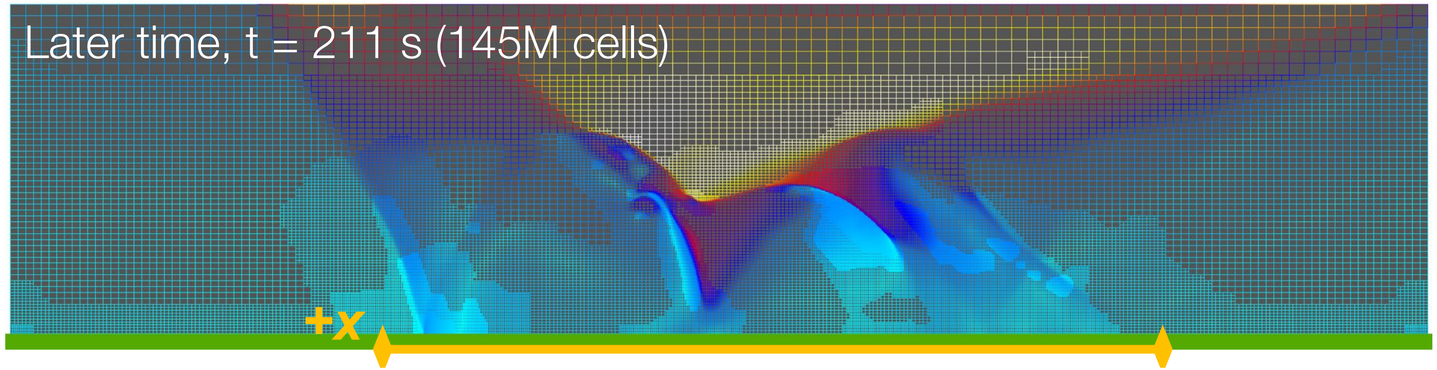


Temperature and mesh

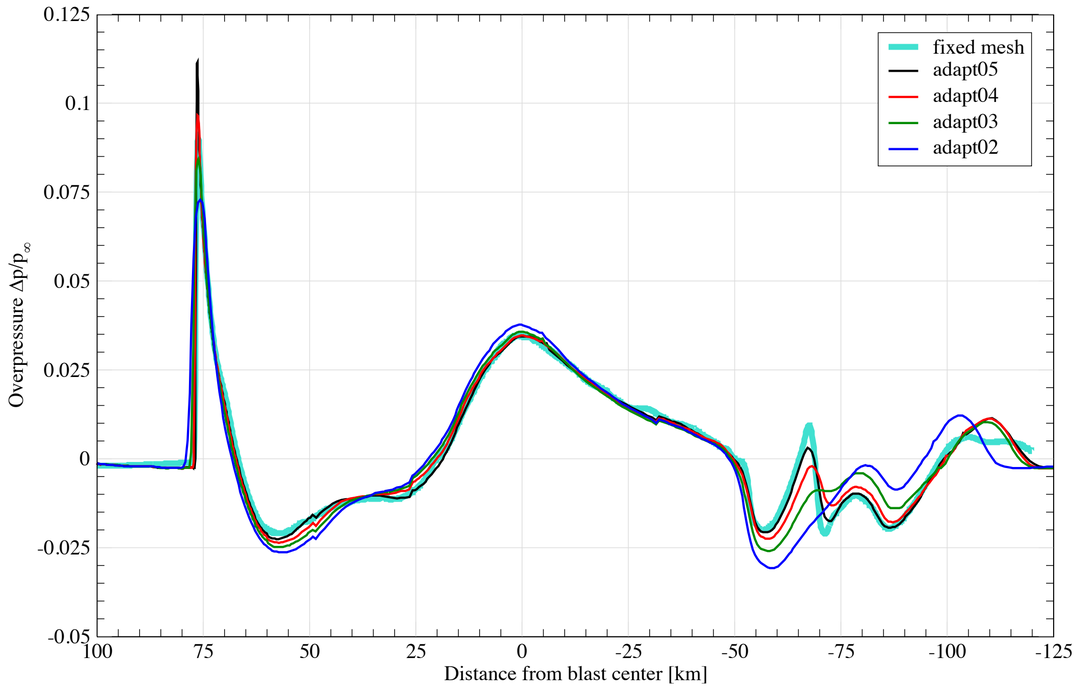


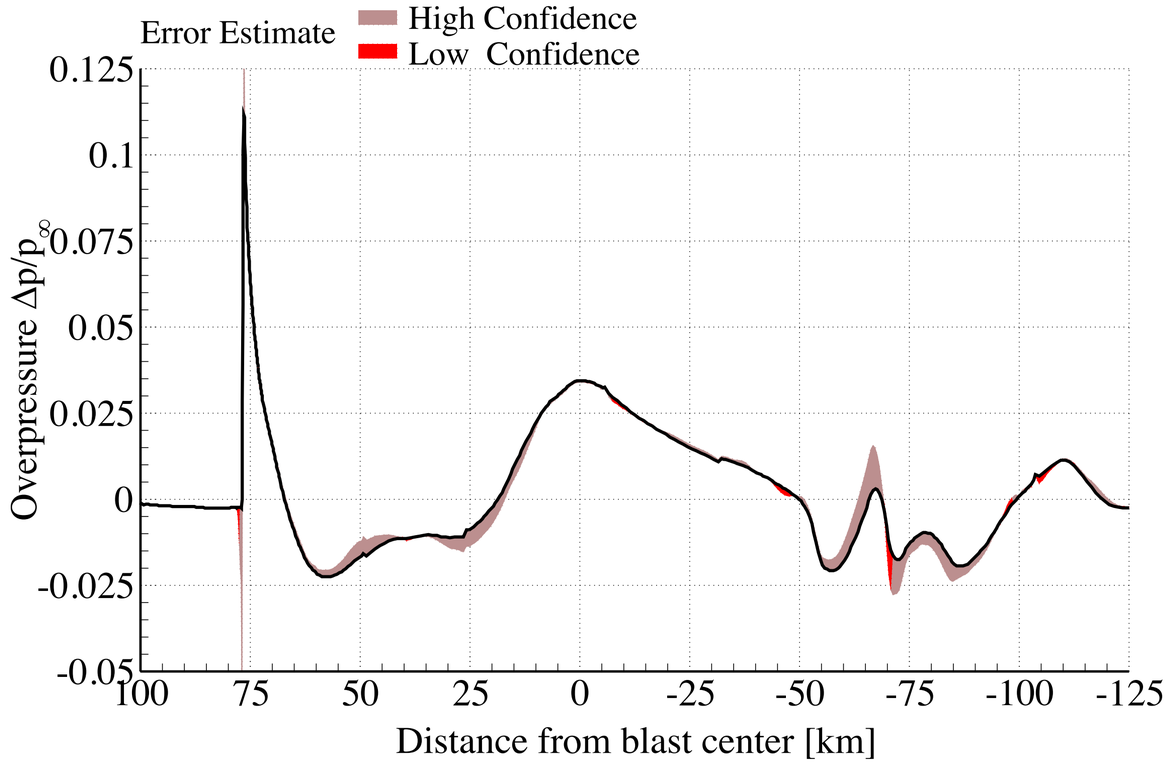
Mesh convergence for unsteady cases

SMD/ATAP



- Sequence of adapted meshes allows use of Richardson extrapolation to assess mesh convergence of solution
- Without exact solution or adjoint, cannot directly monitor error estimate

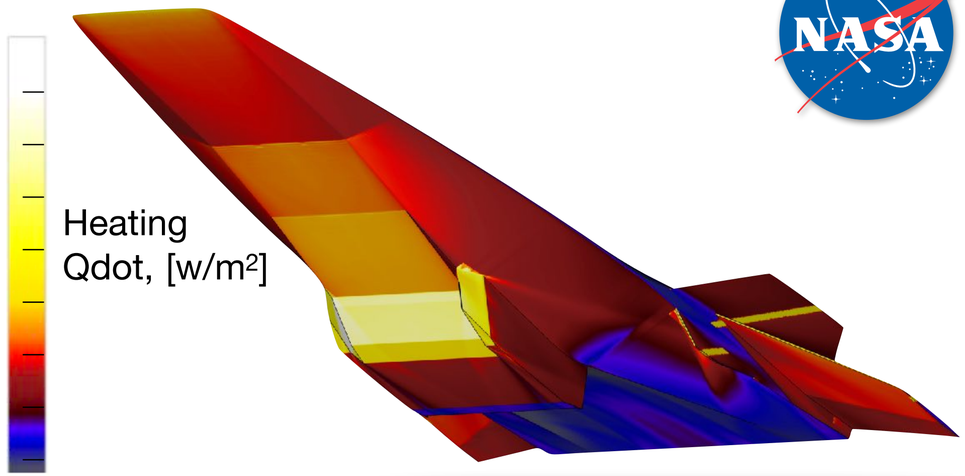




Exploration, Space Technology & Hypersonics

Atmospheric Hypersonics

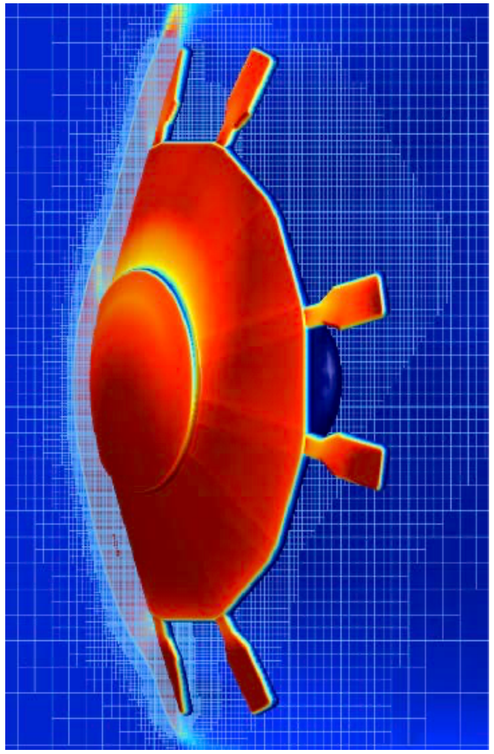
- Cart3D-CBAero coupling for rapid modeling for hypersonic aerothermodynamics
- Anchor CBAero boundary layer using Cart3D inviscid solution
- Aerothermal error estimation, mesh adaptation and design
- Space Act Agreements supporting DOE, USAF & other agencies
- Support dozens of commercial SUAs



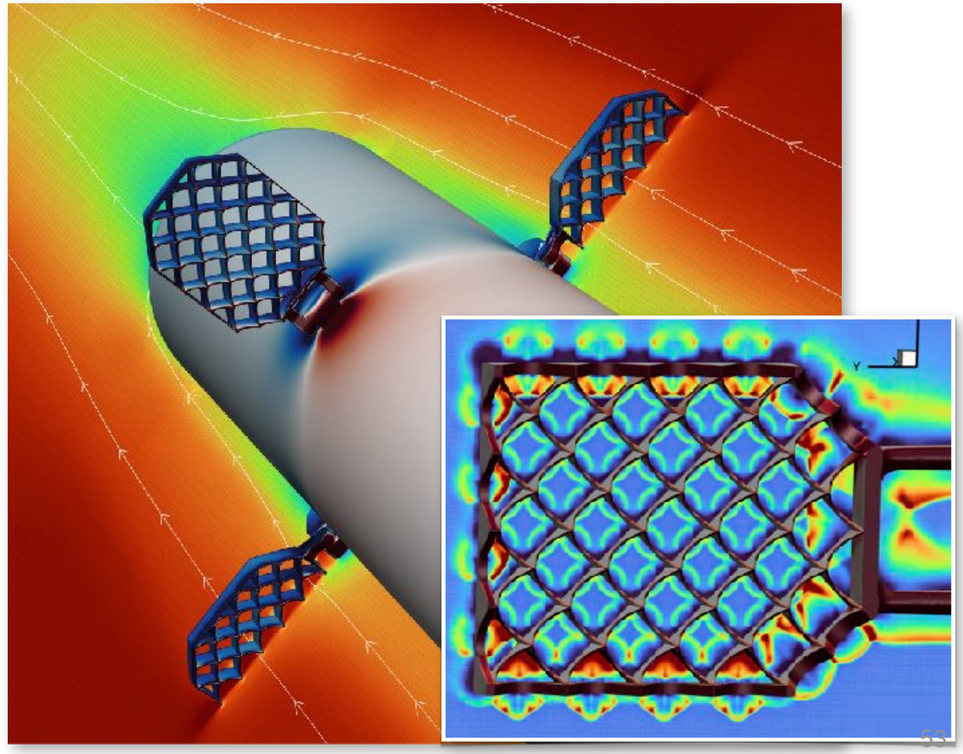
Exploration and Space Technology

- Launch vehicle and re/entry
  - Artemis: SLS & Orion
  - Unmanned, Pterodactyl, Dragonfly, MSR, etc..
- Commercial crew & launch vehicles
  - SpaceX, Boeing, Blue Origin, Relativity, Venus, Andrews, Axient, Firefly, etc..
- Equilibrium air solver for Earth re/entry
- Extension to generalized equilibrium gas solver to support Mars, Venus, Titan & other extraterrestrial atmospheres

Planetary Probes



Commercial launch vehicles

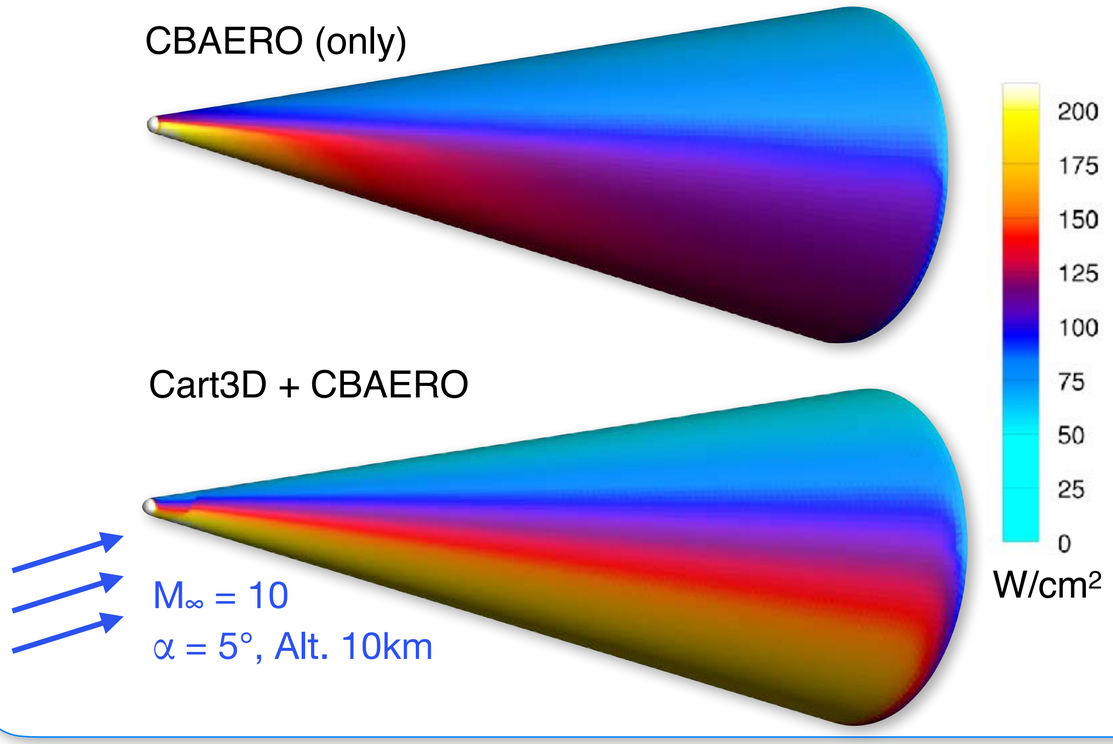


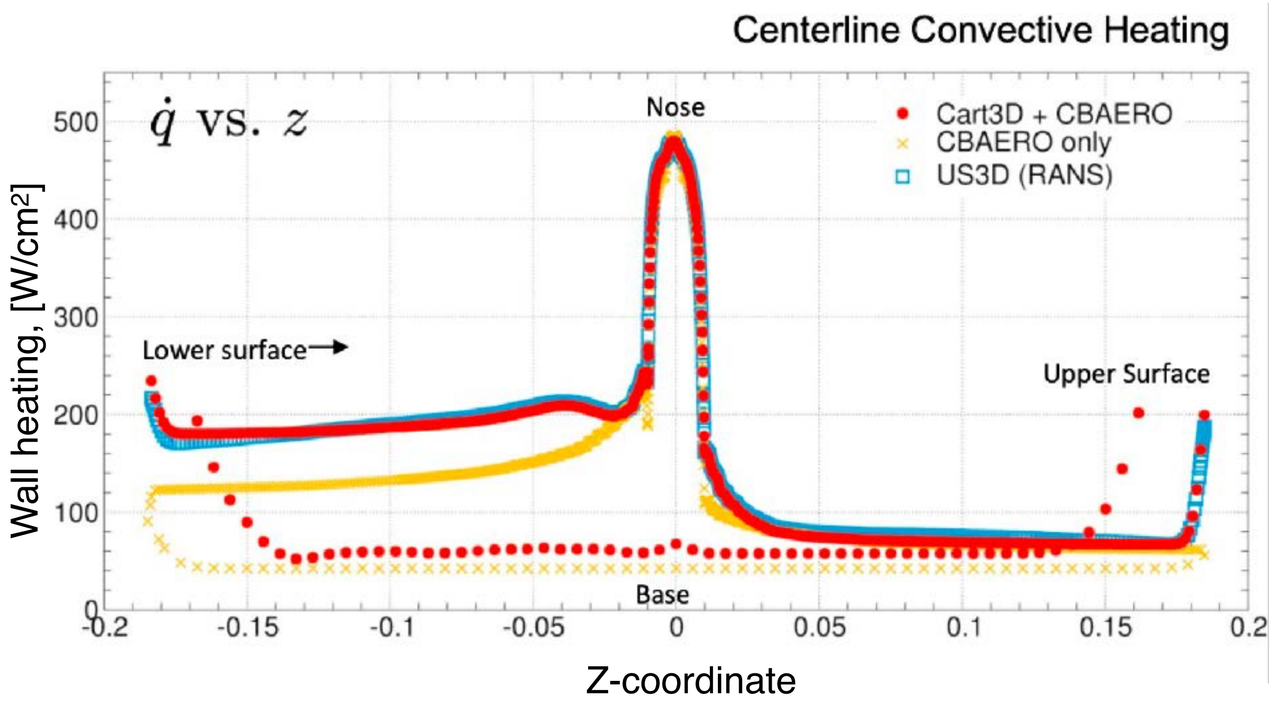
Exploration, Space Technology & Hypersonics

Rapid modeling for hypersonic aerothermodynamics

- Joint work with Dave Kinney (ARC-AA)
- Couple Cart3D & CBAero by running CBAero boundary-layer against Cart3D inviscid solution
- Single-pass approach, anchors CBAero B-L with the Cart3D inviscid solution, typically 50-150x faster than RANS
- Support for both perfect gas and equilibrium gas
- Provide aerothermal outputs, (surface temperature & wall heating & BL quantities)

DOE STREAM Geometry

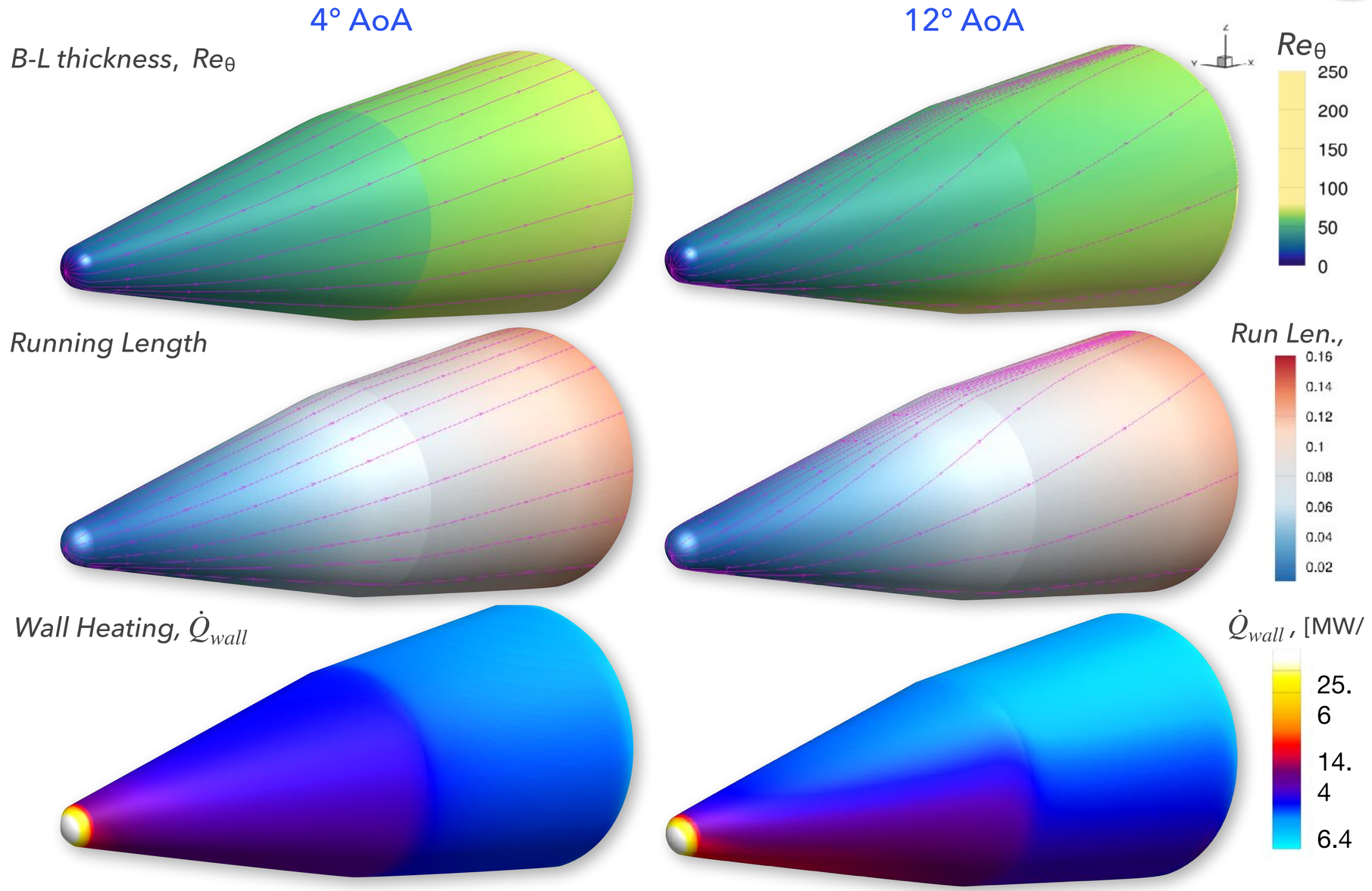




Rapid modeling for hypersonic aerothermodynamics

NASA TP-2213 Biconic: Boundary layer & heating

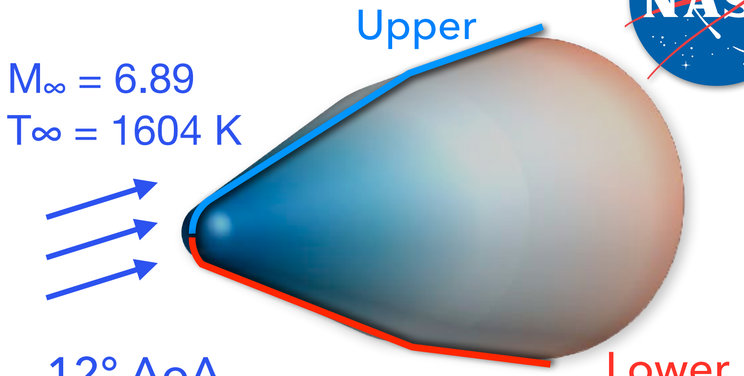
- CBAero v6.0.5 anchored against Cart3D inviscid solution
- Freestream:
  $M_\infty = 6.89$
  $p_\infty = 2182$ Pa
  $\rho_\infty = 0.00473$ kg/m^3
  $T_\infty = 1604$ K
  $\alpha = 4° \& 12°$
- Const wall temp BC:
  $T_{Wall} = 321$K @ 4°AoA
  $T_{Wall} = 350$K @ 12°AoA



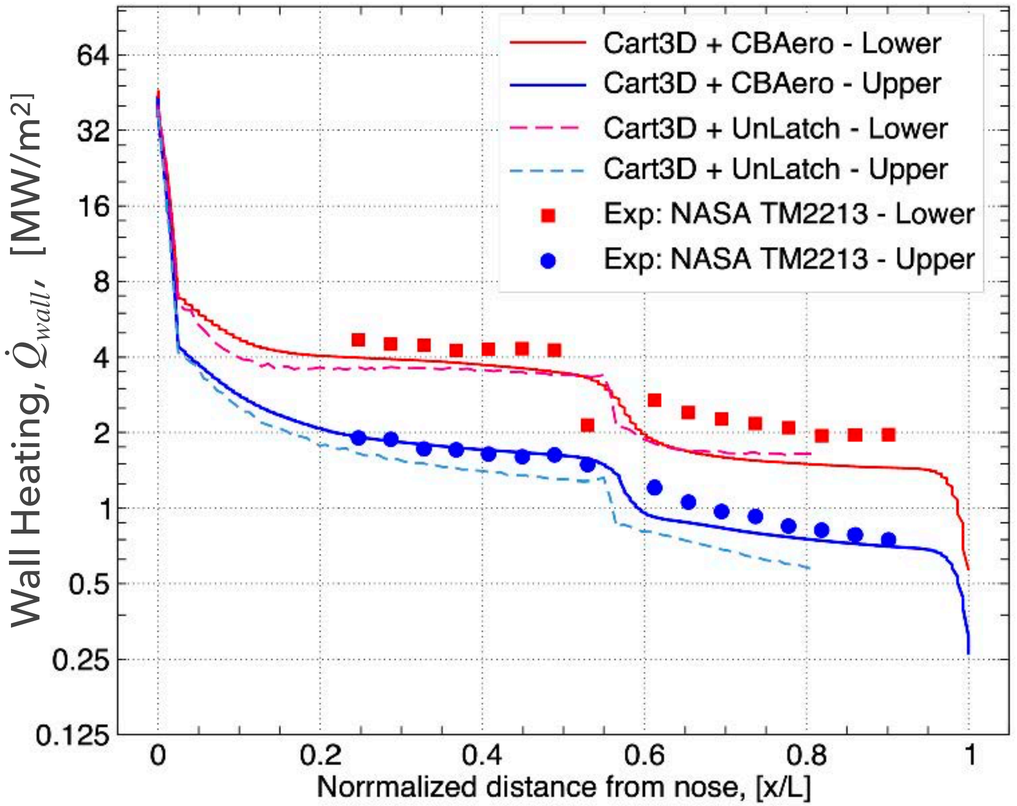
Rapid modeling for hypersonic aerothermodynamics

NASA TP-2213 Biconic: Boundary layer & heating

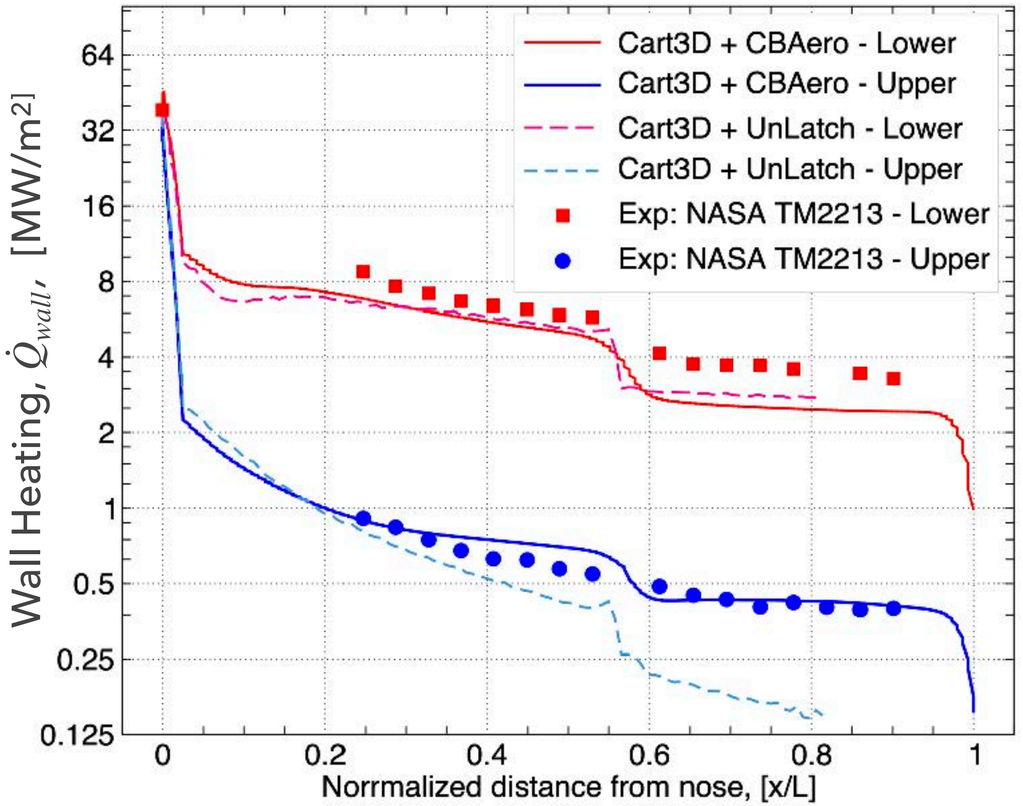
- Comparison with experimental data & LaRC UNLATCH heating code
- Run assuming constant wall temperature
- In general good agreement, significant improvements over UNLATCH
- Similar agreement as RANS results published by Miller & Gnoffo‡



4° AoA



12° AoA

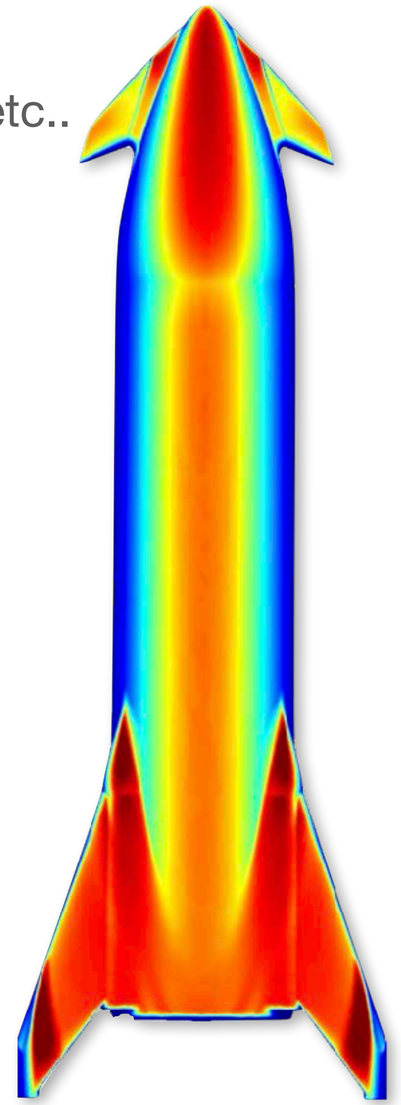


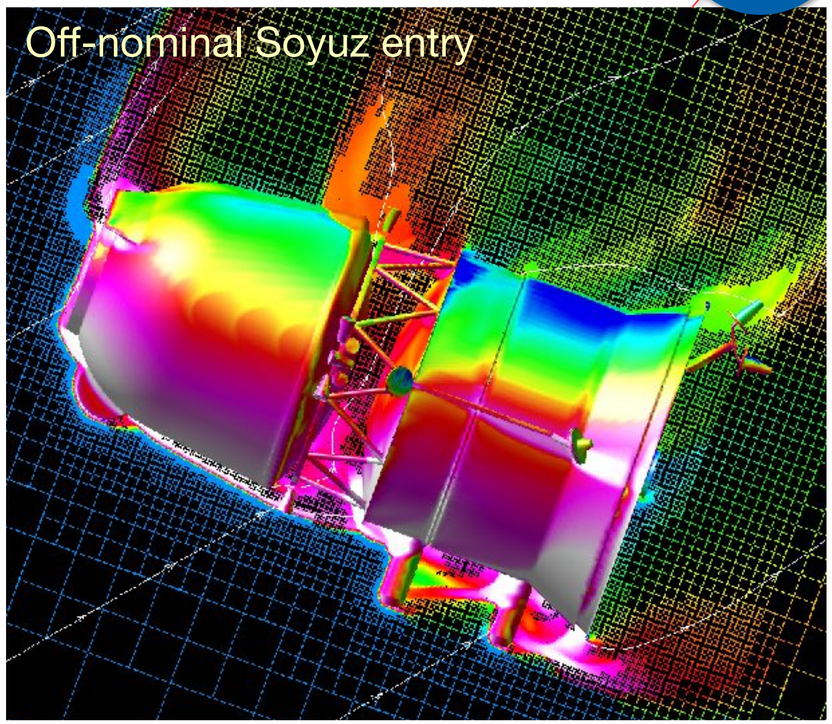
‡ *Miller, Gnoffo & Wilder, JSR **23**(3):225-352*

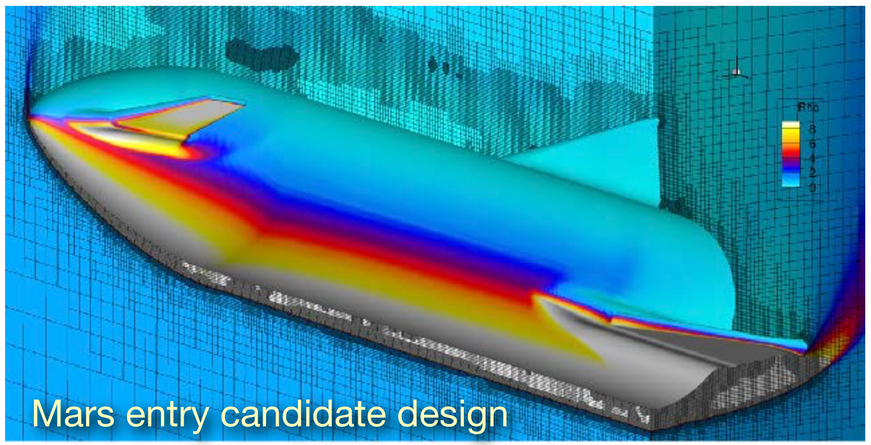
Exploration, Space Technology & Hypersonics

Improved equilibrium solver for air and extraterrestrial atmospheres

- Improve accuracy for terrestrial hypersonics
- Permit equilibrium gas simulations on Mars, Venus etc..
- Existing equilibrium gas solver based on Prabhu‡
  - Table-lookup based implementation
  - Tables need custom lookup functions
  - Existing tables have restricted range of applicability
- Modernize to use CEA2, CEA3, or Mutation++
  - Greater accuracy for air (Earth)
    - Broader conditions & higher temperatures
    - Better for lunar and Mars re/entry
  - Permit for arbitrary gas mixtures
  - Extraterrestrial atmospheres
  - Agnostic to chemistry solver





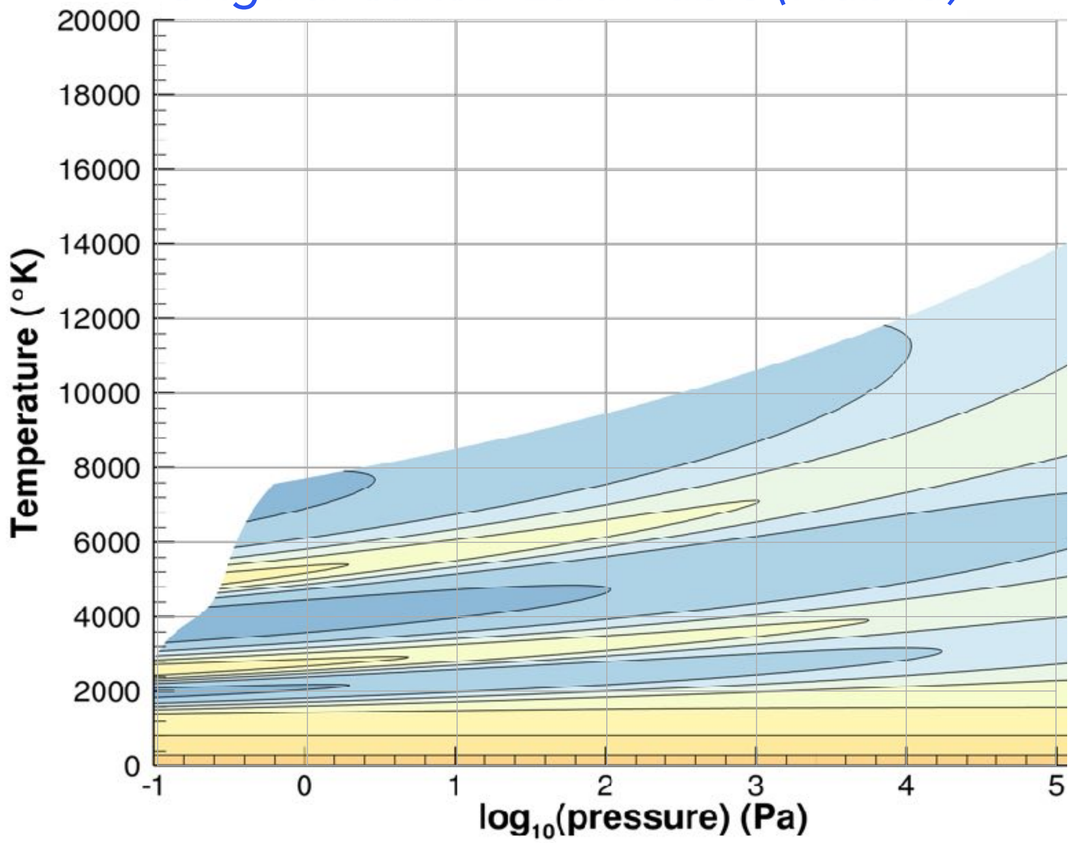


‡ *See: Prabhu & Wayne, NASATP-2792, 1988*

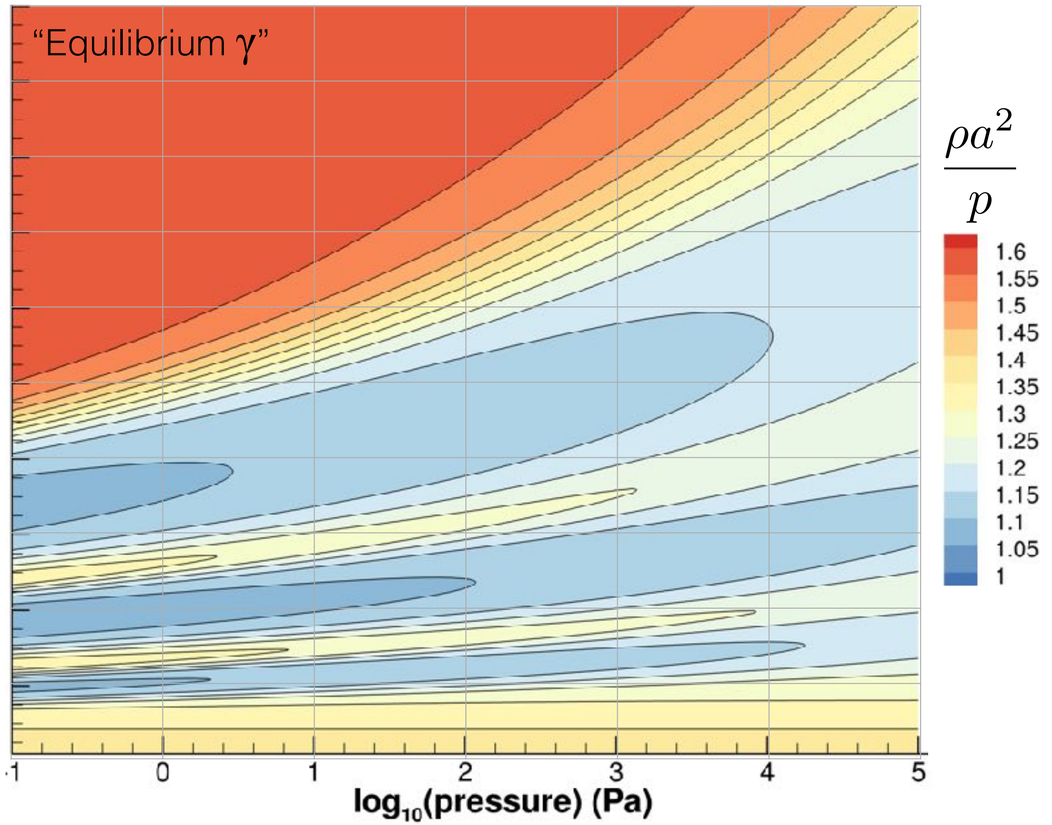
Planned development for hypersonics

Improved equilibrium solver for air and extraterrestrial atmospheres

Original Cart3D Earth Table (Prabhu)



Mutation++

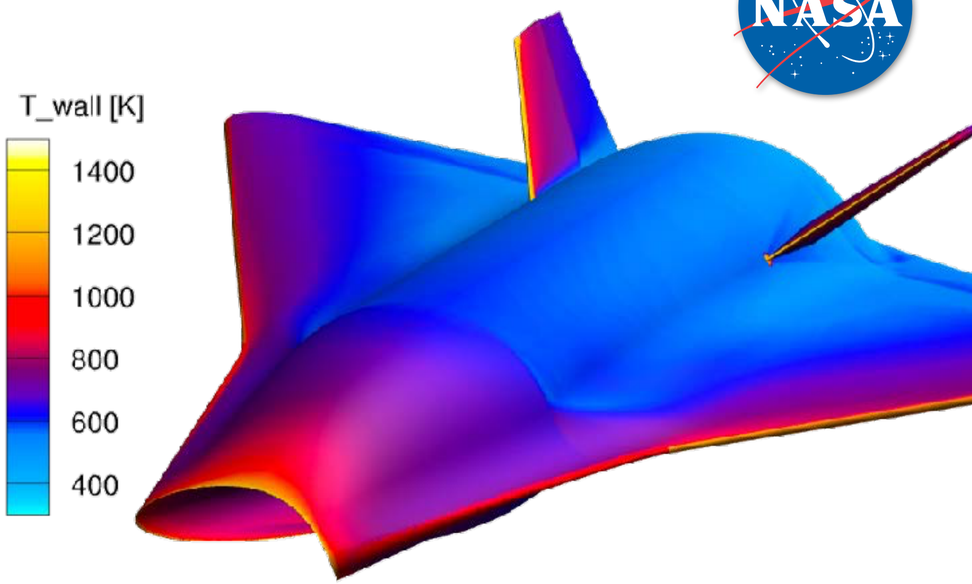


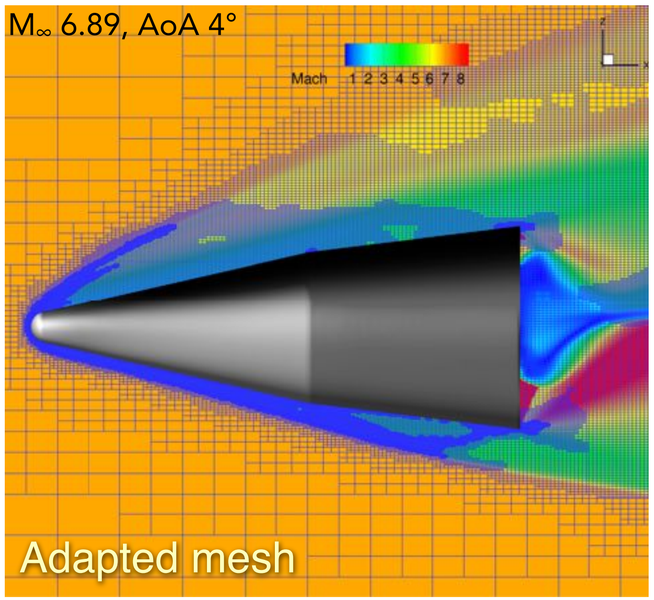
- CEA coverage is similar and table is extremely similar to the Mutation++ map
- Both CEA and Mutation++ offer expanded coverage and higher resolution than current table

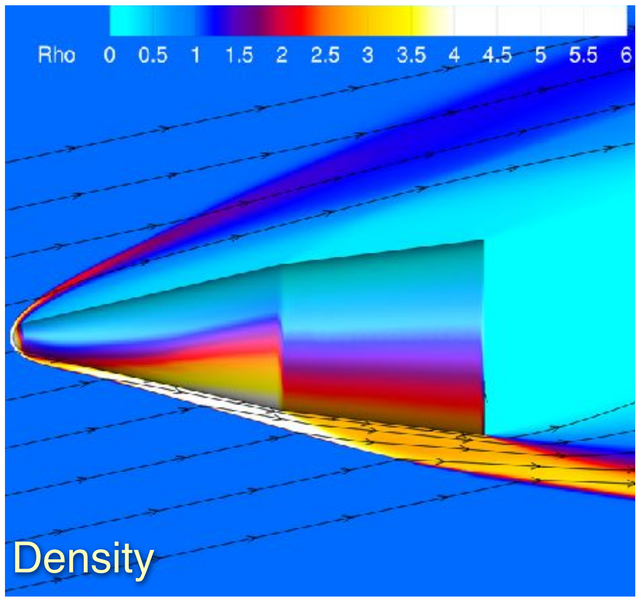
Exploration, Space Technology & Hypersonics

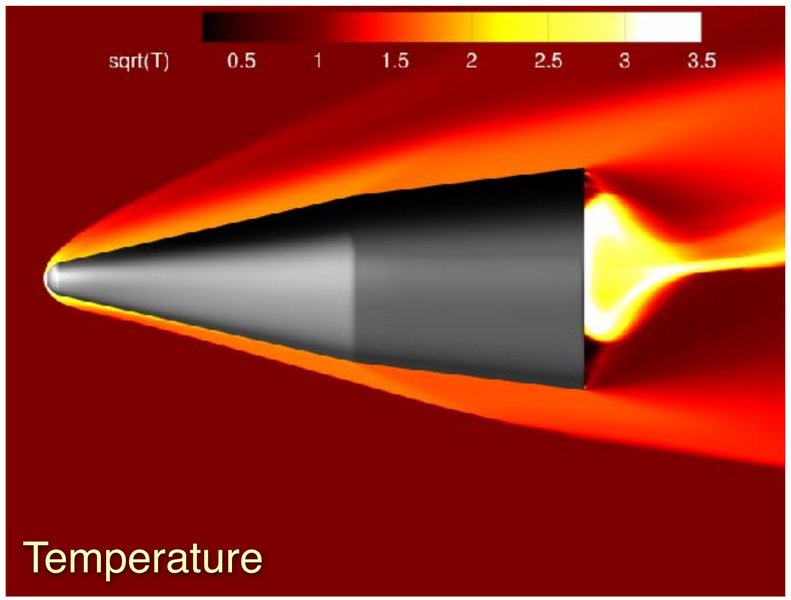
Planned development for hypersonics

- Coupling of Cart3D and CBAero adjoints
  - CBAero currently adding adjoint sensitivities (v7.X)
  - Multi-physics coupling mechanism similar to sBOOM
  - Enable mesh adaptation and error estimation for wall heating or wall temp.
  - Enable aerothermal design (e.g. minimize heat flux)









Near term opportunities & development

Planned development in fy26 and beyond

- OpenMDAO integration
- Commercial supersonics & X-59
  - Phase 2 & phase 3 support
  - Low-boom design
- Science Mission
  - Long range blast propagation and Lamb wave formation
  - Asteroid driven tsunami
- Hypersonics
  - Upgraded equilibrium solver
  - Aerothermodynamics
- Exploration
  - Extraterrestrial atmospheres
  - Mars entry, descent and landing (EDL)

Thank You!



NASA Advanced Supercomputing Division

ARMD Commercial Supersonics and LBFD

ARMD Transformational Tools & Technologies

SMD Planetary Defense Coordination Office

Photo credit: NASA ID: P25-007-07

Thanks!

Thank You!



Photo credit: NASA ID: P25-007-06